"Sapienza" University of Rome

Department of Chemical Engineer

"Industrial Chemical Processes" PhD Program (XXIV cycle)

DEVELOPMENT OF PROCESSES FOR METALS RECOVERY FROM SPECIAL WASTE WITH PRODUCTION OF NANOPARTICLES

by Giuseppe Granata

Supervisor: Prof. Luigi Toro

ACADEMIC YEAR 2010/2011

Index

Abstract

According to the European Guideline 66/2006 within next years several goals must be achieved about collection and recycling of batteries. In particular, 45% of spent devices must be collected by September 2016 and recycling processes for their valorization must ensure at least a 50% of recycling by average weight. By this work the recycling of most common rechargeable batteries such as lithium ion, nickel metal hydride and primary lithium batteries was examined as an answer to the European Guideline. Moreover the production of nanoparticles has been investigated with the future aim to produce nanomaterials downstream of a hydrometallurgical process for battery valorization. In particular based Mn and Co nanoparticles have been produced because of the large amounts of Mn and Co contained in the above mentioned devices.

This thesis has been organized as a series of papers among which someone has been already published whilst someone else is still under reviewing.

At first a hydrometallurgical process to recover cobalt and lithium from lithium ion batteries was developed by studying operations like leaching, purification and metal recovery. The input material of this investigation consisted in a fine powder coming from a mechanical pretreatment made by a small enterprise in northern Italy. The effect of adding a secondary purification step by solvent extraction was evaluated in terms of product purity and economical feasibility of the process.
Then three mechanical routes of pre-treatments were developed in order to dismantle nickel metal hydride, lithium ion and primary lithium batteries recovering valuable fractions either directly saleable (ferrous and non ferrous metals) or further valorizable (electrodic powders) by hydrometallurgical operations for Co, Mn and Ni recovery. Moreover, in order to recycle these devices together, without a preliminary sorting, an unique mechanical process was developed and a solvent extraction procedure for Mn-Co-Ni separation was optimized. Besides, leaching of nickel metal hydride electrodic powder was investigated as well as recovery of rare earths by precipitation.
Aiming to a future production of nanoparticles downstream of a hydrometallurgical process for recycling of batteries, nanoparticles of manganese carbonate were produced by inverse micelles and operating conditions like reactants concentration and water-surfactant molar ratio were investigated. All product were characterized by X-ray diffraction and by Transmission Electron Microscope to determine their crystalline structure and morphology.

Under the same purpose the electronucleation of cobalt on a copper electrode was studied as preparatory study for the synthesis of metallic nanoparticles by pulsed electrodeposition.

1. Introduction

A battery is an electrochemical device able to convert chemical energy to electrical energy. Based on the specific chemical reaction occurring at the electrodes different amounts of electrical energy can be produced and hence several kind of devices can be found on the market. Sometimes the difference between two kinds of batteries can be due also to their electrolytes.
A battery contains mainly the electrodes (anode and cathode) responsible for the specific chemical reaction, charge transfer electrolytes, polymeric or paper separators and the external case, often made up of either ferrous metals or plastic.
There are two basic types of household batteries: single use primary cells and rechargeable secondary cells.
Among primary cells, the most used are the zinc-carbon and the alkaline batteries. Typically these batteries come in sizes AAA, AA, C, D and 9V. The zinc-carbon represent 39% of the European portable battery market whilst the alkaline cells are 51% of the European market [2]. The zinc-carbon batteries have a zinc electrode but in the past they contained also 0.05- 0.5% of lead and 0.01-0.05%. of cadmium to improve mechanical properties of electrodes. Besides cadmium and lead some batteries used to contain mercury, which was most commonly used to coat the zinc electrode to reduce corrosion and thereby enhance battery performance but nowadays batteries are usually produced without these elements [1,3–5].
In general, zinc-carbon batteries have a carbon rod in contact with carbon and MnO_2 as cathode and a zinc case as anode. A paste of NH_4Cl and $ZnCl_2$ is the acid electrolyte. On cylindrical cells the zinc electrode is usually recovered with a stainless steel jacket. A plastic or paperboard separator and an asphalt seal are usually present.
Alkaline-manganese batteries were developed after the zinc-carbon ones. These are usually composed of a brass rod in contact with powdered zinc as anode and a steel case in contact with carbon and MnO2 as cathode. A paste of KOH is used as alkaline electrolyte (pH 14) [1,3,4]. The reactions responsible of their functioning are:

$$Zn\ (s) + 2OH^-\ (aq) \rightarrow ZnO\ (s) + H_2O\ (l) + 2e^-$$
$$2MnO_2\ (s) + H_2O\ (l) + 2e^- \rightarrow Mn_2O_3\ (s) + 2OH^-\ (aq)$$

The rechargeable batteries represent 8% of the European portable battery market. Among rechargeable batteries, nickel-cadmium (NiCd) represents 38%, nickel-metalhydride (NiMH) 35% and lithium-ion 18% of the European market [2,6,7].
Among rechargeable batteries the NiCd were the most used from 1950 to the last decade in both industrial and civil application [8] but several years ago their production has been forbidden because the Ni-Cd system is considered one of the most hazardous in terms of disposal [9]. In fact their cathode was made of cadmium and their anode included Ni(OH), whilst the electrolyte was usually a mixture of KOH. Since these devices are rechargeable the reaction responsible of their working is reversible and it can be summarized as following:

$$Cd + 2NiO(OH) + 2H_2O \rightarrow 2Ni(OH)_2 + Cd(OH)_2 \qquad (1)$$

Nickel metal hydride (NiMH) batteries were developed in 1989 and commercialized primarily in Japan in 1990 mainly to replace NiCd systems. They have high electrochemical capacity, as well as safety and good environmental compatibility. In addition, NiMH batteries are found to be efficient in a wide range of temperatures (−20 to 60 ◦C) and to possess long lives (500–1000 cycles) and low self-discharge rates. The positive electrodes is a porous nickel coated with nickel oxy-hydroxide whilst the anode is made of a hydrogen storage alloy based on mischmetal (mainly cerium, lanthanum, praseodymium and neodymium) like Mm–Ni–Co (Mm = misc. metal) on a metal-mesh

substrate. An inert insulating layer made of polypropylene or polyamide separates the two electrodes [10] and KOH is usually used as electrolyte [11, 12]
Their working is based on the anodic reaction 2 and on the cathodic reaction 3:

$$MH + OH^- \rightarrow M + e^- + H_2O \quad (2)$$
$$NiO(OH) + e^- + H_2O \rightarrow Ni(OH)_2 + OH^- \quad (3)$$

Based lithium devices can be considered as the newest generation of portable batteries and accumulators and their advantages are related to the electrochemical properties of lithium. The highest redox potential Li/Li^+ and the smallest size and mobility of Li^+, provide to lithium devices higher open circuit potentials (even twice than a based zinc battery), lower self discharge rates and lower weights. Regarding this kind of devices a distinction between primary and secondary systems must be done. Primary lithium (metal) uses metallic lithium as anode whilst the cathode can be made of many different compound in several physical states. The most used cathode is a manganese oxide (MnO_2) but other oxides (MoO_3, V_2O_5, TiO_2, $Ag_2V_4O_{11}$, Ag_2CrO_4, CuO, Bi_2O_3, SO_2) can be found instead of the manganese one. The electrolyte is often a lithium salt like lithium perchlorate dissolved in an organic solvent such as propylene carbonate and dimethoxyethane.
Even if these batteries contain no toxic metals there is the possibility of fire if metallic lithium is exposed to moisture while the cells are corroding. For a proper disposal, these batteries must be fully discharged in order to consume all metallic lithium content.
Secondary lithium batteries are rechargeable devices whereas lithium is never contained as a metal but it's always present as Ion. These devices make use of crystallized carbon on a copper layer as anode and lithium cobalt oxide on an aluminum foil as cathode even though other oxides like $LiNiO_2$, $LiNi_{(1-x)}Co_xO_2$ or $LiMn_2O_4$ can be found on the market. In this system ions of Lithium can migrate through an electrolyte solution such as $LiPF_6$, $LiCLO_4$ or $LiBF_4$ in organic solvent like polyethylencarbonate and polypropilencarbonate [13-15].
The chemistry of this intercalated system can be summarized by the following reactions:

Positive Electrode	$LiCoO_2 \leftrightarrow Li_{(1-x)}CoO_2 + xLi^+ + xe^-$
Negative Electrode	$C + xLi^+ + xe^- \leftrightarrow CLi_x^+$
Battery as a Whole	$LiCoO_2 + C \leftrightarrow Li_{(1-x)}CoO_2 + CLi_x$

Lithium-ion-polymer batteries are similar to Li-ion, but because of a solid electrolyte instead of a lithium one like in the common lithium ion batteries, a slim geometry and simpler packing is allowed [16].
On the market lithium accumulators are available in prismatic and cylindric shapes (Fig. 1 and 2). The prismatic one has been developed in the early 1990 to response to consumer demand for thinner geometry and nowday is mainly used for mobile phones and for both lithium ion and lithium polymer accumulators. Whereas the Li-ion accumulators are available in both shapes the lithium-polymer devices are sold exclusively in a prismatic shape.

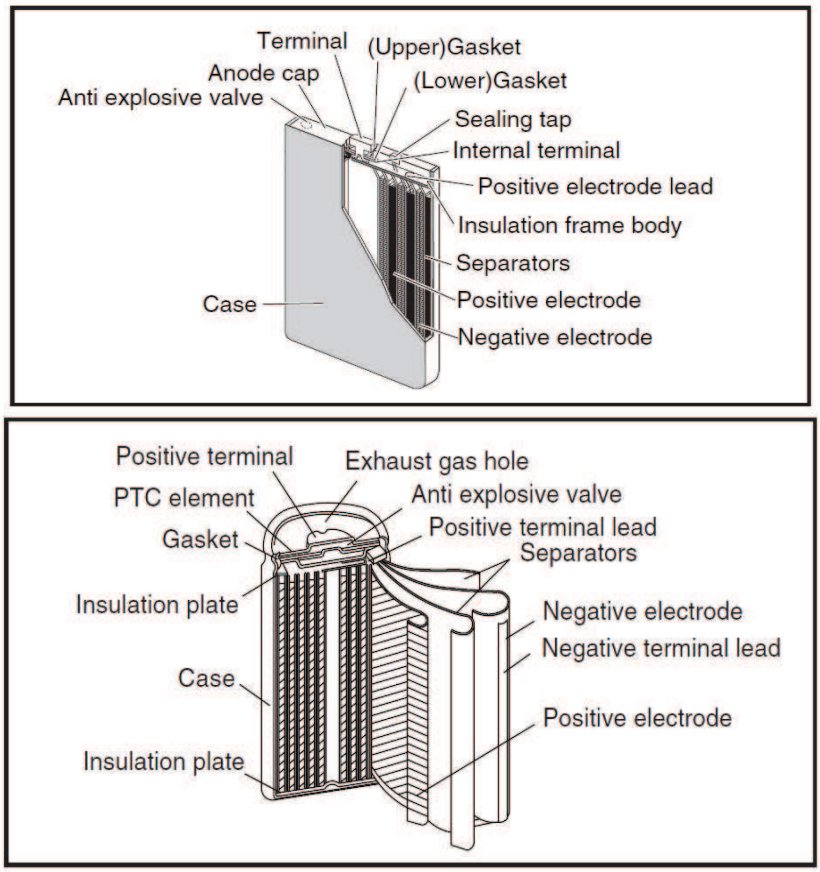

Fig 2: structure of a cylindrical shape battery

1.1 European Guideline for Batteries (2006/66/EC)

The EU market for batteries is estimated to be about 800,000 tonnes of automotive batteries, 190,000 tonnes of industrial batteries and 160,000 tonnes of consumer batteries every year

European Guideline 66/2006 [17], aims to minimize the negative impact of batteries, accumulators and their waste on the environment**.**

The guideline acts in several aspects of the problems related to batteries and their waste, from the placing batteries on the market to their end of life.

Regarding the placing of these devices on the market, the directive 66/2006 put several limits about the content of hazardous substances:

- batteries containing more than 0.0005 % of mercury by weight are prohibited except for button cells with mercury content of no more than 2 % by weight
- portable batteries containing more than 0.002 % of cadmium are prohibited except for emergency and alarm systems, medical equipment and cordless power tools.

Furthermore, according to the guideline Member States should promote, even with economical instruments, the research related to the improving of batteries' environmental performances over their whole life-cycle.

The guideline promotes high levels of collecting and recycling of batteries and battery' waste fixing some minimum goals which must be achieved in the next years. In particular Member Countries should ensure:

- 25% and 45 % of collecting respectively within 2012 and 2016.

- 65% by average weight for lead-acid batteries, 75% for nickel-cadmium and 50% for other kinds of batteries (12.4 and Annex IIIB)

By guideline 66/2006 landfills or incinerator are going to be forbidden as final destination for spent batteries, accumulators and their waste and the necessity to use the best technology to recycle these spent devices has been enhanced.

1.2 Market and Recycling of Batteries

According to EPBA data, the European portable battery market is dominated by primary batteries and EPBA has calculated that 92% of sold batteries in 2003 were primary devices (Figure 3). This data does not include lead-acid secondary batteries, and do not seem to include custom made battery packs. The primary battery market is largely dominated by alkaline batteries, followed by Zinc Carbon batteries (Figure 4). The recent evolution of the market tends to confirm this trend for future years, with the proportion of alkaline increasing at the expense of other primary batteries (mainly Zinc Carbon batteries).

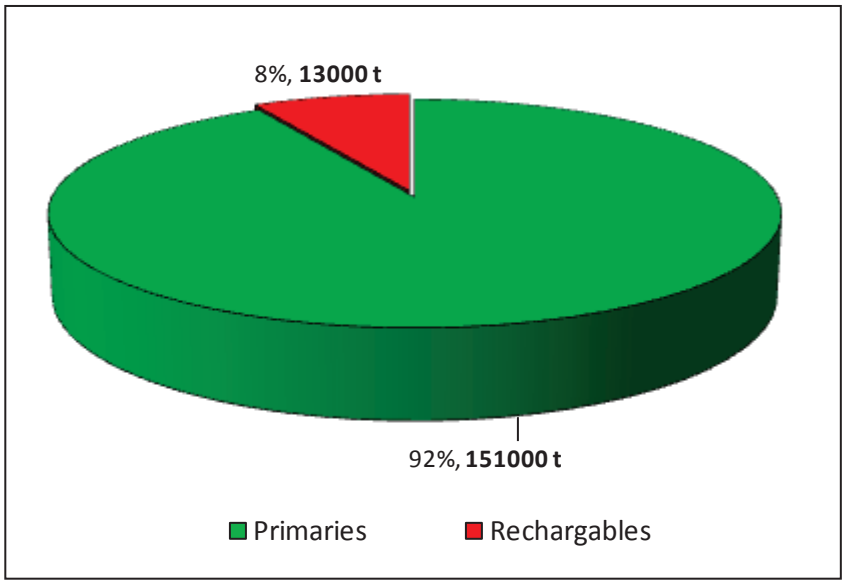

Fig. 3: market of primary and rechargeable batteries

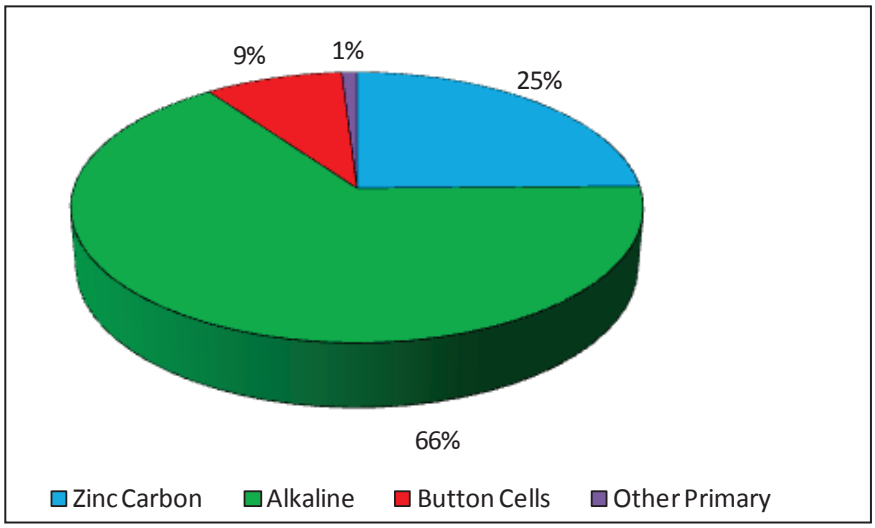

Fig.4:market of primary batteries

Among rechargeable batteries up to 2003 the nickel cadmium ones were the most sold but with the guideline 66/2006 a strong modifying in the statistics is expected. Ni-MH have in fact replaced NiCd batteries for toys, cordless phones, household devices and power tools and nowday no more NiCd devices are available on the market. In fig.5 it can be also noticed as lithium-ion/lithium polymer accumulators have found a constant increasing in their use because of a wide diffusion of mobile phones and notebooks.

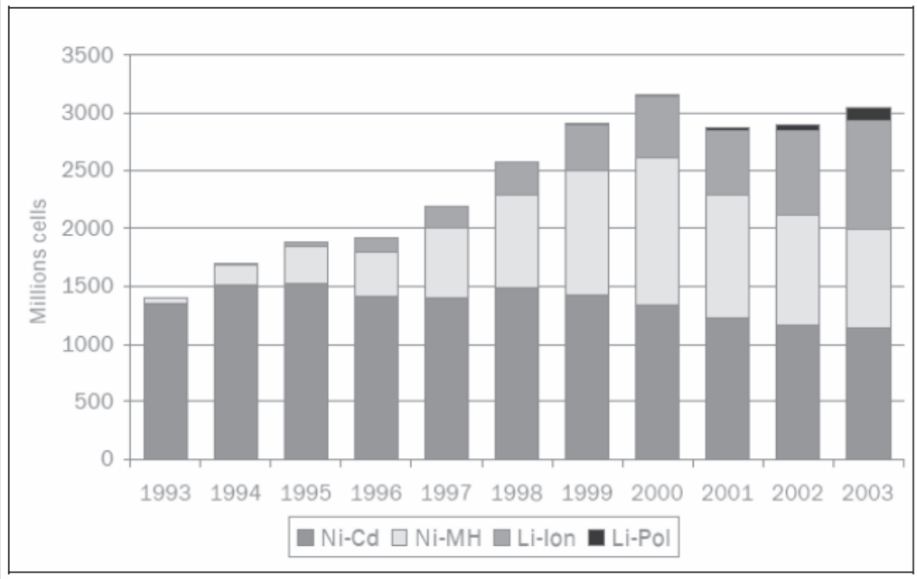

Fig.6: market of portable rechargeable batteries

The European Battery Recycling Association has estimated that on hundreds of thousands tonnes of sold portable batteries only 27000 t have been collected for recycling in 2008, an amount equal to around 14% in weight which must be doubled in 2010 to achieve the European collection target of 25%.

A life cycle assessment (LCA) study carried out by the environmental consultant ERM on behalf on the British Government in November 2000 [18] has confirmed that the recycling of batteries gives an environmental benefit, especially when using existing material recovery technologies such as in the steel industry. This is also valid for the recycling of other battery systems such as NiCd, NiMH, button cells and Li batteries.

1.3 Recycling Technologies

There are many different technologies to recycle batteries and accumulators and all of them require a preliminary physical treatment in order to dismantled the spent devices allowing the recovery of interesting fractions either directly salable or further valorizable by metallurgical technologies.

1.3.1. Pyrometallurgical processes

Pyromtallurgical processes can be either specifically designed to recycle wastes or are associated with the production of steel.. When using batteries as raw materials in steel production, metals such as iron, chromium, nickel and manganese, are used as feed materials to adjust the steel composition but this solution can be used only controlling the metal composition otherwise there would be a worsening of steel properties. One of problems related to the pyrometallurgical processes is the dust generation: zinc and cadmium as volatile compounds are often recovered by condensation from fly ash whilst to avoid mercury accumulation in the bottom ash a pyrolytic step

can be applied as a pre-treatment to remove also organic matter [19]. Usually this kind of processes have been applied for zinc-carbon and manganese-alkaline batteries. For instances the Imperial Smelting Process (ISP) is used in Duisburg to produce zinc recycling zinc-carbon and zinc-air batteries [20] whilst The WAELZ one, is famous to allow the recovery of metals such as Zn, Cd and Pb from dusts by a rotary furnace [21,22].
Whereas a process is specifically designed to recycle batteries in includes several step such as pyrolysis, reduction and incineration. In the pyrolysis water and mercury are evaporated, separated and condensed whilst organic compounds are thermally destroyed and emitted as a gas. By the reduction step at around 1500 ◦C with carbon as reducing agent the metallic fraction is reduced producing metallic alloys. In the incineration, gasses generated by pyrolysis are incinerated at temperatures around 1000 ◦C and then quenched to avoid the generation of dioxins. The sludge generated on the process still contains mercury and they must be treated by distillation. Among pyrometallurgical processes the RECYTEC one has been developed in Swiss 1989 to specifically recycle mixture of batteries [23]. Currently it is used for the recycling of all types of batteries with the exception of NiCd batteries, as well as in the recycling of mercury lamps [24–25]. CITRON is a French technology developed by the homonymous company to recycle different materials by mechanical processing, pyrolysis and metal reduction [26]. The SUMIMOTO Process is a Japanese technology used to recycle of all types of batteries (with the exception of NiCd batteries) producing a ferromanganese alloy by pyrolysis and reduction. BATREC is a swiss technology deriving from SUMIMOTO process which allows to treat any waste containing heavy metals (batteries, dental wastes, thermometers, scraps, etc.) zinc by distillation, and the metallurgical difficulties associated with the separation of nickel and iron.

1.3.2. Hydrometallurgical processes

Hydrometallurgical processes are connected to leaching steps in acid or alkaline medium and purification processes in order to dissolve the metallic fraction, in order to recover metal solutions that could be used by the chemical industry [27].
A typical hydrometallurgical process aims to recover a specific metal from its primary source and it is composed by several operations.

1.3.2.1 Leaching

In a leaching operation one or more metals are extracted from their primary source by an acid or alkaline agent. Many operating conditions such as type of leachant and its concentration, temperature, stirring, presence of reducing/oxidizing agent are important in determining the extent of the reaction. Usually high temperatures, high concentrations and smaller particles of solid material promote higher extractive yields. The choice of the leachant is important in order to define in which form the metal will be solubylized.
Sulphuric Acid is the most used leachant since it's considered environmental friendly and it is able to extract many metals from many different sources according to the reaction:

$$MeO + H_2SO_4 \rightarrow MeSO_4 + H_2O \quad (4)$$

Many hydrometallurgical processes for waste valorization use hydrocloridric acid as leachant extracting in this way all metals as chloride, for instance according to the reactions:

$$MeFe_2O_4 + 2HCl \rightarrow MeCl_2 + Fe_2O_3 + H_2O \quad (5)$$

$$MeO + 2HCl \rightarrow MeCl_2 + H_2O \quad (6)$$

$$Me + 2HCl \rightarrow MeCl_2 + H_2 \quad (7)$$

Some hydrometallurgical process uses acetic acid as leachant (i.e. UBC-Chaparral Process), solubylizing all metals as acetates:

$$CH_3COOH + MeO \rightarrow Me(CH_3COO)_2 \quad (8)$$

Since not all metals are soluble as acetates this leachant is able to determine a higher selectivity towards some specific elements but anyway it doesn't find wide use because acetic acid is more expensive than other leachants.
Because of the amphoteric behavior owned by some metals, alkaline agents such as sodium or calcium hydroxide can be used to determine their selective solubilization. For instances

$$ZnO + 2NaOH \rightarrow Na_2ZnO_2 + H_2O \quad (9)$$

$$PbO + 2NaOH \rightarrow Na_2PbO_2 + H_2O \quad (10)$$

$$2Na_2ZnO_2 + 2H_2O \rightarrow 2Zn + 4NaOH + O_2 \quad (11)$$

$$Al_2O_3 \bullet H2O + 2NaOH \rightarrow Na_2OAl2O_3 + 2H_2O \quad (12)$$

Anyway even though the extraction can split metals from their primary source, in an alkaline media with sodium, some complex and insoluble salt can be formed.

1.3.2.2 Purification

Since the leaching can solubylize other metals acting as impurities in further operations, a purification step of leach liquors can be made enriching the solution of targeted metals. Selective precipitations are the most common ways to purify a leach liquor and they consist in a separation of different metals taking advantage from their different solubility as hydroxides or other salts.
If there are no appreciable differences as solubility constants between hydroxides or salts a purification by precipitation can't be used. In this case a solvent extraction procedure can lead to selective separation of targeted metals.
In the most common extractive procedure, by using a biphasic system (aqueous/organic) a mass transfer from one phase to another one takes place through a mechanism of repartition based on the different hydrophilicity/liphophylicity of substances. Whereas this substance is a metal which need to be selectively separated from other metals in solution, a particular kind of "solvent extraction with reaction is required. In this operation, dissolving into an organic phase a molecule able to react selectively with a metal in the aqueous phase forming a complex, a mass transfer can be determined.
A typical reaction can be represented by the equation:

$$M^{n+} + nRHorg \leftrightarrow MR_n\ org + nH^+ \quad (13)$$

Where M^{n+} is the metal ion in the aqueous phase, RHorg is the acidic form of complexant agent in the organic phase and MR_n org is the complex metal-complexant in the organic phase.

The equilibrium constant of previous reaction (K) can be written as:

$$K = [MR_{n\ org}]\ [H^+]n/[M^{n+}][RH_{org}]^n \quad (14)$$

and for the metal of interest a Dilution Ratio (D) between organic and aqueous phases can be defined as:

$$D = \frac{[MR_{n\ org}]}{[M^{n+}]} \quad (15)$$

Replacing the equation (3) in (2) and taking into a logarithm:

$$logD = logK + nlog[RHorg] + npH \quad (16)$$

and as it can be seen in (), for the same extraent, the distribution coefficient of a metal depends on the extraent concentration in the organic phase and on the pH of the aqueous phase.
When two metals (M1 and M2) can be extracted at the same time, a factor β to quantify the separative capacity is defined as ratio of their dilution ratios:

$$B = D_{M1}/D_{M2} \quad (17)$$

1.3.2.3 Recovery

Crystallization

Crystallization refers to the formation of solid crystals from a homogeneous solution and it can be used as both purification and recovery technologies in many branches of chemical manufactures.

A typical crystallization takes place in two successive steps called Nucleation and Crystal growth.

Nucleation refers to the formation of first elementary aggregates of solids as results of several surface depositions and theoretically in order to get this first step the limit solubility concentration must be reached in the solution. Actually under this condition the induction time, defined as time necessary to get the first nucleus, is infinitive and hence, since the Induction time decrease proportionally increasing oversaturation or overcooling grade, this concentration/cooling must be passed.

Nucleation is metastable phenomenous easily understandable by considering the free energy changes associated with the formation of the nucleus. The statement that the free energy per molecule of the new phase is less than that of the solvated phase only applies to the bulk of the new phase. The surface is a different matter. Because the surface molecules are less well bound to their neighbors than are those in the bulk, their contribution to the free energy of the new phase is greater. The difference between the free energy per molecule of the bulk and that of the surface is referred to as the interfacial free energy (It is sometimes called the surface free energy). The interfacial free energy is always a positive term and acts to destabilize the nucleus. As a consequence, at very small size when many of the molecules reside at the surface, the nucleus is unstable. Adding even one more molecule just increases the free energy of the system. On average, such a nucleus will dissolve rather than grow. But once the nucleus gets large enough, the drop in free energy associated with formation of the bulk phase becomes sufficiently high that the surface free energy is unimportant, and every addition of a molecule to the lattice lowers the free energy of the system. There is an intermediate size at which the free energy of the system is decreased whether the nucleus grows or dissolves, and this is known as the critical size. This phenomenon is referred to as the Gibbs-Thomson effect. Of course, if the supersaturation is high enough, the critical size can be reduced to less than one growth unit.

The existence of a critical size has a number of implications. First and foremost, because nucleation of the new phase is the result of fluctuations that bring together sufficient numbers of molecules to exceed the critical size, the probability of nucleation will be strongly affected by the value of the critical size. This means that nucleation can be controlled, to some extent, by modulating the critical size, which is in turn a function of the interfacial energy. The smaller the interfacial energy, the smaller the critical size and the more likely nucleation becomes for any given supersaturation. As a consequence, by varying either the solution composition or the supersaturation, the probability of nucleation can be manipulated.

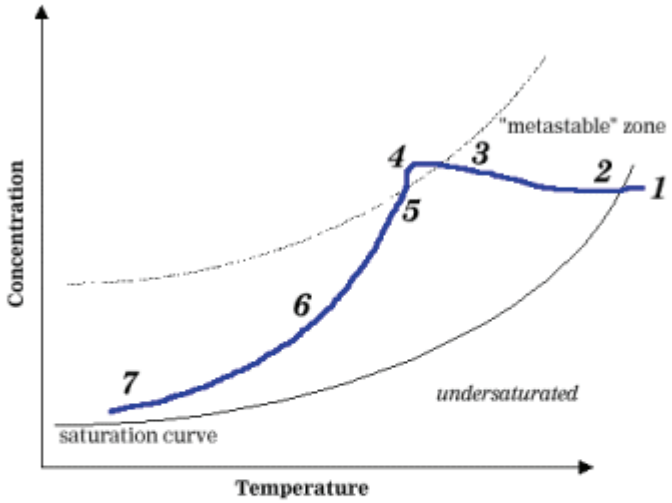

Fig. 7: crystallization equilibrium towards oversaturation and overconcentration

Nucleation on foreign surfaces

The presence of a foreign surface can be used to exert even greater control over nucleation because, quite often, the interfacial energy between a crystal nucleus and a solid substrate is lower than that of the crystal in contact with the solution (Neilsen 1964; Abraham 1974; Chernov 1984; Mullin 1992; Mutaftschiev 1993). This is because the molecules in the crystal can form bonds with those in the substrate that are stronger than the bonds of solvation. Because the enthalpic contribution to the free energy comes primarily from chemical bonding, stronger bonds lead to a smaller interfacial free energy.

For simplicity, we consider a spherical nucleus of radius *r*, as illustrated in Figure 8, nucleating within the bulk solution. (This is referred to as homogeneous nucleation.) The free energy change per molecule (Δg) is given by the sum of bulk (Δgb) and surface terms (Δgs), namely:

$$\Delta g = \Delta g_b + \Delta g_s = \{[(4/3)\pi r^3]/\Omega\}\Delta\mu + 4\pi r^2\alpha \qquad (18)$$

where Ω is the volume per molecule, and α is the interfacial free energy. The first term is negative and varies as the cube of *r*, while the second term is positive and varying as r^2. As shown in Figure 8, the sum of the two terms has a maximum that occurs when $d\Delta g/dr = 0$. The value of *r* at this point can be found by taking the derivative of (8) and setting it equal to zero. This is known as the critical radius, r_c, and is given by:

$$r_c = 2\Omega\alpha/\Delta\mu = 2\Omega\alpha/kT\sigma \qquad (19)$$

In this equilibrium of formation and dissolution of new nuclei and hence attachments and detachments', once the first nucei have been formed the liquid-solid transition goes on resulting either in the formation of new nuclei or in a growth of previously formed nuclei.

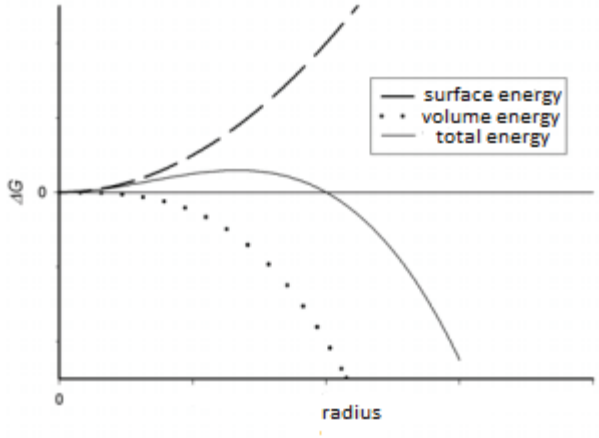

Fig.8: free energy in the formation of a critical radius nuclei

Electrochemical recovery

Electrowinning refers to an operation of electrodeposition of non-ferrous metals from a leached solution to the working electrode of an electrochemical cell.

When a specific voltage is applied to an electrochemical cell, if this potential is higher than the cell's electromotive force, the cell will behave as an electrolytic cell. Whereas an electrolysis occurs the reactions which require a lower electric work take place at the electrodes: the most oxidants species can be reduced at cathode whilst the most reducing species can be oxidized at anode.

In order to have an electrolysis a voltage V must be applied to the electrodes:

$$V = (E_a - E_c) + V_s + iR$$

Where

- V is the total applied voltage
- E_a and E_c are respectively the anodic and cathodic potentials, by Nernst equation
- V_s is the total overvoltage
- i is the faradic current
- R is the cell resistance

From a quantitative point of view the deposition of substances at the electrodes follows the Faraday's law according to the amount of reacting substances is proportional to the current intensity which cross the electrodes during the process. In particular when 96500 Coulomb cross the cell, one equivalent of subastance react on the electrodes.

<u>Over potential</u>

Overpontial is a part of the total applied voltage which is necessary in order to have reactions with an appreciable rate and it can be meant as a measurement of reversibility of an electrodic reaction. Overpotential increases with corrent density and it usually decreases with temperature but the most important factor which determine its value is the electrodic material type.

Since the reactions which require less work are favorite, overpotential could be seen as impediment but actually many electropositive metals can be reduced only because the overpotential increases the required potential for the theoretically favorite hydrogen reduction.

Overpotential value can be seen as a kinetic impediment and it value can't be pre-calculated but it must be determined only by a specific experimentation.

An electrolyc process can be carried out:

a. *At constant applied voltage*

When applied voltage is constant, since Ea – Ec increases during the electrolysis current intensity must decrease and it means that chemical reactions occur until applied voltage holds a value higher than electromotive force of the cell. When the applied voltage equals Ea – Ec current intensity decreases to 0 and electrolysis is over. This technique determines good selectivity but slow processes

b. At constant current

Increasing gradually the applied voltage, current value can be kept constant during the electrolysis. In this way the electrolysis is faster because current doesn't decrease but the electrodic potential can reach soon a value where another redox couple could react. This lost in terms of selectivity can be avoided only when electroactive species have a quite different decomposition potential.

c. *At controlled working potential*

Controlling the working potential is possible to obtain the bet selectivity whereas there are more electroactive species. Working electrode potential can be kept constant towards a third reference electrode by modulating the total voltage applied to the cell in order to balance all variations during the electrolysis. Electrolysis at controlled potential grant good selectivity and relatively fast processes.

References

[1] H. Lund, The McGraw-Hill Recycling Handbook, 2nd ed., McGraw-Hill, New York, 2001.
[2] European Portable Battery Association, 2 April 2003. http://www.epba-europe.org.
[3] W. Baumann, A. Muth, Batterien—Daten und Fakten zum Umweltschutz, Springer, Berlin, 1997, 593 pp.
[4] F. Hiller, R. Giercke, H.A. Kiehne, Entsorgung von Gerätebatterien, Expert-Verlag, Hannover, 1998, 61 pp.
[5] C.C.M.B. Souza, D.C. Oliveira, J.A. Tenório, Charaterization of used alkaline batteries powder and analysis of zinc recovery by acid leaching, J. Power Sour. 103 (2001) 120–126.
[6] J.C. Bartels, How to calculate collection rates for spent batteries, in: Proceedings of the Fifth International Battery Recycling Congress, Deauville, France, 1999.
[7] N.F. Oldershausen, VFW-Rebat, a private, profit-oriented battery collection, in: Proceedings of the Fifth International Battery Recycling Congress, Deauville, France, 1999.
[8] F. Putois, Market for nickel-cadmium batteries, J. Power Sour. 57 (1995) 67–70.
[9] Choice of Battery Chemistries, 2 April 2003. http://www.cadex.com.
[10] P. Zhang, T. Yokoyama, O. Itabashi, Y. Wakui, T.M. Suzuki, K. Inoue, Hydrometallurgy 50 (1998) 61–75.
[11] C.J. Rydh, B. Svärd, Sci. Tot. Environ. 302 (2003) 167–184.
[12] D.C.R. Espinosa, A.M. Bernardes, J.A.S. Tenório, J. Power Sources 137 (2004) 134–139.
[13] W. Qunwei, L. Wenquan, P. Jai, Characterization of a commercial size cylindrical Li-ion cell with a reference electrode, J. Power Sour. 88 (2) (2000) 237–242.
[14] C. Iwakura, Y. Fukumoto, H. Inoue, S. Ohashi, S. Kobayashi, H. Tada, M. Abe, Electrochemical characterization of various metal foils as a current collector of positive electrode for rechargeable lithium batteries, J. Power Sour. 68 (2) (1997) 301–303.
[15] J.M. Chen, C.Y. Yao, S.P. Sheu, Y.C. Chiou, H.C. Shih, The study of carbon half-cell voltage in lithium-ion secondary batteries, J. Power Sour. 68 (2) (1997) 242–244.
[16] I. Buchmann, What's the best battery? 2 April 2003. http://www.batteryuniversity.com.
[17] EU Battery Directive Extended Impact Assessment (2003)
[18] Recharge http://www.rechargebatteries.org/MarketDataRechargableBatteries.pdf
[19] A. Vassart, A chemical recycling scheme for used primary batteries, in: Proceedings of the Global Symposium on Recycling Waste Treatment and Clean Technology (REWAS'99), vol. II, TMS, 1999, pp. 1139–1146.
[20] W.D. Schneider, B. Schwab, New ways for economical and ecological battery recycling, in: Proceedings of the Fifth International Battery Recycling Congress, Deauville, France, 1999.
[21] B. Egocheaga-Garcia, Developing the Waelz process: some new possibilities for the preparations of the load in the Waelz process and ultradepuration of the volatile fraction obtained in this process, in: Proceedings of the Third International Conference on the Recycling of Metals, ASM, 1997, pp. 387–402.
[22] W.S. Moser, G.T. Mahier Jr., R.T. Knepper, M.R. Kuba, F.J. Pusateri, Metals recycling from steelmaking and foundry wastes by horsehead resource development, in: Proceedings of the International Conference on Electric Furnace, 1992, pp. 145–157.
[23] J.F. Equey, Recymet: our experience in the recycling of spent batteries, in: Proceedings of the Fourth International Battery Recycling Congress, Hamburg, Germany, 1998.
[24] H. Jordi, A financing system for battery recycling in Switzerland, Journal of Power Source. 57 (1995) 51–53.
[25] P. Ammann, Economic considerations of battery recycling based on recytec process, J. Power Sour. 57 (1995) 41–44.

[26] J. Frenay, Ph. Ancia, M. Preschia, Minerallurgical and metallurgical processes for the recycling of used domestic batteries, in: Proceedings of the Second International Conference on Recycling of Metals, ASM, 1994, pp. 13–20.
[27] A.M. Bernardes, D.C.R. Tenorio, J.A.S Espinosa. Recycling of batteries: a review of current processes and technologies, Journal of Power Sources 130 (2004) 291–298.

2. Product recovery from Li-Ion battery wastes coming from an industrial pre-treatment plant: lab scale tests and process simulations.

2.1 Introduction

Lithium ion batteries (LIB) are widely used as electrochemical power sources in modern electronic equipments, mainly because of their high energy density, high cell voltage, long storage life, low self discharge rate and wide temperature range of use [1].
European Guideline 66/2006 declared the necessity of reducing pollutant effects related to the wastes of end of life batteries and accumulators. Mandatory collection rates and target material recovery were then established: 25% and 45% collection rates within 2012 and 2016, respectively, and 50% material recovery for LIB [2].
New hydrometallurgical processes should be then developed in order to satisfy such targets. Literature survey showed that research has been mainly focused on the optimization of operating conditions for leaching operation. Most works reported experimental results of acid-reductive leaching where H_2O_2 is generally used as reducing agent along with sulphuric acid [3-6]. Otherwise organic reducing agents can be used such as citric acid [7] and oxalic acid [8]. Some works also compared different leaching mixtures: Zhang and coworkers [9] investigated three acids (nitric, sulphuric and chloridric) and evaluated the effect of acid concentration, temperature, leaching time and solid-to-liquid ratio. They found that hydrochloric acid gave the best performance in agreement with experimental results reported by Contestabile et al. [10]. Nitric acid was also tested in leaching experiments using LIB electrodic powder [11].
Few works were published addressing the complete process route to recover Co and/or Mn products [5, 12] or to regenerate lithium cobalt oxide [13,14]. All the works cited above used powder samples obtained by manual dismantling of batteries or laboratory scale mechanical dismantling. This can seriously affect the scalability of process outputs obtained in these studies for two main reasons. First the sequence and type of mechanical pretreatments used for large scale dismantling can completely alter the composition of the input material of leaching section. In particular considering the internal structure of LIB (made up of thin layers of electrodic material within alternate sheets of Al and Cu), the manual dismantling and the selective recovery of electrodic material gives a solid sample completely different from that obtained from real battery grinding. Then hand-made separation of electrodic material gives an input material which is not representative of ground material from large scale plants. In addition, treatment of few units of batteries means that feed heterogeneity is completely neglected. On the other side process development and feasibility analysis required that input material come from large scale treatment to be representative of real wastes that will be treated in plant scale.

Another general observation about literature papers reported above is the complete lack of economic analysis for the proposed process. Then two main limits emerged from the state of the art of literature:

- use of LIB powders coming from few samples of manually or lab-scale dismantled batteries,
- focus on leaching section rather than on the whole process feasibility.

The aim of this work is overcoming these limits by addressing the process economics of different routes to recover Co and Li products from LIBs using a real waste fraction coming from a large scale pre-treatment plant.
Innovative aspects are then:

- LIB powder which is representative of what would be treated in large scale facilitating the scale-up of the process.

- economical feasibility of different process options to recover lithium and cobalt products from LIB wastes. In particular, the effect of adding a secondary purification step by solvent extraction was estimated in terms of product purity and process economic feasibility.
- use of glucose as reducing agent: this carbohydrate (potentially coming from waste of food factories) have been already used for Mn(IV)oxides leaching [15], but never tested for cobalt reductive leaching.

2.2 Materials and methods

Materials

The input material used in leaching experiments was kindly provided by "S.E.Val. s.r.l.", an Italian medium enterprise working in the recycling of wastes of electric and electronic equipments, batteries and accumulators. LIBs were treated in a large scale mechanical route of pre-treatment (5000 t/y), which was made up of a combination of crushing, milling, sieving, and physical separations such as eddy current separator, magnetic, pneumatic and densimetric splitter.

All chemicals (H_2SO_4, NaOH, Na_2CO_3, di-2-ethylhexylphosphoric acid, D2EHPA) were analytical grade reagents (Sigma-Aldrich). The extractant Cyanex 272 was supplied by Cytec USA Incorporation and was used without further purification. Low boiling point kerosene (180–270 °C) was used as diluent.

Granulometric anasysis and acid digestion

The input material was vibro-sieved 3 times for 10 min using 6 sieves with different cut-off: 2 mm, 1mm, 0.5 mm, 0.25 mm, 0.2 mm, 0.125 mm. After sieving samples of each fraction (2 g) were digested using 40 mL of aqua regia (HCl:HNO3 = 3:1) for 5 h, filtered and analyzed by an Inductively Coupled Plasma Optical Emission Spectrometer (ICP-OES, Varian Vista-MPX Simultaneous CCD) in order to determine concentration in solid of each metal (x0). For each digestion three replicates were performed and average values reported.

Leaching

Leaching experiments were carried out in 0.5 L Pyrex jacket reactors provided of impeller stirrer, vapor condenser and thermometer. Heating was provided by an external thermostatic apparatus. H2SO4 solutions were put inside the reactors at the desired temperature. Then the desired weight of solid input material (m0) and the reducing agent (if present) were added under stirring. Experimental conditions (temperature, amount of acid expressed as g of acid per gram of solid, reducing agent concentration expressed as % stoichiometric excess) used in all leaching tests were listed in Tables 1 and 2.

Stoichiometric concentration of glucose was calculated according to reaction 1:

$$24LiCoO_2 + 36H_2SO_4 + C_6H_{12}O_6 = 24CoSO_4 + 12Li_2SO_4 + 6CO_2 + 42H_2O \quad (1)$$

During leaching time, leach liquor samples (2 mL) were periodically drawn, filtered and analyzed by ICP-OES.

At the end of each experiment, residual solids were separated by filtration, washed with water, dried in a oven, weighted (mf) and digested as reported in paragraph 2.2 to determine the residual concentration of each metal in solid phase (xf). Extractive yields for each metal were the determined as:

$$extractive\,yield\,(\%) = \frac{x_0 m_0 - x_f m_f}{x_0 m_0} * 100 \qquad (2)$$

where x_0 is the metal concentration (g/g) in the solid before leaching, m_0 is the weight (g) of solid used for leaching, xf is the metal concentration in solid residue after leaching, and mf is the weight of solid residue after leaching.
Treatments were arranged according to two factorial designs [16] for the preliminary optimization of the operating conditions using HCl (Table 1) and H_2SO_4 plus glucose (Table 2) at fixed solid liquid ratio (s/l=100 g/L). A third set of experimental tests was performed using $2gH_2SO_4$/gpowder with 50% of stoichiometric excess of glucose at 90°C in order to investigate the effect of solid-liquid ratio by increasing the solid concentration from 100 g/L to 135 g/L, and finally to 200 g/L.

Primary purification: precipitation
Iron, aluminum and copper were removed by leach liquor by adding sodium hydroxide pellets up to pH 5.0 under stirring at room temperature. After 2 hour stirring suspensions were filtered and solutions analyzed by ICP-OES.

Solvent Extraction
Cyanex 272 and D2HEPA (extractants) were dissolved in kerosene (diluent) until reaching the same molar concentration of cobalt in the leach liquor (0.84 M) and then partially saponified (65%) by adding a NaOH solution (5 M) under stirring [17,18]. 10 mL of purified leach liquor (50 g/L of Co, 10 g/L of Li, 5 g/L of Ni, 1.5 g/L of Mn) were shacked for 5 min with the organic phase. The volume of aqueous phase was kept constant for all experiments, while the volume of the organic phase was varied from 10 to 60 mL. Then the ratio between organic phase volume and aqueous phase volume, O/A, changed from 1 to 6. Considering that the molar concentration of the extractant in the organic phase is the same of Co in aqueous phase, working with variable O/A ratios means working under different stoichiometric conditions (O/A=molSLV/molCo, where molSLV are the mol of extractant in organic phase). After shacking the two phases were separated by a separating funnel. pH values of leach liquors were adjusted by the addition of NaOH or H2SO4 solution in the range 1-6. All experiments were performed at room temperature (25±1 °C) in duplicates. Raffinates (aqueous phase after extraction) were analyzed by ICP-OES to determine the amount of extracted Co2+, Li+, Ni2+, and Mn2+. Stripping tests for metal recovery from organic phase were carried out using 4 M H2SO4 solution at 25±1°C with the same volume of organic phase and aqueous phase (O/A=1).

Cobalt recovery
Cobalt was recovered as carbonate from solutions coming both from primary purification (NaOH precipitation) and secondary purification (stripping solution after solvent extraction). A saturated Na_2CO_3 solution was added to purified leach liquors under stirring in order to have a final pH of 9-10. After 2 hours under stirring, suspensions were filtered and analyzed by ICP-OES. Solid precipitates were washed with water to remove soluble salt (as Na_2SO_4) and then dried at 60°C for 24 hours. In order to evaluate the purity of obtained products, cobalt carbonate samples were dissolved in water and solutions analyzed by ICP-OES.

Lithium recovery
Lithium was recovered as carbonate from raffinates. A saturated Na_2CO_3 solution was added to raffinates under stirring up to pH 8. After 2 hours under stirring, suspensions were filtered and

analyzed by ICP-OES. Solid precipitates (mainly Ni, Mn, and Cu carbonates) were removed by filtration and the residual solution was evaporated leaving different amounts of residual water (tested degree of evaporation: 70, 80, 90%). Lithium carbonate was separated by filtration, washed in hot water and dried. Lithium carbonate samples were dissolved in water and solutions analyzed by ICP-OES.

2.3 Results and discussion

2.3.1 Input material composition and metal distribution in the different fractions

The input material used in leaching experiments contains Co (250 ± 30 mg/g), Cu (60 ± 20 mg/g), Al (50 ± 20 mg/g), Li (35 ± 5 mg/g), Mn (15 ± 3 mg/g), and Ni (3 ± 1 mg/g). Considering this composition and in particular the amount of cobalt (lithium can be also contained in the electrolyte), it can be evaluated that LiCoO2 is 50%w/w of the input material. Granulometric distribution shows that 41% of mass weight has a diameter (d) which is <0.125 mm, 8% has 0.125<d<0.200 mm, 5% has 0.200<d<0.250 mm, 10% has 0.250<d<0.500 mm, 4% has 0.500<d<1 mm ,12% has 1<d<2 mm, and 19% has d>2 mm. According to the charts showed in Figure 1, all metals are mainly contained in the fractions with d<1 mm (82% of Li, 81% of Co, 88% of Mn, 62% of Ni) with the exception of copper and aluminum, which are concentrated in the fraction with d>1 mm (67% of Al, 79% of Cu).

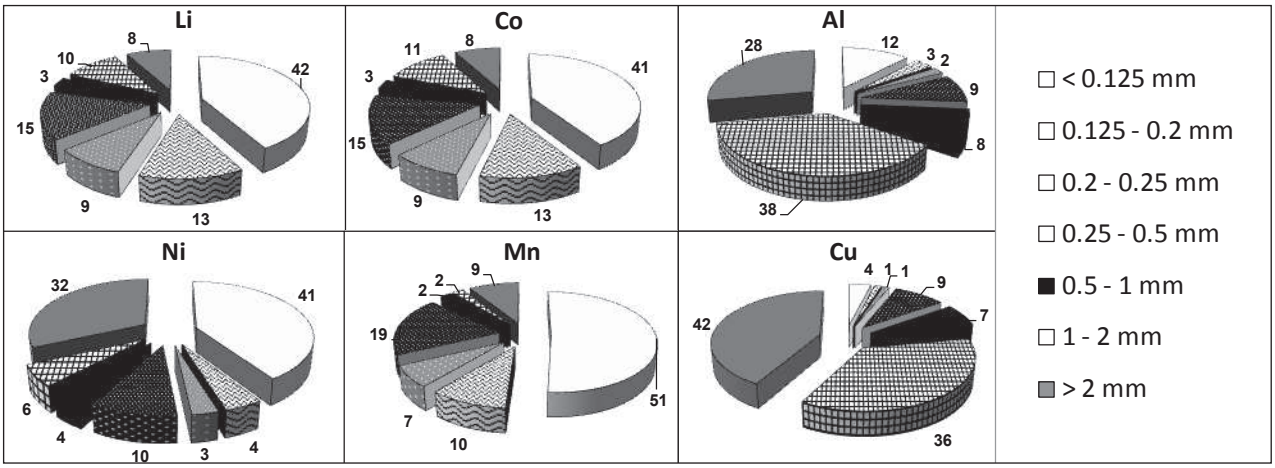

Fig. 1 Distribution of all investigated metals

2.3.2 Leaching

Metal extraction yields obtained using HCl are reported in Table 1: temperature (changing from 30 to 90°C) and acid amount (changing from 1.5 to 2.0 g of acid per gram of electrodic powder) exhibit significant effects (95% significance level) [16] only for Al, Co and Fe as evidenced in Fig. 2. In particular analysis of variance shows:

- positive effect of temperature (A factor) on Al and Co extraction;
- negative effect of acid concentration (B factor) on Co extraction;
- positive effect of the interaction temperature-acid concentration (AB) on Co and Fe yields.

Li extraction is not significantly affected in the range of operating conditions considered here, while Co extraction yield is maximized working at the high level of temperature and the low level of acid. According to these findings acid concentration could be used at the lower level in order to save reagents and minimize Fe extraction, which is an impurity. In these preliminary optimized

conditions (90°C, 1.5 g HCl per g of solid) acid leaching using HCl is able to extract quantitatively Co, Li, Ni, Mn, Al and Cu (see Table 1).

T (°C)	[HCl] (g/g_{powder})	Treatments	Al	Co	Cu	Fe	Li	Mn	Ni
30	1.5	1	99	98	100	100	88	72	100
			98	95	98	100	97	100	99
90	1.5	a	100	100	100	58	99	100	100
			100	98	98	79	99	100	100
30	2.0	b	99	58	99	100	88	93	100
			98	48	98	91	76	61	99
90	2.0	ab	100	98	100	100	95	96	100
			99	98	99	100	98	100	100

Table 1: Metal extraction yields (%) using HCl in a full factorial design replicated twice (A: temperature, B:HCl concentratiion, s/l ratio = 10)

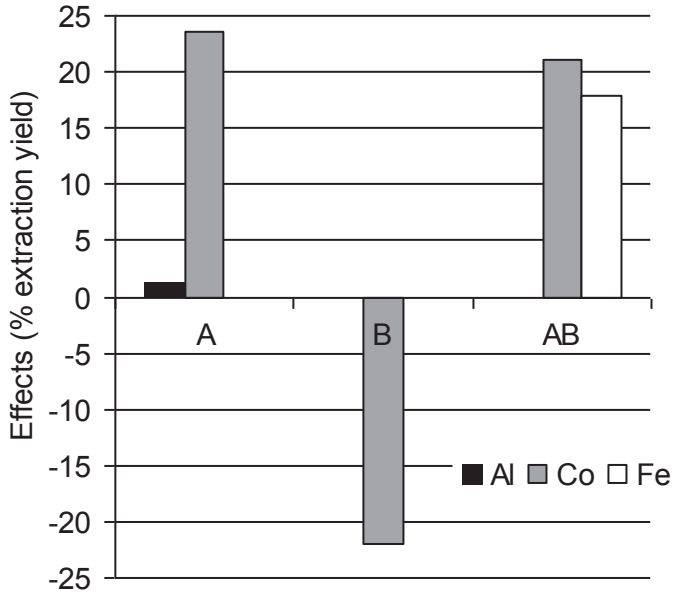

Fig. 2: Estimates of significant effect on metal extraction yield (%) for acid leaching with HCl: A) temperature; B) HCl concentration (Solid-liquid ratio 10)

Preliminary tests (not reported here) using only H_2SO_4 to leach the input material show that the acid without reducing agents does not extract quantitatively both Co and Li: at 90°C extraction yields were lower than 50% and 80% for Co and Li, respectively). In presence of a reducing agent Co(III) is reduced to Co(II) and extraction yields arrive to values higher than 90%. Based on these results a factorial design is arranged for H_2SO_4 considering the effect of three factors (A: temperature; B: acid concentration; C: glucose stoichiometric excess) (see Table 2 for the complete list of treatments of this factorial design).

Extraction yields in acid-reducing conditions (H_2SO_4 plus glucose) are listed in Table 2, while the estimates of significant effects (95% significance level) are reported in Figure 3.

Table 2: Metal extraction yields (%) using H_2SO_4 in a full factorial design replicated twice (A:temperature; B:H2SO4 concentration; C:stoichiometric excess of reducing agent, s/l ratio = 10)

T (°C)	[H_2SO_4] (g/g_{powder})	[glu] (% exc)	Treatments	Al	Co	Cu	Fe	Li	Mn	Ni
30	2.0	50	1	75	48	38	70	77	67	97
				70	51	51	75	77	62	97
90	2.0	50	a	99	97	98	89	98	100	100
				98	98	99	90	99	100	100
30	2.5	50	b	89	82	79	85	90	87	98
				72	64	55	39	77	67	96
90	2.5	50	ab	99	98	97	31	98	100	100
				99	97	97	28	98	100	99
30	2.0	100	c	74	64	54	64	79	73	96
				75	61	59	72	77	71	96
90	2.0	100	ac	97	94	87	84	98	100	100
				98	96	89	85	98	100	100
30	2.5	100	bc	98	97	97	90	98	100	99
				99	93	98	88	98	100	100
90	2.5	100	abc	64	33	28	43	67	64	95
				70	51	54	27	77	73	97

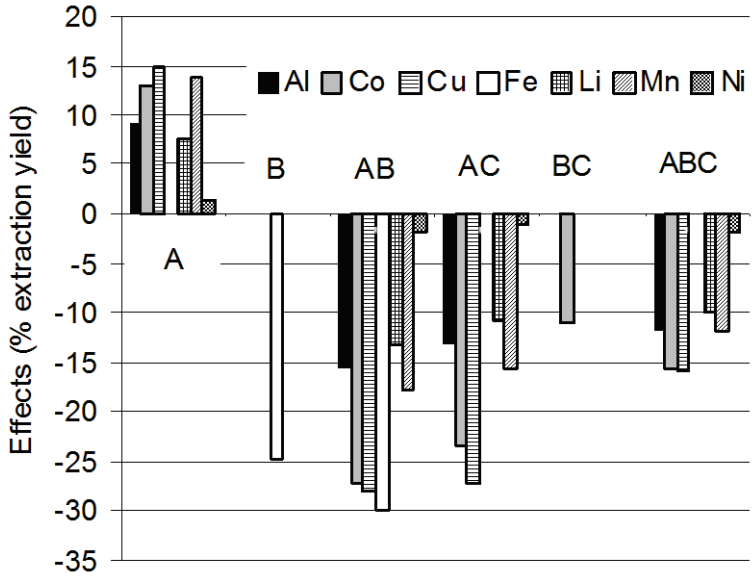

Fig. 3: Estimates of significant effect on metal extraction yield (%) for acid reducing leaching with H_2SO_4: A) temperature; B) H_2SO_4 concentration; C) reducing agent concentration (Solid-liquid ratio 10)

Analysis of variance shows that only temperature (factor A) has a positive effect on all metals (except Fe), while the other factors and their interactions negatively affect metal extractions. According to these data, preliminary optimized conditions for acid-reducing leaching are 90°C, 2 g of H2SO4 for each gram of solid and 50% of stoichiometric excess of reducing agent. These data confirm the efficiency of carbohydrates as reducing agent in leaching processes, as already verified for the leaching of electrodic powder from alkaline and Zn-C batteries [15].

The effect of solid-liquid ratio (solid concentration) is evaluated performing leaching experiments with sulphuric acid (90°C, 2 g of H2SO4 for each gram of solid and 50% of stoichiometric excess of reducing agent) varying the weight of treated solid. Experimental results reported in Figure 4 show that increasing the solid concentration from 100 to 200 g/L determines a 10% decrease of both cobalt and lithium extractive yields.

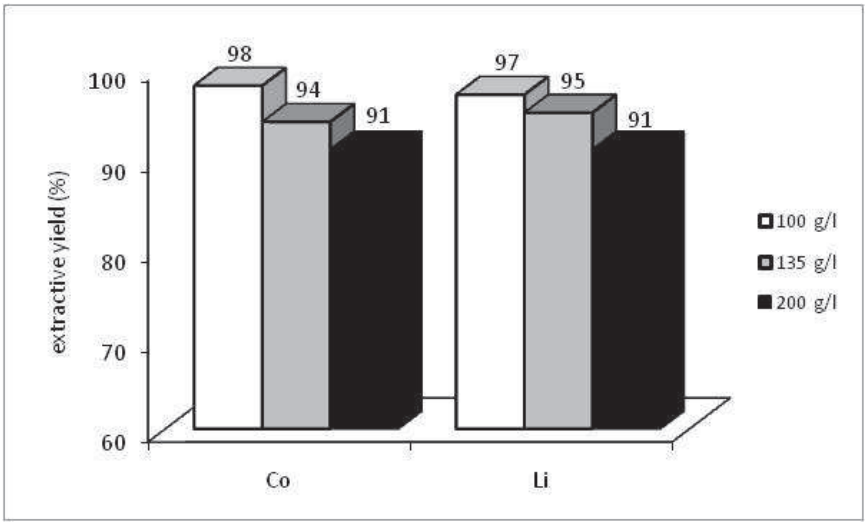

Fig. 4: Effect of solid-liquid ratio (leaching conditions: 90°C, 2 g of H_2SO_4 for each gram of solid and 50% of stoichiometric excess of reducing agent).

Anyway operating in large scale plants this decrease could be negligible compared with the reduction of leaching reactor volume obtainable by increasing the solid-liquid ratio.

2.3.3 Primary purification: chemical precipitation

Leach liquor composition obtained in optimized conditions using acid-reducing leaching (90°C, 2 g of H2SO4 for each gram of solid, and 50% of stoichiometric excess of reducing agent) is: 50 g/L of Co, 10 g/L of Li, 7 g/L of Al, 5 g/L of Ni, 2 g/L of Fe, 3 g/L of Cu, 1.5 g/L of Mn. Primary purification determines the removal of metal impurities and, in particular, complete removal of iron and aluminum, and 60% removal of copper.

2.3.4 Secondary purification: solvent extraction

Solvent extraction is performed testing the selectivity of two extractants, D2EHPA and CYANEX 272, on leach liquors after primary purification. Solvent extraction operation aims to separate cobalt from nickel in order to recover high purity cobalt products.

Metal extraction occurs according to the following mechanism [19]:

$$M_{Aq}^{2+} + A_{Org}^{-} + 2(HA)_{2Org.} \rightarrow MA_2 \cdot 3HA_{Org.} + H_{Aq}^{+} \qquad (2)$$

where $A_{Org}^{-} + 2(HA)_{2Org}$ represents the extractant saponified by the following reaction:

$$Na_{Aq}^{+} + 1/2(HA)_{2Org} \rightarrow NaA_{Org} + H_{Aq}^{+} \quad (3)$$

The efficiency of metal extraction was evaluated by the distribution coefficient of metal in aqueous and organic phase

$$D_{Co} = \frac{[Co]_{org}}{[Co]_{aq}} \quad (4)$$

$$D_{Ni} = \frac{[Ni]_{org}}{[Ni]_{aq}} \quad (5)$$

where metal concentration in organic phase is determined by a mass balance considering the residual concentration in aqueous phase.

An index of the extraction selectivity (β) can be then evaluated considering Ni as the main competitor of Co during solvent extraction

$$\beta = \frac{D_{Co}}{D_{Ni}} \quad (6)$$

Experimental results showed that for both extractants (D2HEPA and CYANEX 272) the minimum stoichiometric ratio (moles of extractant per moles of cobalt) which is necessary to extract quantitatively cobalt was 4 (fig. 5a, 5b). Increasing D2HEPA amount above this value, all the investigated metals were extracted simultaneously, while increasing CYANEX 272 nickel started to be significantly extracted only after cobalt extraction is complete. This result denoted the higher selectivity of CYANEX 272 for Co with respect to D2HEPA as confirmed by the trend of the selectivity coefficient reported in fig. 6a.

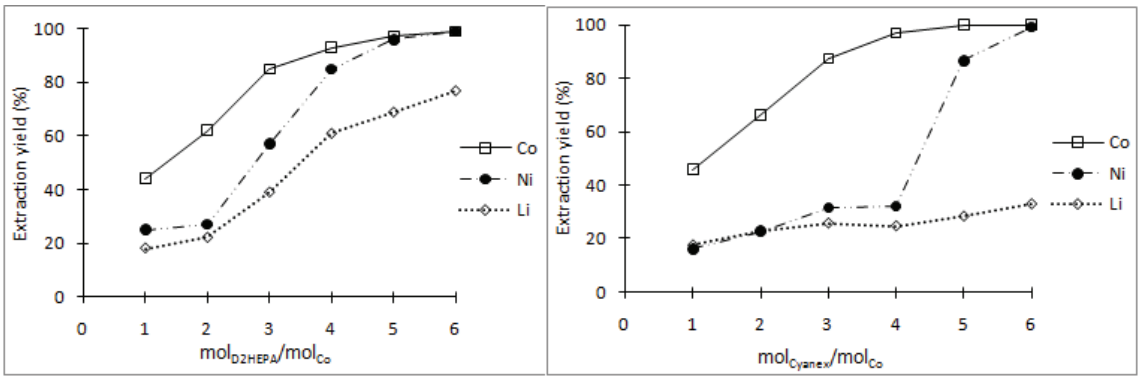

Fig.5: Effect of stoichiometry on the extraction with D2EHPA (a) and Cyanex 272 (b) at pH 5.5

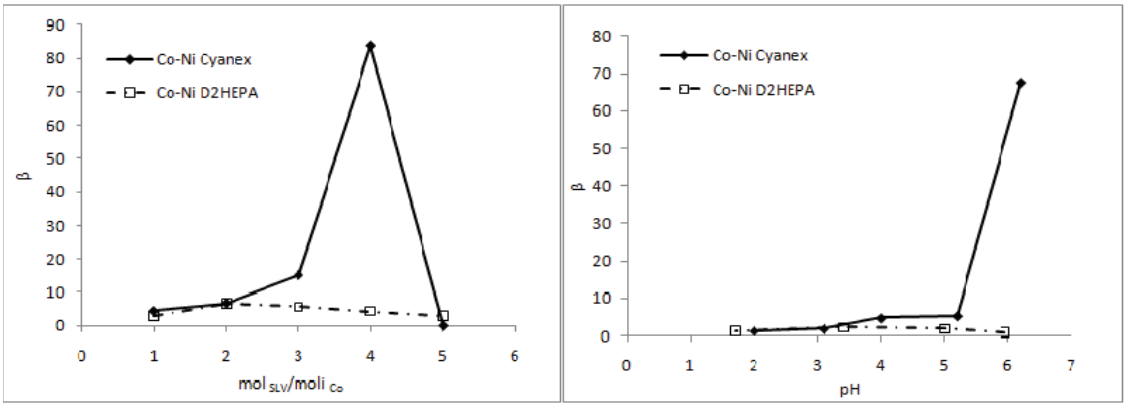

Fig.6: Selectivity index for Ni-Co separation versus stoichiometry (a) and versus pH (b).

As for the effect of pH (fixing the stoichiometric ratio at 4) it was found that optimal pH value to have a quantitative extraction of cobalt was 6 for both extractants (fig 7a, 7b). Further increase of pH determined Co and Ni precipitation. Analyzing the selectivity coefficient versus pH (fig. 6b) it is evident that CYANEX 272 is significantly better that D2HEPA for Co-Ni separation.

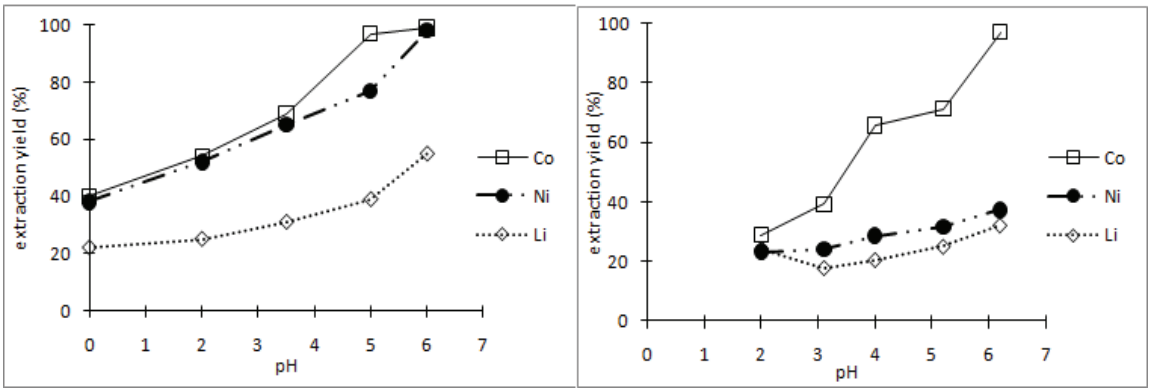

Fig.7: Effect of pH on the extraction with D2EHPA (a) and Cyanex 272 (b) (stoichiometric ratio = 4 mol_{SLV}/mol_{Co})

Stripping tests were performed to re-extract cobalt in aqueous phase. Experimental results showed that cobalt can be quantitatively re-extracted by using 1:1 v/v of 4 M H_2SO_4 solution.

2.3.5 Product recovery

Cobalt is recovered as carbonate (98% yield) from both solutions (primary and secondary purification). Co carbonate recovered after secondary purification has a cobalt content of about 47%w/w, while carbonate recovered after primary purification had 36-37%w/w Co content. These data show that only performing solvent extraction it is possible to have a product satisfying the commercial standard required for this chemical (45-47%w/w of Co content).

Lithium is recovered as carbonate with a yield of 80% and with a purity higher than 98% by evaporation of 80% of water volume.

2.3.6 Process simulations

Process simulations consisted in mass and energy balances for the two process routes reported in Figure 8 which differ for the presence or not of secondary purification by solvent extraction.

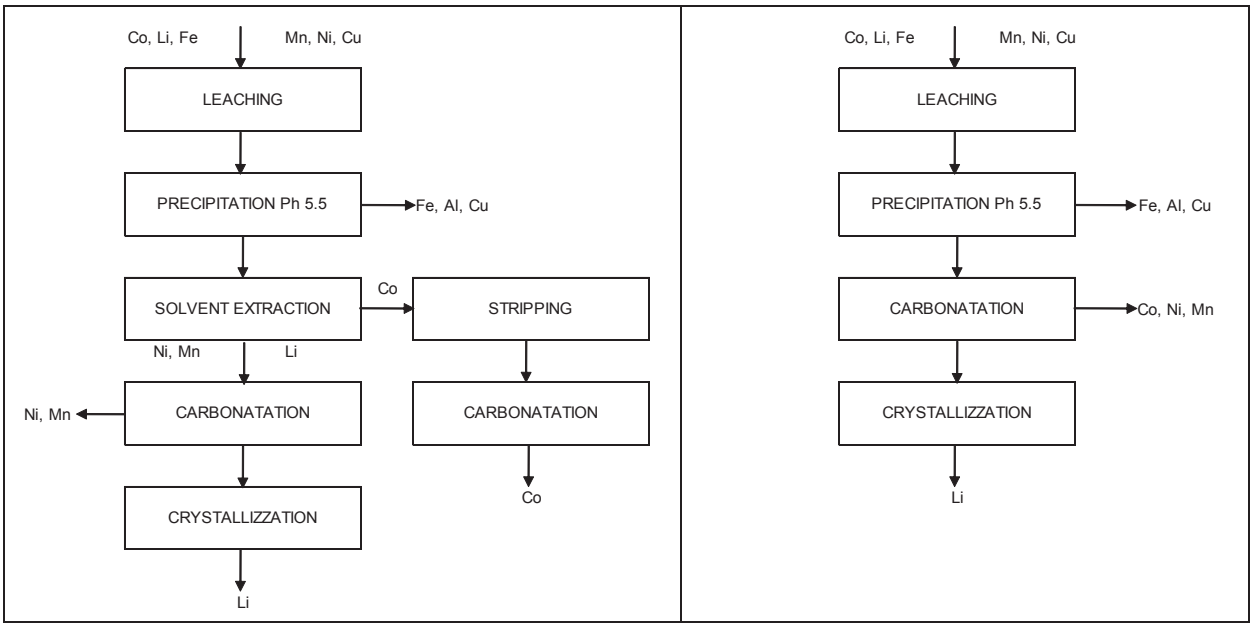

Fig. 8: Simulated flowcharts

Simulation were performed by a dedicated software (Super Pro Design) using as input data the lab-scale results obtained for leaching, purification (only primary or both primary and secondary) and recovery operations as detailed before. In particular yields of operation (leaching, purifications, product recovery), consumption of chemicals, energy requirements, and operation scheduling are estimated for each units according to experimental data reported above. Other economic parameters (cost of materials, utilities, waste treatment, process potentiality, equipment characteristics) are fixed as reported in Table 3. Cost of raw materials is taken from sellers, while the selling prices of high purity products ($CoCO_3$ and Li_2CO_3) are taken from the International market of chemicals (Table 3). Costs of the mechanical pre-treatment section are not included in simulations and then they should be used only for comparison among the two different process routes considered here (with and without solvent extraction).

Table 3: Main inputs and outputs of process simulations

	AMOUNT PURCHASED OR SOLD (t/y)	COSTS FOR PROCESS WITH SOLVENT EXTRACTION ($)	COSTS FOR PROCESS WITHOUT SOLVENT EXTRACTION ($)
Processed powder	100-250	500 t^{-1}	500 t^{-1}
$CoCO_3$ selling price	110-560	45000 t^{-1}	5000-18000 t^{-1}
Li_2CO_3 selling price	18-50	5000 t^{-1}	5000 t^{-1}
Solvent purchasing price	1.5-3.2	35000 t^{-1}	-
H_2SO_4 purchasing price	180-500	70 t^{-1}	70 t^{-1}
Na_2CO_3 purchasing price	100-275	50 t^{-1}	50 t^{-1}
Water	265-675	20 t^{-1}	20 t^{-1}
Electricity		0.20 $(kWh)^{-1}$	0.20 $(kWh)^{-1}$
Wastewater treatment		50 t^{-1}	50 t^{-1}
Solid waste disposal	40-120	100 t^{-1}	100 t^{-1}
Total Operating Cost		1542000-2127000 y^{-1}	1301000-1550000 y^{-1}
Total equipments		2300000-4000000	1500000-2300000
Total Capital Investment		2500000-4500000	1500000-2500000

Once all input parameters have been chosen, mass and energy balances are obtained for the two process options along with other technical (equipment size and chemical and energy consumption) and economical outputs such as:

- total capital investment,
- operating costs,
- Total Revenues
- gross margin (%) = Total Revenues-Operating Cost)/Total Revenues *100
- payback time (the time necessary to balance the investment by the total revenues)

Simulations are performed considering

- the effect of the input flow rate for both processes (with and without solvent extraction)
- the effect of the selling price of low purity CoCO3 obtained without solvent extraction.

As for the first point: simulations are performed for different input flow rates in order to under stand the minimum amount of waste which should be processed to have a feasible process. Input amounts are based on real amounts of spent batteries which were collected in Italy in 2008. In particular, the chosen amount 100, 185 and 250 t/y of input material correspond to the 20, 37 and 50% of the total collected wastes, respectively. Input material of the leaching section is about 50% in weight of the initial waste before physical pretreatment (experimental data not reported here).
As for the second point: since the international market of chemicals does not give any selling price for low purity CoCO3 obtained without solvent extraction, several simulations are carried out for different selling prices of this product (from 10 to 18 $/kg). The aim of these simulations is to understand for which selling price of low purity CoCO3, the processes with and without solvent extraction give the same economical outputs (i.e. gross margin and payback time).
Process simulations show that for both processes the economical benefits (gross margin and payback time) are proportional to the input flow rate of treated wastes (see Figure 9a for the process with solvent extraction and data reported in Table 4 for the process without solvent extraction). The diffusion of this kind of plants can be then favored by promoting collection strategies.

Table 4: Process simulations for the option without solvent extraction

Processed Powder (t/y)	$CoCO_3$ selling Price ($/kg)	Total Capital Investment ($)	Operating Costs ($/y)	Total Revenues ($/y)	Gross Margin (%)	Return of Investment (%)	Payback Time (y)
100	7.5	1687000	1301000	1025000	-	-	12
185	7.5	2398000	1480000	1896000	22	19.1	5.2
250	7.5	2570000	1550000	2562000	39.5	39.5	3.1
100	10	1687000	1301000	1305000	3.0	8.7	8.7
185	10	2398000	1480000	2414000	38.7	32.1	3.1
250	10	2570000	1550000	3262000	52.5	48.7	2.1
100	18	1687000	1301000	2200000	40.9	40.6	2.4
185	18	2400000	1480000	4070000	63.4	73.2	1.4
250	18	2570000	1550000	5500000	71.5	100	1.0

Process simulations also show that the total investment for the process including solvent extraction is significantly higher than that without solvent extraction (Table 3).

As for the effect of selling price of low purity CoCO3, fixing this price at 18 $/kg and feeding the hydrometallurgical section with at least 250 t/y of electrodic powder both processes reach the same economical benefits (see gross margin and payback time obtained in these conditions for both processes in Figures 9). If either the selling price of low purity CoCO3 or the input flow rate of wastes decrease (i.e. price < 18 $/kg or feed flow rate <250 t/y), the economical outputs without solvent extraction become worst than those with solvent extraction.

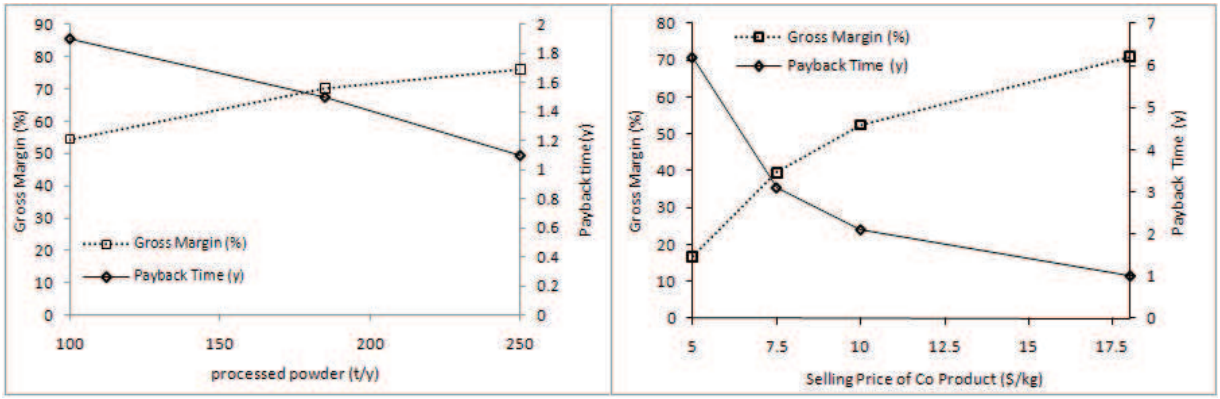

Fig. 9: Main economical results for the process analysis with solvent extraction (a) and without solvent extraction (b) for several sell prices of $CoCO_3$ (input flowrate: 250 t/y)

2.4. Conclusions

In this paper two hydrometallurgical processes to recover lithium and cobalt from lithium ion batteries were analyzed. Co and Li were extracted from an input material coming from a large scale mechanical route of pre-treatment of a recycling plant in the Northern Italy. This powder was successfully leached using 2g/g of sulphuric acid in the presence of an excess of 50 % of a reducing agent as glucose, which could be also a waste of food factory. Iron, aluminum and copper (partially) were removed by precipitation as hydroxides at pH 5.0. When solvent extraction was performed high purity cobalt carbonate (47%w/w of cobalt) was obtained by precipitation. Performing the same operation without solvent extraction a product containing 36-37%w/w of Co was obtained.

Lithium was recovered by crystallization (yield 80%) with 98% purity. Solvent extraction allows to obtain high purity products but this operation is one of the most expensive in hydrometallurgical processes. Process simulations showed that, for the same input flow rate, process with solvent extraction gives economical outputs (gross margin and payback time) which are better than those for the process without solvent extraction. Processes present the same economical indices for a feed flow rate of at least 250 t/y if low purity cobalt carbonate (produced without solvent extraction) could be sold at 18 $/kg.

References

[1] A.M. Bernardes, D.C.R. Espinosa, J.A.S. Tenório, J. Power Sources 130 (2004) 291–298.
[2] P.V.D. Bossche, The current legislative development in the EU waste policy: challenge or opportunities for metal industry, Cobalt Development Institute, January 2006.
[3] S.M. Shin, N.H. Kim, J.S. Sohn, D.H. Yang and Y.H. Kim, Hydrometallurgy 79 (2005), 172–181.
[4] G. Dorella, M. B. Mansur, J. Power Sources 170 (2007), 210–215.
[5] B. Swain, J. Jeong, J.C Lee, G.H Lee, J.S Sohn, J. Power Sources 167 (2007), 536–544.
[6] D. A. Ferreira, L. M. Zimmer Prados, D. Majuste, M. B. Mansur, J. Power Sources 187 (2009), 238–246.

[7] L. Li, J. Ge, F. Wu, R. Chen, S. Chen, B. Wu, J. Haz. Materials 176 (2010), 288–293.
[8] J.S. Sohn, D.H. Yang, S.M. Shin, N.H. Kim, H.T. Sohn, in: K.I. Rhee, J.K. Oh (Eds.), Proceedings of the International Symposium on Green Technology for Resources and Material Recycling, November 24–27, 2004, Seoul, Korea, 316–320.
[9] P. Zhang, T. Yokoyama, O. Itabashi, T.M. Suzuki, K. Inoue, Hydrometallurgy 47 (1998) 259–271.
[10] M. Contestabile, S. Panero and B. Scrosati, J. Power Sources 92 (2001), 65–69.
[11] S. Castillo, F. Ansart, C. Laberty-Robert and J. Portal, J. Power Sources 112 (2002), 247–254.
[12] J.F. Paulino, N.G. Busnardo, J. C. Afonso, J. Haz. Materials 150 (2008) 843-849.
[13] C.K. Lee and K.I. Rhee, Hydrometallurgy 68 (2003), 5–10.
[14] J. Nan, D. Han and X. Zuo, J. Power Sources 152 (2005), 278–284.
[15] G. Furlani, E. Moscardini, F. Pagnanelli, F. Ferella, F. Vegliò, L. Toro, Hydrometallurgy 99 (2009) 115–118.
[16] D.C. Montgomery, Design and Analysis of Experiments, 4th edition, John Wiley & Sons, New York (1997).
[17] K. Sarangi, B.R. Reddy, R.P. Das, Hydrometallurgy 52 (3) (1999) 253–265.
[18] S.K. Sahu, A. Agrawal, B.D. Pandey, V. Kumar, Miner. Eng. 17 (2004) 949–951.
[19] B. Swain, J. Jeonga, J.C Lee, G.H Lee, Sep. Purif. Technol. 63 (2008) 360–369

3. Valorization of nickel metal hydride batteries

A process to valorize wastes from nickel metal hydride batteries has been developed at first studying the physical operation required to dismantle the spent devices and then focusing on the hydrometallurgical operations necessary to recover valuable metals from the electronic poweder.

As better explained below, since the most difficult operation of the process was the separation between cobalt, nickel and manganese which are contained in this kind of devices, a well structured way of solvent extraction for their separation has been optimized. The obtained results for both the hydrometallurgical physical routes suggested the possibility to study an unique way of treatment for nickel metal hydride, lithium ion and nickel metal hydride batteries. As follows resulted in a paper: "MECHANICAL PRETREATMENT ROUTES AND SOLVENT EXTRACTION PROCEDURES TO RECOVER MATTER FROM NICKEL METAL HYDRIDE, LITHIUM ION AND PRIMARY LITHIUM BATTERIES".

3.1 Introduction

Both technological innovation and market expansion lead to a dramatic increase in the production of electric and electronic equipments, such as mobile phones, computers, cameras, and consequently batteries.

According to the European Guideline, 2006/66/EC [1] which aims to minimize the environmental impact of spent batteries, their waste and battery productive process, in the next years several goals must be achieved about collection and recycling. In particular 25% of spent devices must be collected by September 2012 and 45% by September 2016. Moreover the guideline established that recycling processes of batteries must ensure to achieve at least a 50% of recycling by average weight.

To solve the environmental problems related to batteries and their waste, researchers in relevant fields have carried out some studies [2] and it seems urgent to develop economically and environmentally sound processes for their recycling. Moreover, since waste batteries contain considerable amounts of valuable materials, recycling processes become important subjects, even considring all possible economical benefits for investors in this field. Economical benefits are related to the possibility of both selling all recovered products and earning public money just by the activity of collecting and recycling [3]. In this context even if some kinds of batteries do not contain metals much suitable to be sold, there is anyway a high interest about their recycling.

In the current literature there are many works concerning the hydrometallurgical treatment of batteries and accumulators. Most of them focused on the treatment of a single-type of devices such as Li-Ion [4-6] and NiMH accumulators [7-10]. Important reviews summarizing the technologic advances about battery recycling have been also published [11,12].

In addition only few researchers focused on the recycling of primary lithium batteries [13] and this could be due to the more hazardous and less valuable substances such as Li and Mn, contained in this kind of devices [14].

Many authors mainly focused on leaching investigations and they found up the required operating conditions to dissolve all metals from the electrodic powders. Anyway most works were performed by preliminary manual dismantling of samples in a lab-scale without considering the upstream operations of dismantling [15-24] and this choice could affect the representativity of final powders. Moreover, in order to develop a complete process, this choice doesn't take into account that sometimes a preliminary operation of sorting can be expensive and it must be specifically developed in the desired scale.

Rufino et al. [25] developed a pre-treatment route to treat more kinds of batteries working on battery samples of the order of 400 kg which can be considered as representative of real wastes.

They proposed a mechanical route to treat spent batteries but they didn't focus on the real possibility to further recover metals from obtained fractions. In fact in order to satisfy the European Guideline by recycling at least the 50% of batteries by average weight, a chemical treatment of electrodic powders must be included in every eventual process. For this purpose it's important to obtain a fine fraction having a composition which allows all required separations by chemical operations. In this scenario the aim of this work was:

- To develop mechanical routes for the treatment of NiMH, Li-Ion and primary lithium batteries evaluating also the technical feasibility of a unique pre-treatment route for a mixture of these batteries in order to obtain a fine fraction enriched in valuable metals (Co, Ni, Mn).
- To optimize the chemical separation of metals extracted from this fine fraction as a function of the feed composition. By this way we can predict the optimal chemical route to recover metals depending on the feed composition of battery wastes.

Primary lithium batteries, Li-Ion and NiMH accumulators were treated by the same mechanical route and different fractions (ferrous metals, non ferrous metals, electrodic powders) were obtained and characterized. Based on the compositions of fine fractions, several leach liquors were formulated to simulate real solutions coming from a leaching of different mixtures of powders. Therefore a solvent extraction procedure has been developed to separate Ni, Co and Mn from these solutions.

Novelty aspects:

- An unique pre-treatment route for spent primary lithium, Li-ion, and NiMH batteries
- All mechanical routes have been developed in a medium scale in order to obtain waste fractions which are representative of what achievable in large scale.
- The treatment of Primary lithium batteries which haven't been investigated yet from this point of view.
- Correlation between purification scheme and upstream feed composition.

Even if NiMH batteries are known to contain valuable substances like rare earths (10-15% by battery average weight) we've preliminary focused our attention only on Mn, Co and Ni, because rare earths separation has been already studied and it appears easily performable. Mass balances obtained by this work will better explain which fractions need to be recovered in order to accomplish the European Guideline as minimum recycling of batteries

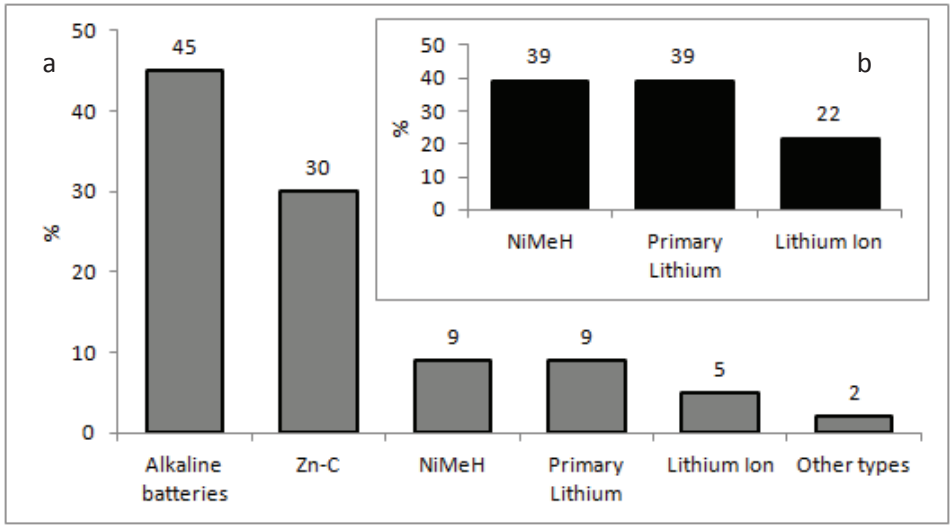

Fig.1a: Statistics of sampling considering all kind of spent portable devices

Fig.1b:Statistics considering only nickel metal hydride, lithium ion and primary lithium batteries

3.2 Material and methods

Material

Around 100 tonnes of portable batteries were collected by S.E.Val. s.r.l. between March 2009 and March 2010. In the same period a total amount of 3 tonnes of batteries was classified in three times, (1 ton for each time) in order to find the input composition and its variability in a year. Results of classification are listed in fig. 1. Once composition was determined, 50 kg of each kind of devices were thoroughly mixed by the ring and cone method and quartered three times in order to get a more representative sample., NiMH, Li-Ion and primary lithium batteries used in this work were drawn from these samples.

All metal salts ($CoSO_4 \bullet 7H_2O$, $NiSO_4 \bullet 6H_2O$, $MnSO_4$) and other chemicals such as HCl (37%), HNO_3 (65%), H_2O_2 (40%$_{w/v}$), H_2SO_4 (96%), and NaOH, used for the experiments were bought by Sigma-Aldrich as reagent grades. The extractant Cyanex 272 was supplied by Cytec USA corporation and it was used without further purification. Low boiling point kerosene (180–270 °C) was used as diluents. All reagents were used without further purification.

Analysis for metal determinations were performed by a Inductively Coupled Plasma Optical Emission Spectrometer (Varian Vista-MPX Simultaneous CCD)**.**

Mechanical treatment tests

All thermal treatments performed in this work were made at 300 °C in a silite furnace. Whereas there was the possibility of explosions the treatments were carried out using a steel vessel as container able to afford all possible explosions and a nitrogen atmosphere was used in order to reduce the sharp oxidation of residual metallic lithium with the air.

Crushing operations were carried out in a two blade rotors crusher (DR120/360 9.2 kW_9/5) without any controlling sieve and in a hammer crusher (ŠK 600 7.5 kW) using a 5 mm sieve. A sieving operation (1 mm) allowed the separation of a fine powders (electrodic poweders) from larger fractions mainly containing pieces of metals. The powders (< 1 mm) were used for chemical tests whilst the larger fractions were sent to further separating operations. Therefore magnetic metals, non ferrous metals and non metals were separated by an Eddy Current Separator with a mobile splitter (EPA SKR-22). All initial, intermediate and final fractions were weighed in order to evaluate the performances of all operations and the weight loss. Hence, based on these results a final mass balance has been obtained.

Laboratory test

The electrodic powders (< 1mm) obtained by mechanical treatments were characterized by acid digestions with HCl-HNO_3 3:1 at room temperature for 4 hours and at 130°C for 2 hours after adding 10%$_{v/v}$ of hydrogen peroxide (40%$_{w/v}$). The resulting solutions, after filtration were analyzed by ICP-OES to evaluate the metal composition.

Cyanex 272 and D2HEPA were dissolved in kerosene and they were partially saponified (65%) by adding a NaOH solution (5 M) under stirring [26,27] and in some tests even adding a phase modifier (TBP, 5 vol.%). 10 ml of solutions were shacked for 5 minutes with a half volume of extractant, and then with another half volume till to reach an equal volume organic-aqueous (O/A). Volumes were kept constant whilst different concentrations of extractants were prepared to investigate the stoichiometric ratio extractant/[Me^{n+}] = 1-4. The two phases were separated by a separating funnel and the pH values of the aqueous solutions were adjusted by the addition of NaOH or H_2SO_4 solution in the range 2-6. All experiments were performed at room temperature (25±1°C). Aqueous raffinates were analyzed by ICP-OES to determine the amount of extracted cobalt, manganese, and nickel.

Stripping tests for metal recovery from organic phase were carried out by using 4 M H_2SO_4 solution, at 25±1 °C.

3.3 Results

3.3.1 Mechanical Routes

Mechanical operations were required since the metallic elements are covered with or encapsulated by plastic or iron shell [28] and by them we separated the electrodic powders contained in the devices aiming to maximize the final mass recovery.

The Flowsheets of developed mechanical routes to treat NiMH, Li-Ion and primary lithium batteries, are listed respectively in figures 2, 3 and 4. These flowsheets contain also the mass balances of every operations as percentage of fractions (the percentages in brackets are referred to the total initial mass of samples). Whereas the total percentage in bracket wasn't one hundred the difference must be considered as weight loss.

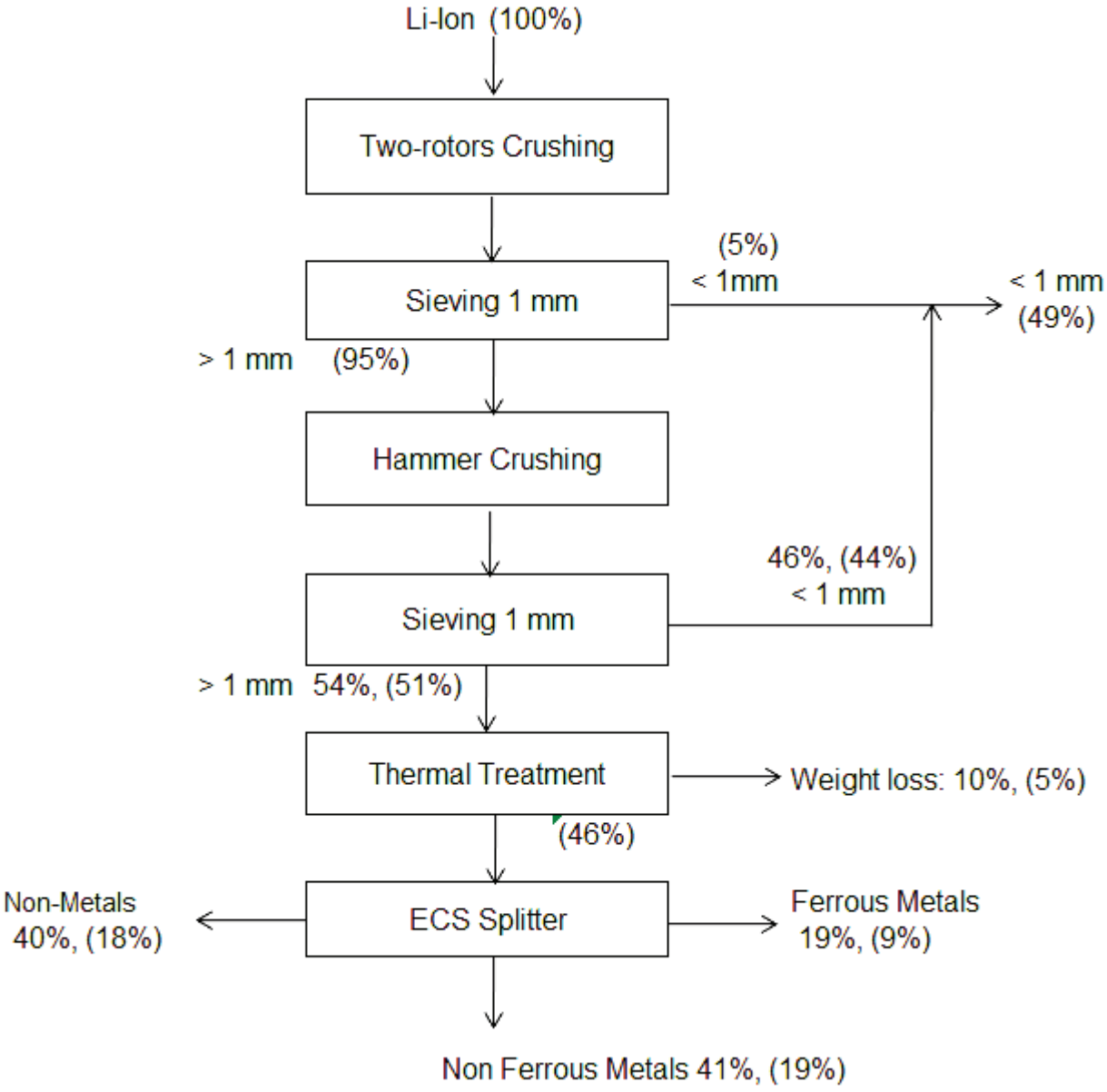

Fig. 2: mechanical route to treat spent Li-Ion batteries

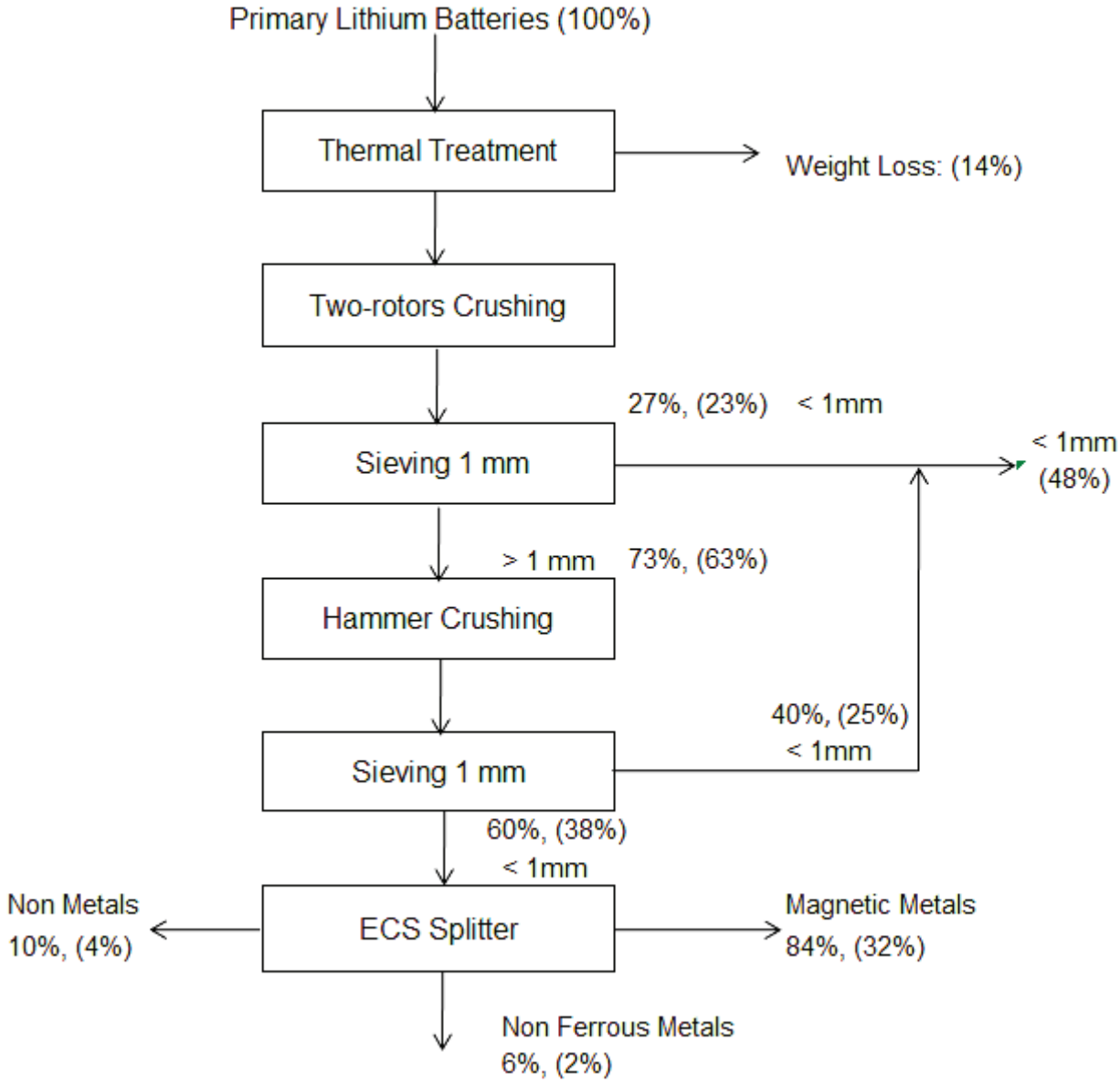

Fig.3: mechanical route to treat Primary Lithium Batteries

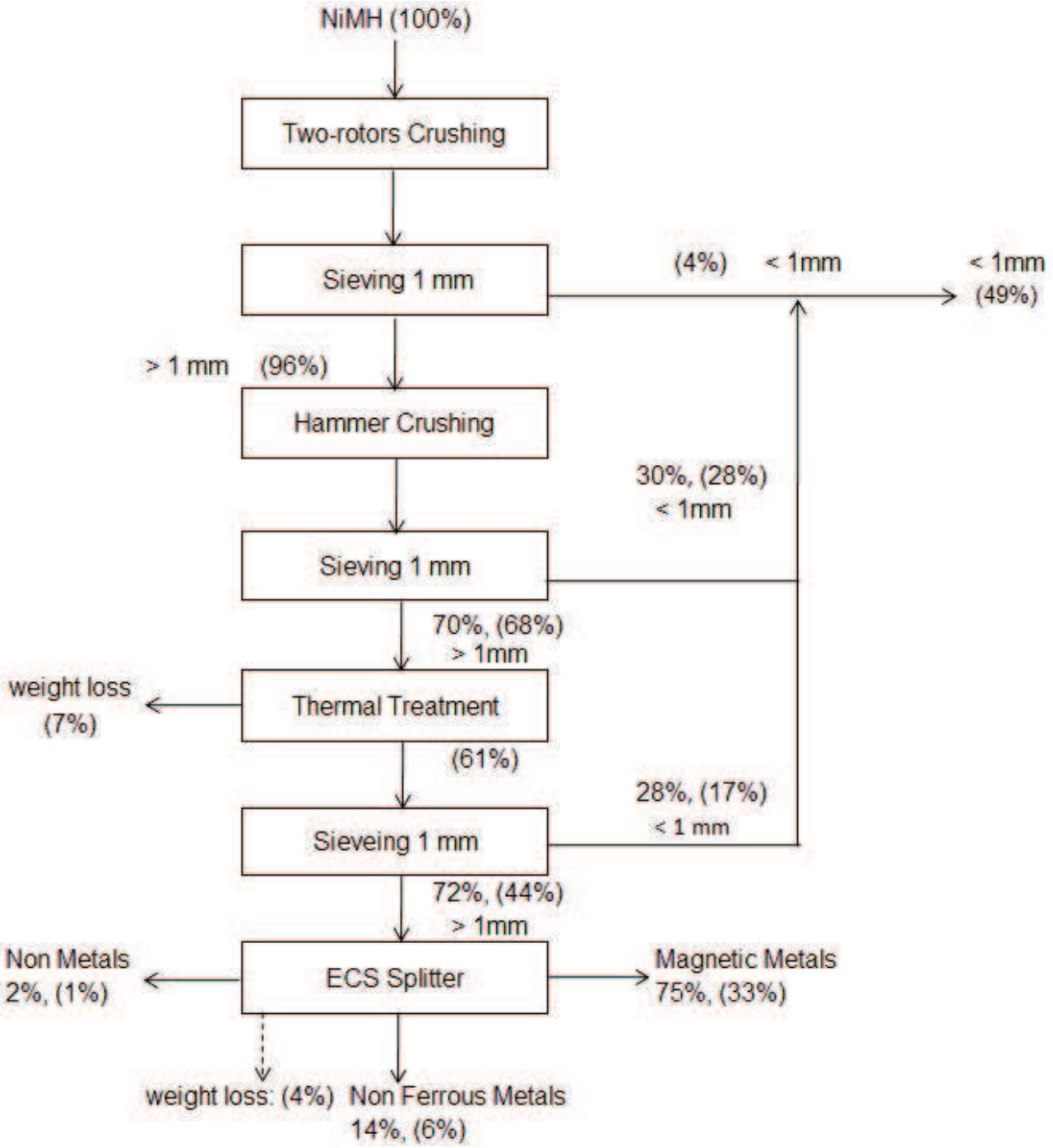

Fig. 4: mechanical route to treat NiMH batteries

As can be seen the central parts of all developed mechanical routes included two operations of crushing and two operations of sieving (1 mm). Hence taking as reference factor the amount of recovered electrodic powder, the performances of a double crushing by a two blade rotor crusher were compared with those of a crushing by a two blade rotor crusher followed by a hammer crushing. Results of this investigation (listed in table 1 as percentage of total mass of samples), showed that hammer crushing was able to maximize the recovery of electrodic powders.

Table 1: Powder recovered after size reduction operations

Input devices	Double Crushing by two blade rotors crusher [%]	Double crushing by two blade rotors and hammer crushing [%]
Primary lithium batteries	37	48
Li-Ion batteries	21	49
NiMH batteries	28	49

The metal content for all characterized powders is listed in table 2:

The metal compositions of all characterized powders recovered by mechanical operations are listed in table 2.

Table 2: composition of powders resulting from mechanical treatments

	Al [%]	**Co** [%]	**Cu** [%]	**Fe** [%]	**Li** [%]	**Mn** [%]	**Ni** [%]
Li-Ion batteries	5 ± 2	25 ± 3	0.2 ± 0.1	3.5 ± 0.5	3.5 ± 0.5	1.5 ± 0.3	6 ± 2
Primary lithium batteries	0.8 ± 0.2	< 0.01	0.08 ± 0.04	3.0 ± 0.5	5.5 ± 0.5	37 ± 1	0.12 ± 0.01
NiMH batteries	0.15 ± 0.01	1.5 ± 0.07	0.5 ± 0.2	1 ± 0.2	< 0.01	3.8 ± 0.2	22 ± 3

It must be observed that NiMH electrodic powder contained also 3.1 ± 0.5% of Ce 6.5 ± 0.7% of La and 4.5 ± 0.5% of Nd.

Developed mechanical routes allowed to recover as valuable fractions (ferrous metals, non ferrous metals and non metals) around 40% of NiMH batteries, 46% of Li-Ion batteries and 38% of primary lithium batteries. These results implies that a hydrometallurgical treatment of electrodic powders obtained by mechanical operations must be carried out in order to reach the 50% of recycling fixed by European Guideline 66/2006 by recovering the most significant components as valuable products.

Since the "cores" of developed mechanical routes were similar each others as types of operations, the technical feasibility of a single mechanical route have been investigated by using as input stream a mixture of spent NiMH-Li Ion-Primary Lithium batteries having the same composition we had found in our sampling in real scale. By this choice several advantages have been observed. For instances by the same operation there was a qualitative "dilution" of the explosive power of lithium and also the concurrent combustion of lighter fractions like papers and the dielectric materials which can cause problems during the ECS separation. In spite of these advantages, by performing only one route, it wasn't possible to recover the plastic fractions by ECS because they

were burnt during the preliminary thermal treatment but this aspect could be improved by a further investigation. This “unique route” is showed in figure 5 with all mass balances.
Since the core of developed mechanical routes is similar each other as types of operations, the technical feasibility of a single mechanical route have been investigated using as input a mixture of spent NiMH-Li Ion-Primary Lithium batteries having the same composition we had found in our sampling in real scale. By this operation several advantages have been observed. For instances by the same operation there was “a dilution” of the explosive power of lithium and also the concurrent combustion of lighter fractions like papers and the dielectric materials which can could interfere during the ECS separation. In spite of these aspects, performing only one route, it wasn’t possible to recover plastic fraction by ECS because it was burnt during the preliminary thermal treatment. A further investigation about this aspect could be carried out with the aim to both oxidize lithium without burn plastics. This developed route is showed in figure 5 with all matter balances.

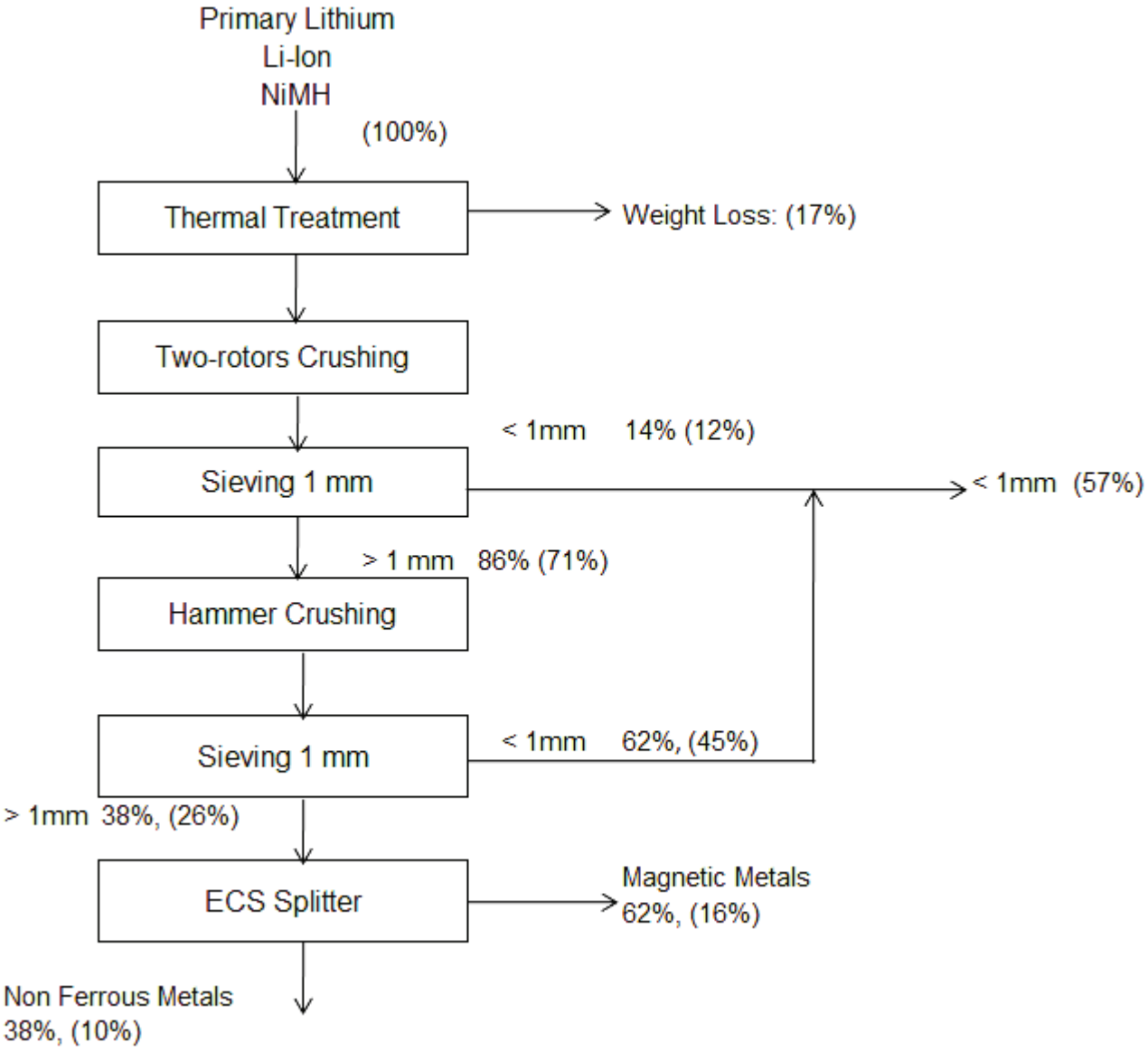

Fig.5: mechanical route to treat a mixture of NiMH-Li Ion-primary lithium batteries

3.3.2 Composition of leach liquors

Leaching operations haven't been investigated from our side because this work had a different purpose and anyway there were already many works showing the possibility to quantitatively dissolve all metals contained in the electrodic powders. Anyway since the compositions of all electrodic powders were well known (also by our characterization) it was possible to estimate the metal concentrations in a hypothetical leach liquor coming from the hydrometallurgical treatment of NiMH, Li-Ion and Primary lithium batteries. In fact, under the justified assumption of a complete dissolution of metals by leaching [8, 10], and considering also an eventual removal of Fe and Al at pH 4 (as also showed in our work recently accepted by Journal of Power Sources) it was possible to formulate several mixture Mn-Co-Ni where their relative concentrations depended on the composition of the input mixture of type of devices. Thus all solution were prepared under the hypothesis of a complete dissolution of metals considering a solid-liquid ratio 1:5 and then they were used to study the solvent extraction procedures. For instance, considering a mixture of 40% NiMH, 40% primary lithium and 20% Li-Ion batteries a quantitative dissolution (S/L ratio 1:5) of their electrodic powders (metal compositions listed in table 2), it results in a solution containing 12 g/l of Co, 31 g/l of Mn and 15 g/l of Ni (Mn relative concentration = 53 %).

3.3.3 Solvent Extraction

Solvent extraction procedure has been studied in order to evaluate the possibility to separate cobalt, nickel and manganese obtaining three different streams.

Metal extraction takes place according to the following reaction [29]

$$M_{Aq}^{2+} + A_{Org}^{-} + 2(HA)_{2Org} \leftrightarrow MA_2 \cdot 3HA_{Org} + H_{Aq}^{+} \qquad [1]$$

where $A_{Org}^{-} + 2(HA)_{2Org}$ represents the solvent saponified by the reaction:

$$Na_{Aq}^{+} + 1/2(HA)_{2Org} \rightarrow NaA_{Org} + H_{Aq}^{+} \qquad [2]$$

The efficiency of single metal extraction was evaluated by extractive yields and selectivites.

Extractive yield (EY) towards a specific metal (Me) was calculated as:

$$EY\ (\%) = [Me]_{org}/[Me]_{tot} \quad *100 \qquad [3]$$

Where:

[Me]tot is the total concentration of a metal determined on the aqueous solution before the extraction

[Me]org is the extracted metals determined as difference between *[Me]tot* and concentration on the aqueous phase after extraction

Extractive selectivity of metal (Me1) against a competitor (Me2) was evaluated by a factor (β) calculated as ratio:

$$B = D_{Me1}/D_{Me2} \qquad [4]$$

Where D is a distribution coefficient for a specific metal calculated as:

$$D = [Me]_{org}/[Me]_{aq} \qquad [5]$$

There are several works in literature which well describe the possibility to separate Ni and Co using Cyanex 272 [30-31]. Here a further investigation about cobalt separation (20 g/l of cobalt) has been made first for several nickel concentration (from 10 to 300 % of cobalt: 2, 10, 20 and 60 g/l of nickel) and then in presence of Manganese. Pseudo-isotherms were preliminary determined to estimate the behavior of the extractants towards single metals and results (not listed here) suggested as pH 5-6 and [Cyanex 272]/Co = 3-4 were the best operating condition for an efficient

separation of Co. Separation Co-Ni was then investigated on a multi-metals solution prepared as above written.

As can be seen in figure 6, by increasing nickel concentration the extractive yields were almost constant and even with high concentrations of nickel ([Ni]/[Co]=3), cobalt could be quantitatively extracted by Cyanex 272. Separating factors towards cobalt in general decreased when increasing Ni concentration but for the lowest [Ni]/[Co] ratio this factor was a bit higher than expected. Actually this can be easily explained because, even if only a small amount of nickel was extracted, since its concentration was low, the resulting extractive yield was high and hence the separating factor was low too. Anyway selectivity towards cobalt was very high even when nickel was 3 times more concentrated than cobalt and the resulting solution, after stripping, contained had a [Ni]/[Co] ratio =0.35. Hence a second extractive step determined a further enrichment of the extract as cobalt because of a behavior exactly like [Ni]/[Co] = 5 as in fig. 6. After two extractive steps by Cyanex 272 we achieved an aqueous solution containing 95% of cobalt and 5% of nickel from an initial one which had 25% of cobalt and 75% of nickel meaning that cobalt-nickel separation is easy performable in a wide range of Ni/Co stoichiometric ratio.

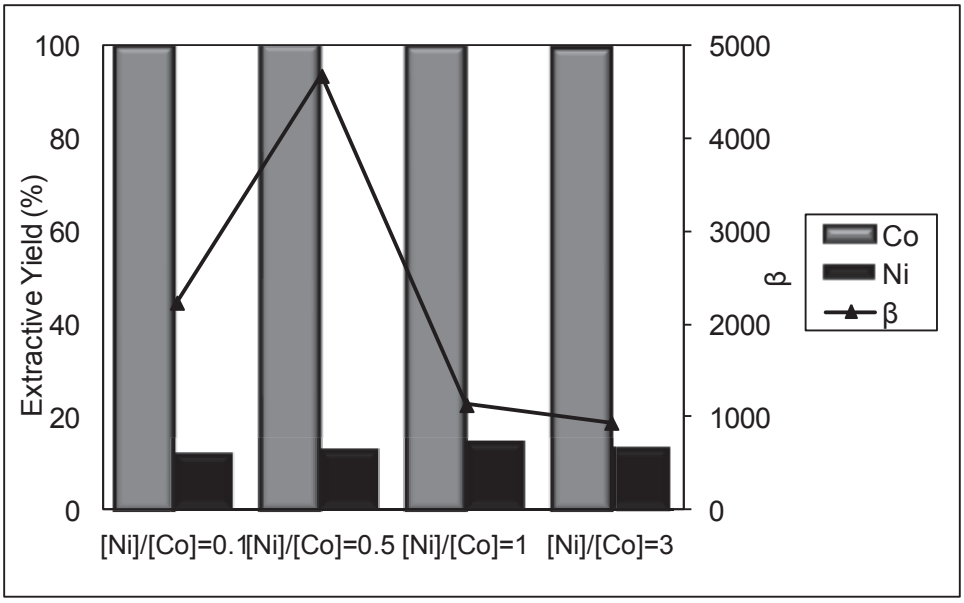

Fig. 6: Cobalt separation with Cyanex 272. Extractive yields and selectivities

After this evaluation, a synthetic leach liquor was prepared including manganese among all contained metals. This operation was made as explained in section 3.2 in order to simulate a solution coming from the leaching of a powder obtained by mechanical treatment of a primary feeding containing 40% of NiMH, 40% of Primary lithium batteries and 20% of Li-Ion as in our classification. The obtained results showed that in presence of 31 g/l of manganese the extractant Cyanex 272 lost completely its selectivity towards cobalt since a large amount of manganese was extracted. Hence another attempt to remove manganese was made reducing its concentration to the value it would have if the main input stream didn't contain the primary lithium batteries, most important source of manganese. As can be seen in fig. 7, even reducing manganese concentration to 6, 4 and 3 g/l, corresponding respectively to an input stream NiMH-Li Ion 50-50%, 40-60% and 25-75%, a selective separation of cobalt by Cyanex 272 wasn't performable.

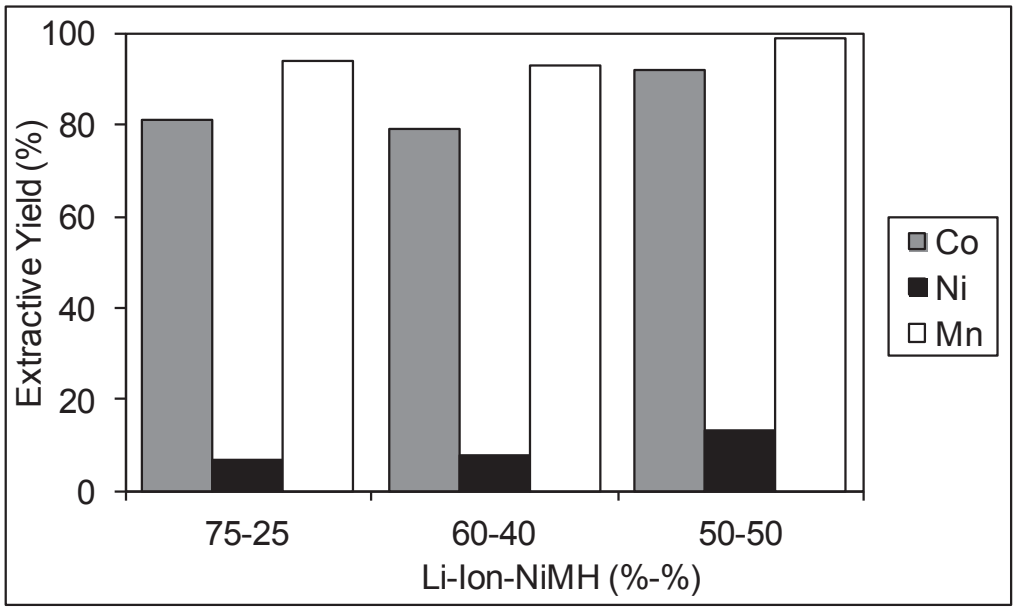

Fig. 7: Cobalt separation In presence of Manganese (no primary lithium batteries)

These results clearly showed the impossibility to selectively extract cobalt in presence of manganese and this implied the necessity to pre-remove manganese. For this purpose a bis2ethylexylphosporic acid (D2EHPA) have been employed as extractant because it was indicated in literature as an agent able to extract many metals among which the manganese [32]. Effects of stoichiometry D2EHPA/Mn has been investigated by modifying the extractant concentration from 1.12 to 2.24 M. The equilibrium pH has been investigated first on a solution containing only manganese (results not listed here) and then on a multi metal solution. As can be seen in fig. 8a, 8b and 8c, by increasing the pH value the manganese extractive yield increased too. This result was due to the further deprotonation of more active sites on D2EHPA molecules and because of this deprotonation other metals were further extracted. The best selectivity was obtained at pH 4 (fig. 9). By increasing the stoichiometric ratio D2EHPA/Mn from 2 to 3 and 4 the extractive yields increased for all metals determining also a decrease of extractive selectivities towards manganese. From a qualitative point of view, it can be also noticed, as D2EHPA granted a high selectivity towards nickel meaning that these operating conditions could be eventually adopted for a separation Mn-Ni.

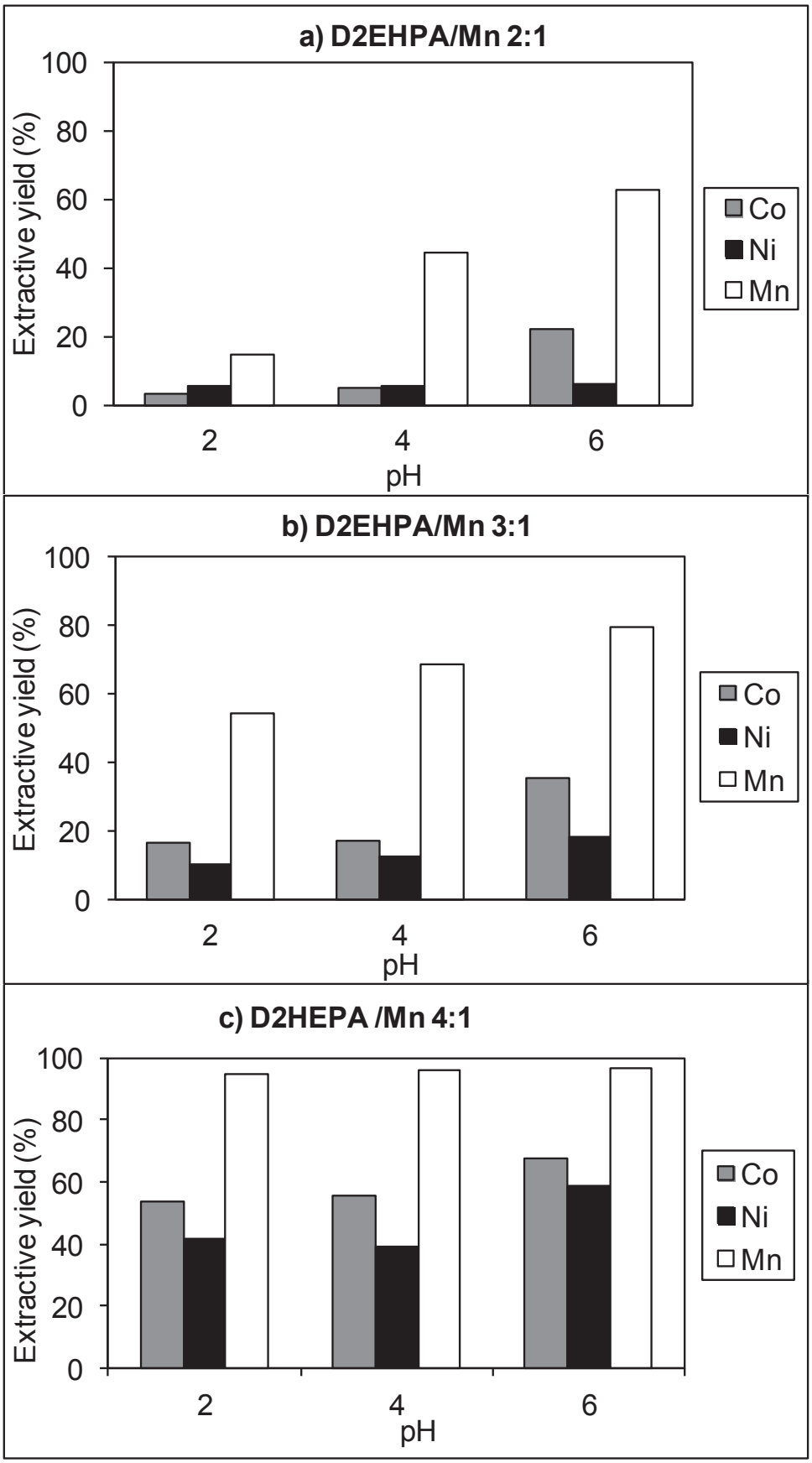

Fig. 8: Extractive yields at different *pH values using three different stoichiometric ratios of D2EHPA/Mn, 2:1 (8a), 3:1 (8b) and 4:1 (8c)*

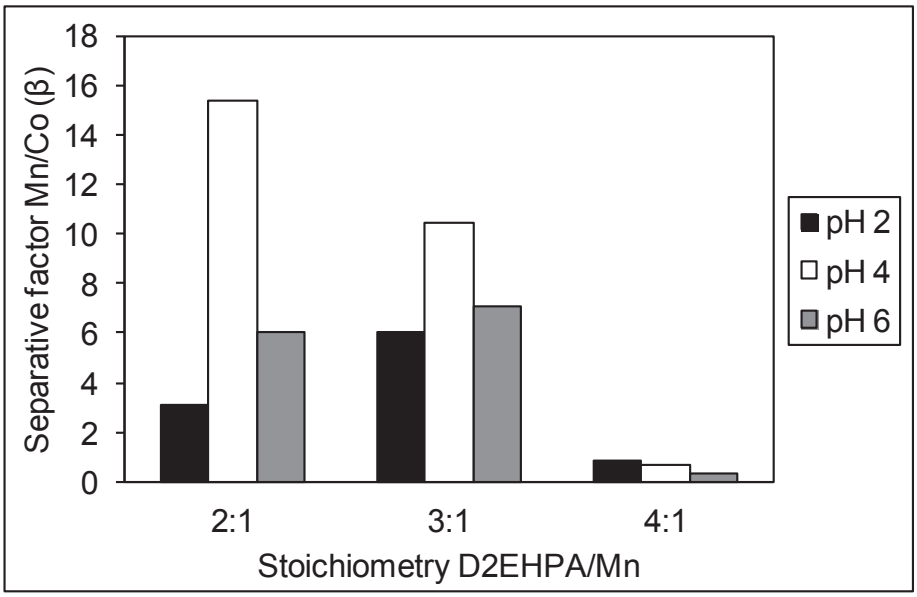

Fig. 9: Separative factors for different stoichiometry and pH values

According to obtained results, in order to selectively remove manganese from the aqueous phase, operating conditions to promote a lower extractive yield and a higher separating factor are preferable because by a multi-step extraction it could be possible to increase the extractive yield keeping high the selectivity. .

Therefore a multi-step extraction on the same solution was carried out using 2 moles of D2EHPA for mole of manganese at pH 4. General results of this experiment are listed in figure 10 where it can be noted that Mn concentration decreased during the extractive procedures whilst Co and Ni content increased. In fact, by following an extractive behavior as in fig. 8a there was a progressive relative enrichment in Ni and Co because the extractive yields towards them was much lower than the one towards manganese.

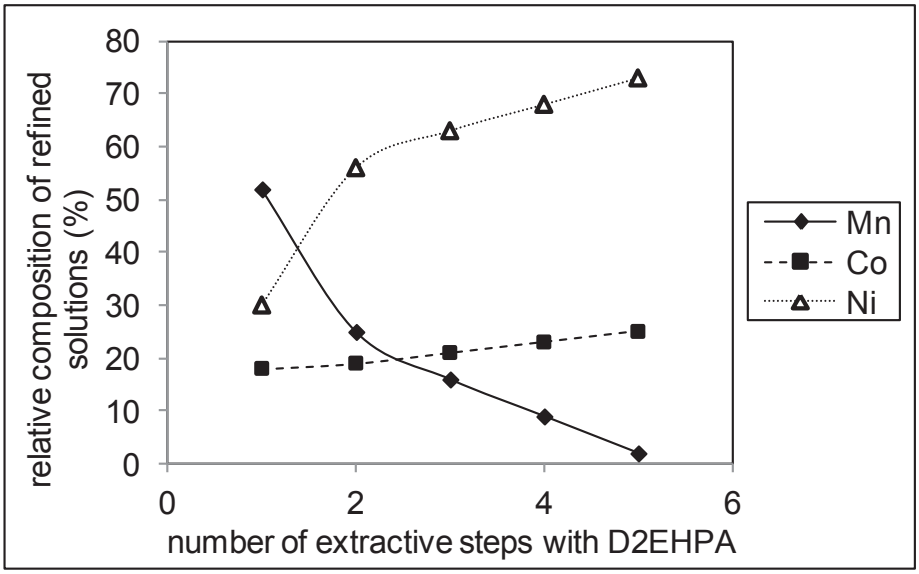

Fig. 10: relative composition of refined solution during the extractive steps with D2EHPA/Mn 2:1

The graph in fig. 10 could be used to estimate the number of required extractive steps to separate manganese when its relative concentration in a ternary mixture Mn-Co-Ni is well known.

Therefore, in the investigated range of concentrations, whereas the upstream composition as spent batteries is well known, it could be also possible to predict the number of extractive steps necessary for manganese removal.

3.4 Conclusions

A mechanical route of pretreatment have been developed in order to treat, NiMH and Li-Ion accumulators as well as primary Lithium Batteries towards which the research didn't pay much attention considering the economical interest behind their recycling.

By this paper the possibility to avoiding a preliminary sorting of these devices has been showed feeding the mechanical section with a mixture of these devices. In this case, once the produced powder has been treated by hydrometallurgical operations, it become necessary to operate a solvent extraction procedure to separate Ni, Co and Mn.

A solvent extraction procedure has been developed to preliminary and selectively remove manganese from the leach liquor using a D2EHPA at pH 4 in a stoichiometric ratio extractant/Mn = 2. In three step it was possible to remove more than 90% of manganese while in four steps the manganese was quantitatively removed enriching the aqueous solution of cobalt and nickel.

Once manganese has been removed removed, cobalt can be selectively separated from nickel in a wide range of nickel concentration using Cyanex 272 in a stoichiometric ratio 3.5:1 at pH 5.5. If necessary a multi step extraction can be easily carried out in order to further separate the cobalt.

As total result Ni-Co and Ni-Mn are always separable with high efficiency using only one solvent whilst in presence of Manganese a preliminary step with D2HEPA is necessary for its removal. Because of these performances in the solvent extraction it could be possible to feed the hydrometallurgical section of a an eventual plant:

a) With only Li Ion batteries because Ni and Co are separable in a wide range of nickel concentration

b) With only NiMH since Ni and Mn were always separable

c) With only primary lithium batteries because they contain only managanese and a solvent extraction isn't required

d) With a mixture of Li Ion and NiMH Accumulators because Ni-Mn and Ni-Co are always separable and Mn has a relative concentration included in the same range as in figure 8.

e) With a mixture of spent devices which represent the composition we have found in industrial scale, that was 40% NiMH, 40% primary lithium batteries, 20% Li Ion Accumulators.

f) Whereas primary lithium batteries are fed in a percentage higher than 40% a further investigation is necessary the possibility of separation and eventually the number of steps required.

Finally, as suggested by the European Guidelines, almost the 50% of total input weight as been recovered just by a mechanical route and this percentage can be easily passed chemically recovering matter after solvent extractions.

3.5 Leaching, recovery of valuable materials and process analysis

Working on the electronic powder obtained by the above mentioned route of mechanical treatment, a leaching procedure has been also studied and obtimized in order to maximize the extraction of metals and hence to allow their successive recovery as valuable products. In literature there were already several works focusing on this problem but here we have performed the present study to truly know the operating conditions and the matter balances required for simulations and process analysis.

3.5.1 Material and methods

Materials

The input material used in leaching experiments was kindly provided by "S.E.Val. s.r.l.", an Italian medium enterprise working in the recycling of wastes of electric and electronic equipments, batteries and accumulators. It was then mechanically treated at Technical university of Kosice in order to develop a mechanical route for waste dismantling. All chemicals (H_2SO_4, NaOH, Na_2CO_3, di-2-ethylhexylphosphoric acid, D2EHPA) were analytical grade reagents (Sigma-Aldrich). The extractant Cyanex 272 was supplied by Cytec USA Incorporation and was used without further purification. Low boiling point kerosene (180–270 °C) was used as diluent.

Leaching

Leaching experiments were carried out in 0.2 L Pyrex jacket reactors provided of impeller stirrer, vapor condenser and thermometer. Heating was provided by an external thermostatic apparatus. 2 g of NiMH electrodic powders and 200 ml of H_2SO_4 solutions (solid-liquid ratio 1:10) were put inside the reactors at the desired temperature. Then the desired weight of solid input material (m_0) was added under stirring. Temperature was investigated in the range 25-80°C, acid concentration was investigated in the range 1-2 M. During leaching time, leach liquor samples (2 mL) were periodically drawn, filtered and analyzed by ICP-OES.

At the end of each experiment, residual solids were separated by filtration, washed with water, dried in a oven, weighted (mf) and digested to determine the residual concentration of each metal in solid phase (xf). Extractive yields for each metal were the determined as:

$$extractive yield\,(\%) = \frac{x_0 m_0 - x_f m_f}{x_0 m_0} * 100$$

where x_0 is the metal concentration (g/g) in the solid before leaching, m_0 is the weight (g) of solid used for leaching, xf is the metal concentration in solid residue after leaching, and mf is the weight of solid residue after leaching.

Treatments were arranged according to a factorial designs for the preliminary optimization of the operating conditions at fixed solid liquid ratio (s/l=100 g/L).

Precipitation of rare earths

Rare earths such as Cerium and Lantanium were precipitated from the leach liquor by adding sodium hydroxide pellets up to pH 1.0-1.5 under stirring at room temperature. After 2 hour stirring suspensions were filtered and solutions analyzed by ICP-OES.

Cobalt recovery

Cobalt was recovered as carbonate from the stripped solution after cobalt extraction, (after precipitations of rare earths and impurity and after manganese extraction). A saturated Na_2CO_3 solution was added to the purified solution under stirring in order to have a final pH of 9- 10. After 2 hours under stirring, suspensions were filtered and analyzed by ICP-OES. Solid precipitates were washed with water to remove soluble salt (as Na_2SO_4) and then dried at 60°C for 24 hours. In order to evaluate the purity of obtained products, cobalt carbonate samples were dissolved in water and solutions analyzed by ICP-OES.

Nickel recovery

Nickel was recovered as hydroxide from raffinates solution of cobalt extraction. Sodium hydroxide pellets were added to purified leach liquors under stirring in order to have a final pH 12. After 2 hours under stirring, suspensions were filtered and analyzed by ICP-OES. Solid precipitates were washed with water to remove soluble salt (as Na_2SO_4) and then dried at 60°C for 24 hours. In order to evaluate the purity of obtained products, nickel hydroxide samples were dissolved and analyzed by ICP-OES.

Manganese recovery

Manganese was recovered as carbonate from its extracted and stripped solution. A saturated Na_2CO_3 solution was added to the stripped solution under stirring in order to have a final pH of 9-10. After 2 hours under stirring, suspensions were filtered and analyzed by ICP-OES. Solid precipitates were washed with water to remove soluble salt (as Na_2SO_4) and then dried at 60°C for 24 hours. In order to evaluate the purity of obtained products, manganese carbonate samples were dissolved and analyzed by ICP-OES.

3.5.2 Results

3.5.2.1 Leaching

Leaching results (fig…) showed that it was possible to quantitatively dissolve all metals after 2 hours of leaching. For metals like Co, Ni and Mn leachant's concentration and temperature didn't exibit a strong influence in the investigated but anyway by using 2M H_2SO_4 at 25°C the higher extractive yields were obtained. On contrary Cerium and Lantanium extractive yields were strongly effected by the temperature in the investigated and in particular the lower the temperature (25°C) was able to determine a better extraction. This could be due to their "inverse solubility" as sulphates which determined a easier oversaturation and precipitation at 80°C. Therefore the leaching operation has been optimized using 2M H_2SO_4 at 25°C for 2 hours.

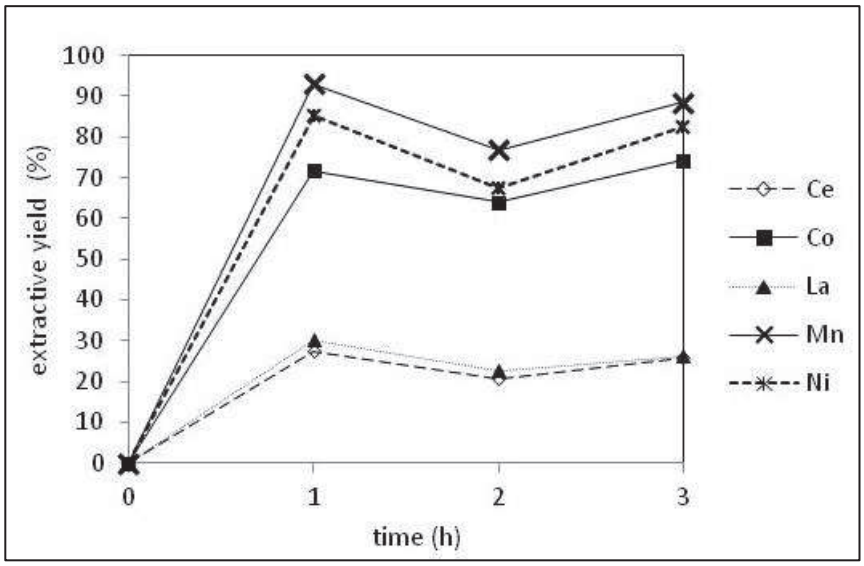

Fig. 11: metal concentrations on time using 1M H_2SO_4 at 80°C

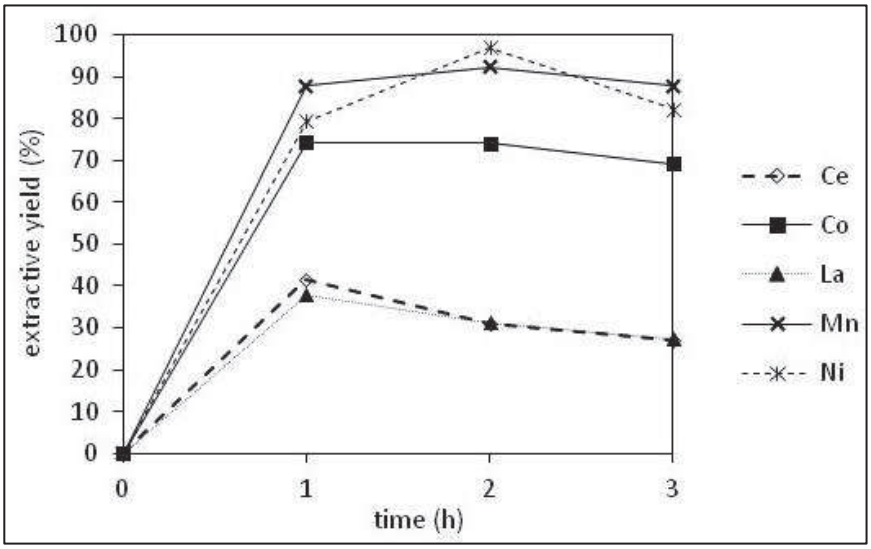

Fig. 12: metal concentrations on time using 2M H_2SO_4 at 80°C

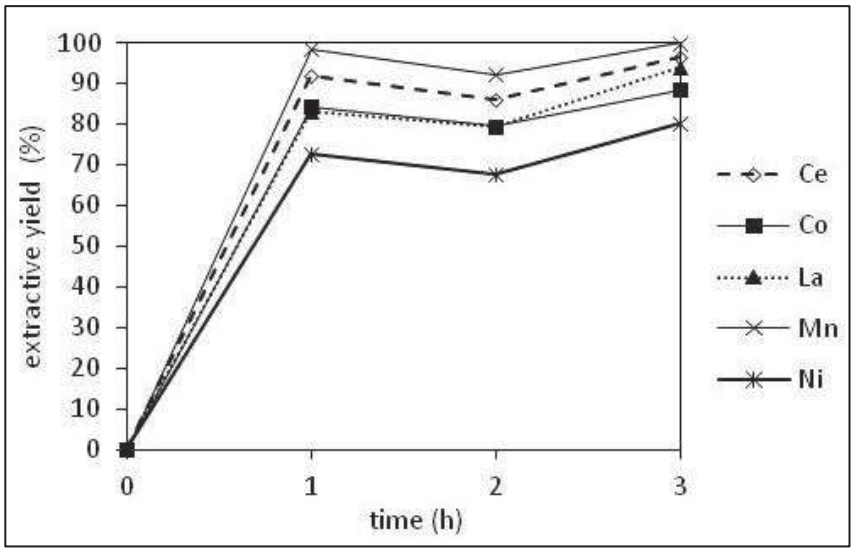

Fig. 13: metal concentrations on time using 1M H_2SO_4 at 25°C

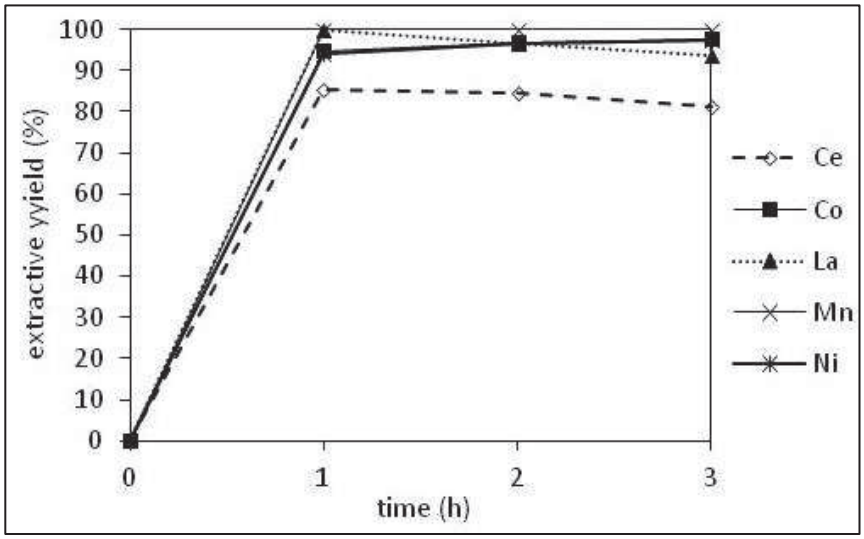

Fig. 14: metal concentrations on time using 2M H_2SO_4 at 25°C

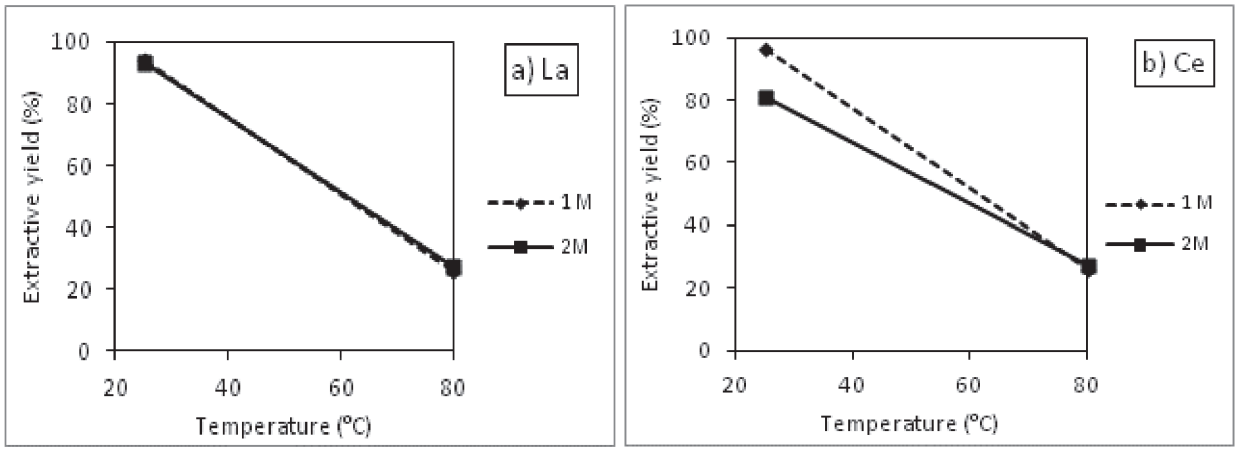

Fig. 15 : effects of leachant's concentration and temperature on extractive yields of La (a) and Ce (b)

3.5.2.2 Recovery of rare earths

Concetrations of Cerium and Lantanium after leaching (pH 0, solid-liquid ratio 1:10) were respectively 2.3 and 6.2 g/l. They were selectively and quantitatively precipitated adding at pH 1.5, as showed in fig 16.

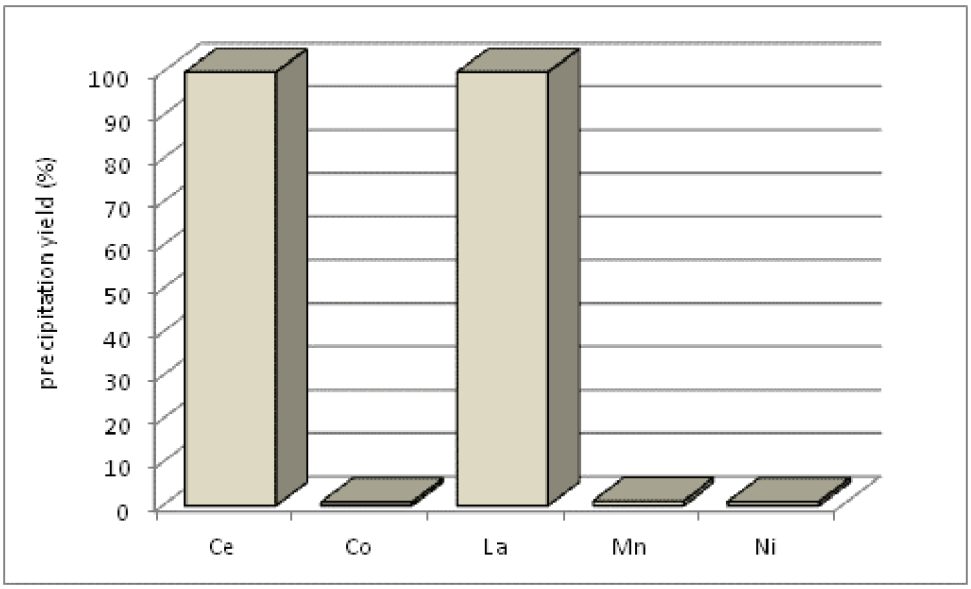

Fig. 16: precipitation yields obtained at pH 1.5

According to literature data (fig.) , for this pH value the rare earths precipitated as mixture of sulphates.

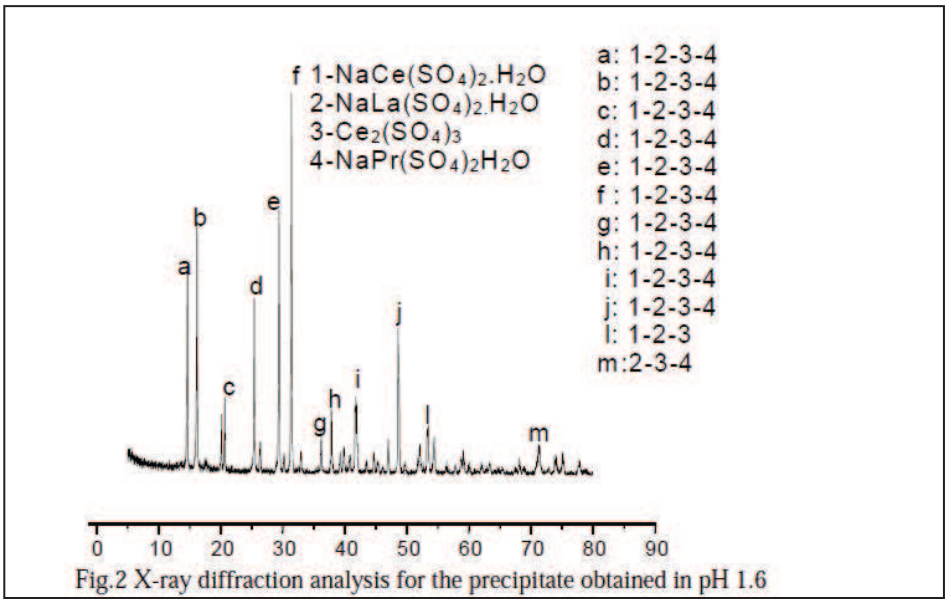

Fig. 17: XRD pattern of precipitated rare earths (J. of Power Sources 193 (2009) 914-923

Since the co-precipitating substances such as $NiSO_4$, $CoSO_4$ and $MnSO_4$ were soluble in water (precipitation was probably due to a massive effects of including in the rare earth flakes) they were easily removed from the precipitate by a washing with water (pH 3) obtaining a final product with a purity higher than 99% as rare earths.

3.5.2.3 Recovery of other products

Cobalt was recovered as carbonate (precipitation yield 98%) after stripping obtaining a product with a cobalt content of about 47%w/w, as required from stardard markets. Nickel was totally precipitated as hydroxide recovering a product containing 58-60% as weight of nickel. Manganese was precipitated as carbonate (precipitation yield 95%) but the obtained product had a lower purity (30-32% as weight of Mn). This was mainly due to the presence of small amounts of co-extracted nickel and cobalt but the obtained product could be better valorizable by further purification or anyway be sold to appropriate refiners.

3.5.2.4 Process Analysis

The developed process for spent NiMH valorization (flowsheet in fig. 18) has been analyzed by simulations using Super Pro Design software as above explained.

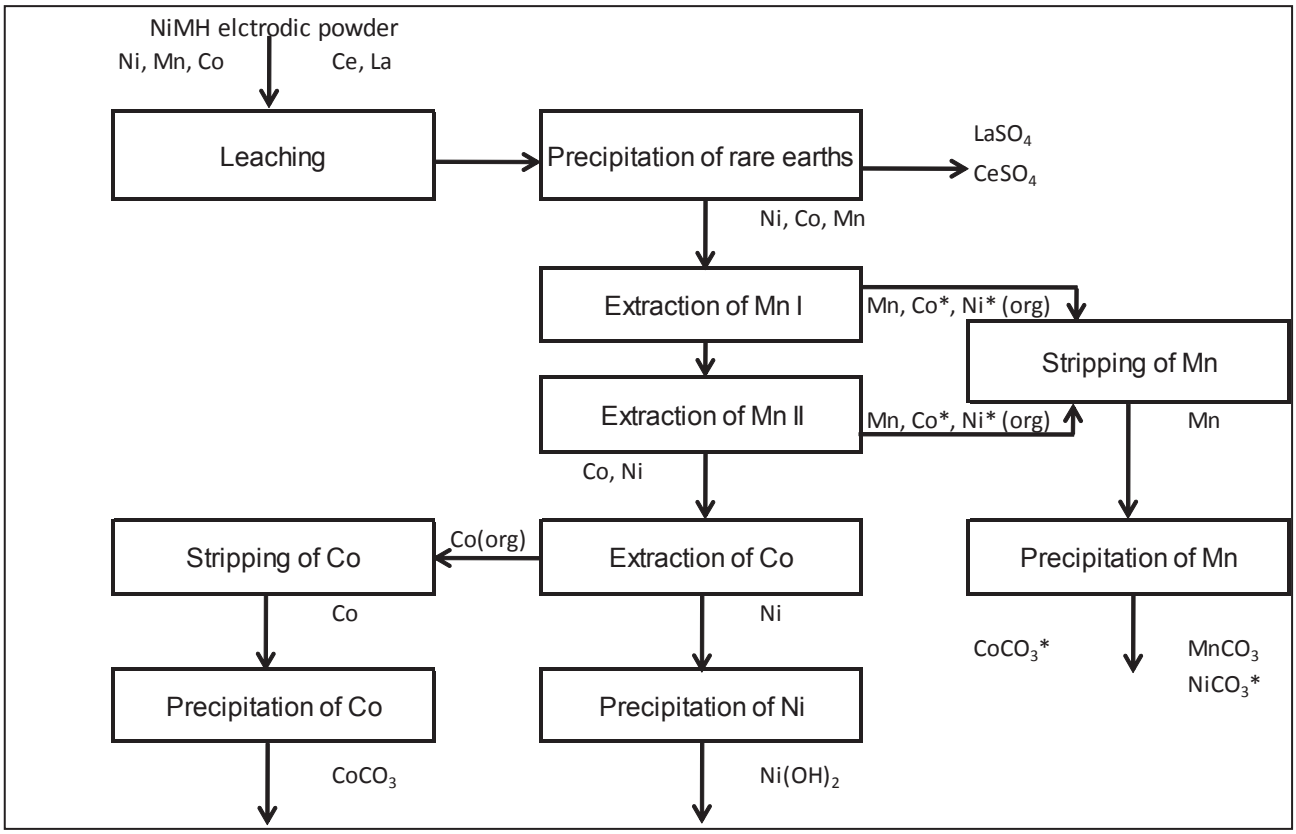

Fig. 18: simulated flowsheet

The used input data for the simulation caome from the lab-scale experiments and the choosed input flowrates were 220, 600 and 1000 tonnes of elctrodic powder. Once more these amounts corresponded to those achievable by collecting and mechanically treating respectively 20, 35 and 50% of the potentially available spent NiMH devices on the Italian market. The table 3 contain the main inputs and outputs of simulations.

All operating conditions such as yields of operation (leaching, purifications, product recovery), consumption of chemicals, energy requirements, and operation scheduling are estimated for each units according to experimental data reported above. Other economic parameters (cost of materials, utilities, waste treatment, process potentiality, equipment characteristics) were fixed as reported in Table 3. Cost of raw materials were taken from sellers, while the selling prices of high purity products (rare earths, $CoCO_3$ and $NiCO_3$) were taken from the International market of chemicals (Table 3). Costs of the mechanical pre-treatment section (not included in the flowsheet) has been estimated to be 250000$.

Table 3: Main inputs and outputs of process simulations

	AMOUNT PURCHASED OR SOLD (t/y)	COSTS ($)
Processed powder	220-1000	500 t^{-1}
$CoCO_3$		45000 t^{-1}
$MnCO_3$		5000 t^{-1}
Cyanex 272		35000 t^{-1}
H_2SO_4		70 t^{-1}
Na_2CO_3		50 t^{-1}
Water		20 t^{-1}
Electricity		0.20 $(kWh)^{-1}$
Wastewater treatment		50 t^{-1}
Solid waste and sludge disposal		100 t^{-1}
Total Operating Cost		2400000-4300000 y^{-1}
Total Capital Investment		6720000-13100000

Economical results of simulations (table 4) showed that processes were always economically suitable in the investigated ranges of input flowrates since payback times were included between approximately 1.5 and 3.5 years. In spite of high costs of investiments and high operating costs the processes grants high revenues by selling rare earths, Ni and Co. Hence high revenues balance high costs and on the whole this process allow similar economical benefit (as payback time) than the one to treat the lithium ion batteries (fig. 19)

Table 4: economical output of the process for NiMH valorization

Processed Powder (t/y)	Total Capital Investiment ($)	Operating Costs ($/y)	Total Revenues ($/y)	Gross Margin (%)	Return on Investiment (%)	Payback Time (y)
220	6722000	2412000	4659000	48.22	28.96	3.45
600	10487000	3580000	12011000	70.2	57.15	1.75
1000	13166000	4298000	19239000	77.66	77.02	1.3

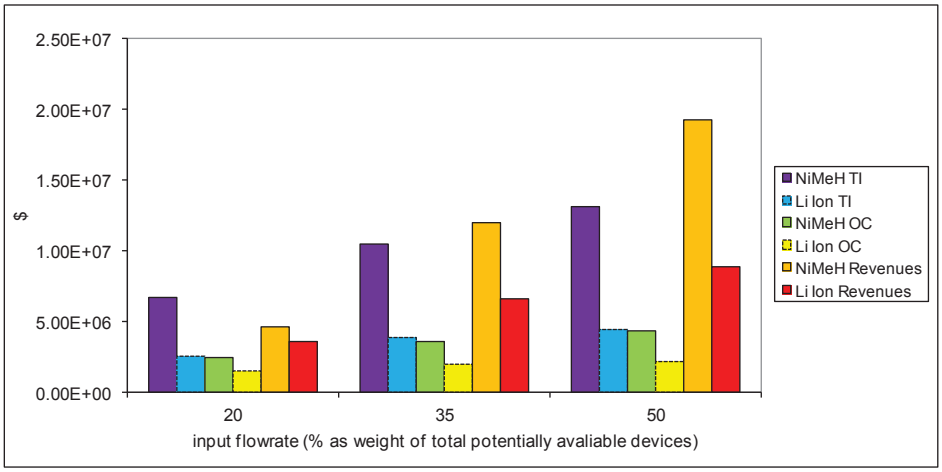

Fig 19: economical comparing between NiMH and Li Ion processes

References

1) Directive 2006/66/EC of the European Parliament and of the Council of 6 September2006. Official Journal of the European Union, 26/9/2006.
2) K. Briffaerts, C. Spirinckx, A. Van der Linden, K. Vranckent al. Waste battery treatment options: Comparing their environmental performance, Waste Management 29 (2009) 2321–2331.
3) F. Ferella, I. De Michelis, F. Veglio. Process for the recycling of alkaline and zinc–carbon spent batteries, Journal of Power Sources 183 (2008) 805–811.
4) D. A. Ferreira, L. M. Zimmer Prados, D. Majuste, M. B. Mansur, Hydrometallurgical separation of aluminium, cobalt, copper and lithium from spent Li-ion batteries, Journal of Power Sources 187 (2009) 238–246
5) Contestabile, M., Panero, S., Scrosati, B., 1999. A laboratory-scale lithium battery recycling process. J. Power Sources 83 (1–2), 75–78.
6) M. J. Lain. Recycling of Lithium Ion Cells and Batteries. Journal of Power Source 97-98 (2001) 736-738
7) L. E. Oliveira, C. Rodrigues, M. B. Mansur. Hydrometallurgical separation of rare earth elements, cobalt and nickel from spent nickel–metal–hydride batteries. Journal of Power Sources 195 (2010) 3735–3741.
8) L. Li, S. Xu, Z. Ju,F. Wu. Recovery of Ni, Co and rare earths from spent Ni-metal hydride batteries and preparation of spherical $Ni(OH)_2$. Hydrometallurgy 100 (2009) 41–46.
9) J. Nan, D. Han, M. Yang, M. Cui. Dismantling, recovery, and reuse of spent nickel-metal hydride batteries, J. Electrochem. Soc., Volume 153, Issue 1, pp. A101-A105 (2006)
10) D. Al Bertuol, A. M. Bernardes, J. A. S. Tenorio. Spent NiMH batteries: Characterization and metal recovery through mechanical processing, Journal of Power Sources 160 (2006) 1465–1470.
11) S. Castillo*, F. Ansart, C. Laberty-Robert, J. Portalfrf. Advances in the recovering of spent lithium battery compounds, Journal of Power Sources 112 (2002) 247–254.
12) J. Xu, H.R. Thomas, R. W. Francis, K. R. Lumb, J. Wang, B. Liang. A review of processes and technologies for the recycling of lithium-ion secondary batteries, Journal of Power Sources 177 (2008) 512–527.
13) J. Jandová, J. Kondás. TMS Fall Extraction and Processing Division: Sohn International Symposium Vol 5 (2006) 299-304.
14) X. Li, H. Koseki. A Study on Hazard of Lithium Primary Batteries, Theory and Practise of Energetic Materials, Vol III (2009) 580-584.
15) Contestabile, M., Panero, S., Scrosati, B., 1999. A laboratory-scale lithium battery recycling process. J. Power Sources 83 (1–2), 75–78.
16) S. M. Shin, N. H. Kim, J. S. Sohn, D. H. Yang, Y. H. Kim. Development of a metal recovery process from Li-ion battery wastes, Hydrometallurgy 79 (2005) 172– 181.

17) C.K. Lee and K.I. Rhee, Reductive leaching of cathodic active materials from lithium ion battery wastes, *Hydrometallurgy* **68** (2003), pp. 5–10.

18) D. A. Ferreira, L. M. Zimmer Prados, D. Majuste, M. B. Mansur. Hydrometallurgical separation of aluminium, cobalt, copper and lithium from spent Li-ion batteries, Journal of Power Sources 187 (2009) 238–246.

19) M. Contestabile, S. Panero, B. Scrosati. A laboratory-scale lithium-ion battery recycling process, Journal of Power Sources 92 (2001) 65±69.

20) C. Lupi, M. Pasquali, A. Dell_Era. Nickel and cobalt recycling from lithium-ion batteries by electrochemical processes, Waste Management 25 (2005) 215–220.

21) J.Nan, D. Han, X.Zuo. Recovery of metal values from spent lithium-ion batteries with chemical deposition and solvent extraction, Journal of Power Sources 152 (2005) 278–284.

22) B. Swain, J. Jeong, J-C Lee, G-H Lee, J-S Sohn. Hydrometallurgical process for recovery of cobalt from waste cathodic active material generated during manufacturing of lithium ion batteries, Journal of Power Sources 167 (2007) 536–544.

23) P. Zhang, T. Yokoyama, O. Itabashi, T. M. Suzuki, K. Inoue. Hydrometallurgical process for recery of metal from spent lithium-ion secondary batteries, Hydrometallurgy 47 (1998) 259-271.

24) T. Müller, B. Friedrich. Development of a recycling process for nickel-metal hydride batteries, Journal of Power Sources 158 (2006) 1498–1509.

25) N. Tzanetakis K. Scott. Recycling of nickel–metal hydride batteries.I: Dissolution and solvent extraction of metals, J Chem Technol Biotechnol 79:919–926 (2004), DOI: 10.1002/jctb.1081.

26) B. Ruffino, M.C. Zanetti, P. Marini. A mechanical pre-treatment process for the valorization of useful fractions from spent batteries, Resources, Conservation and Recycling 55 (2011) 309–315.

27) K. Sarangi, B.R. Reddy), R.P. Das. Extraction studies of cobalt _II/ and nickel _II/ from chloride solutions using Na-Cyanex 272. Separation of Co_II/rNi_II/ by the sodium salts of D2EHPA, PC88A and Cyanex 272 and their misture, Hydrometallurgy 52 _1999. 253–265.

28) S.K. Sahu, A. Agrawal, B.D. Pandey, V. Kumar. Recovery of copper, nickel and cobalt from the leach liquor of a sulphide concentrate by solvent extraction, Minerals Engineering 17 (2004) 949–951.

29) A.M. Bernardes, D.C.R. Espinosa, J.A.S. Tenório. Recycling of batteries: a review of current processes and technologies, Journal of Power Sources 130 (2004) 291–298.

30) B. Swain, J. Jeong, J-C Lee, G-H Lee. Development of process flow sheet for recovery of high pure cobalt from sulfate leach liquor of LIB industry waste: A mathematical model correlation to predict optimum operational conditions, Separation and Purification Technology 63 (2008) 360–369.

31) G. Dorella, M. B. Mansur. A study of the separation of cobalt from spent Li-ion battery residues, Journal of Power Sources 170 (2007) 210–215

32) Cyanex-272, Technical Brochure, American Cyanamid Company, July 1995.

33) M.R. Hossain, S. Nash, G. Rose, S. Alam. Cobalt loaded D2EHPA for selective separation of manganese from cobalt electrolyte solution, Hydrometallurgy 107 (2011) 137–140.

4 Study of Nanoparticles Production

Although nanotechnology is widely talked about, there is little consensus about where the nano-domain begins. Nanoscience can be defined as the study of phenomena and manipulation of materials at atomic, molecular, and macromolecular scales, where properties differ significantly from those at a larger scale, whilst nanotechnologies are the design, characterization, production, and application of structures, devices, and systems by controlling shape and size on the nano scale. Nanomaterials link the two areas together, so these definitions are very appropriate. It is recognized that the size range that provides the greatest potential and, hence, the greatest interest is that below 100 nm.

Just because materials can be made into very small particles does not immediately mean that they have any practical use. However, the fact that these materials can be made at this scale gives them the potential to have some very interesting properties (Table 1).

Table 1:Characteristic lenghts in solide-state science model

Field	Property	Scale Lenght
Electronics	Electronic wavelenght Inelastic mean free path Tunneling	10-100 nm 1-100 nm 1-10 nm
Magnetics	Domain wall Spinn-flip scattering lenght	10-100 nm 1-100 nm
Optics	Quantum well Evanescent wave decay lenght Metallic skinn depth	1-100 nm 10-100 nm 10-100 nm
Superconductivity	Cooper pair coherence lenght Meisner penetration depth	0.1-100 nm 1-100 nm
Mechanics	Dislocation interaction Grain boundiaries Crack tip radii Nucleation/growth defect Surface corrugation	1-1000 nm 1-10 nm 1-100 nm 0.1-10 nm 1-10 nm
Catalysis	Surface topology	1-10 nm
Supramolecules	Kuhn lenght Secondary structure Tertiary structure	1-100 nm 1-10 nm 10-1000 nm
Immunology	Molecular recognition	1-10 nm

Materials at the nanoscale between 1 nm and 250 nm lie between the quantum effects of atoms and molecules and the bulk properties of materials. By being able to fabricate and control the structure of nanoparticles, the scientist and engineer can influence the resulting properties and, ultimately, design materials to give desired properties. The electronic properties that can be controlled at this scale are of great interest. The range of applications where the physical size of the particle can provide enhanced properties that are of benefit are extremely wide.

Manufacturing nanoparticles can be achieved through a wide variety of different routes but summarizable by four generic routes: wet chemical, mechanical, form-in-place, and gas-phase synthesis.

Wet chemical processes include colloidal chemistry, hydrothermal methods, sol-gels, and other precipitation processes. Essentially, solutions of different ions are mixed in well-defined quantities and under controlled conditions of heat, temperature, and pressure to promote the formation of insoluble compounds, which precipitate out of solution. These precipitates are then collected through filtering and/or spray drying to produce a dry powder. The advantages of these wet chemical processes are that a large variety of compounds can be fabricated, including inorganics, organics, and also some metals, in essentially cheap equipment and significant quantities. Another important factor is the ability to control particle size closely and to produce highly monodisperse materials. However, there are limitations with the range of compounds possible, bound water molecules can be a problem, and, especially for sol-gel processing, the yields can be quite low.

New processes that might overcome some of these problems are being developed, such as high-throughput

microreactors. For bulk production, large quantities of starting materials may be required, which can be expensive. Having the nanoparticles well dispersed in a suspension, however, is an advantage if further surface treatment is required to encapsulate or functionalize their surface. These are being used to manufacture materials such as magnetic materials for use in high-density storage devices.

Mechanical processes such as grinding, milling, and mechanical alloying techniques, allow the production of fine inorganic powders or metals using coarse powders as feedstock. In particular, operations like planetary or rotating ball mills grant simplicity and low-cost equipment in spite of some problems such as agglomeration of the powders, broad particle size distributions, contamination from the process equipment itself, and often difficulty in getting to the very fine particle sizes with viable yields.

Form-in-place processes include lithography, vacuum deposition processes such as physical vapor deposition (PVD) and chemical vapor deposition (CVD), and spray coatings. These processes are more geared to the production of nanostructured layers and coatings, but can be used to fabricate nanoparticles by scraping the deposits from the collector. However, they tend to be quite inefficient and are generally not used for the fabrication of dry powders, although some companies are beginning to exploit these processes. A number of universities companies are developing variations on these processes, such as the electrostatic spray assisted vapor deposition process.

Gas-phase synthesis include flame pyrolysis, electro-explosion, laser ablation, high-temperature evaporation, and plasma synthesis techniques. Flame pyrolysis has been used for many years in the fabrication of simple materials such as carbon black and fumed silica, and is being used in the fabrication of man more compounds. Laser ablation is capable of making almost any nanomaterial, since it utilizes a mix of physical erosion and evaporation. However, the production rates are extremely slow and most suited to research uses. Both RF and DC plasmas are being used successfully to make a wide range of materials. The heat source is very clean and controllable and the temperatures in the plasmas can reach in excess of 9000°C, which means that even highly

refractory materials can be processed. However, this also means that the technique is unsuitable for processing organic materials.

The first industrial production of nanomaterials occurred early in the 20th century with the production of carbon black and subsequently, in the 1940s, fumed silica. These materials are still produced and used in large amounts, and some well known companies such as Degussa and Cabot owe their origins to these materials. However, it was not until the latter half of the 20th century that the scientific understanding of materials incorporating ultrafine particulates really developed and it was realized that significant improvements to material properties could be achieved by using them.

During the 1960s, 1970s, and early 1980s there was a gradual expansion as large multinational companies established subsidiaries. The real burst in the commercialization of nanoparticle production has occurred over the last ten years or so. One of the main drivers for this has been the extraordinary growth in the electronics and optoelectonics industries. As the technologies have developed and functionality has increased, the drive has been to produce smaller and smaller products requiring smaller components. This has meant that designers are demanding more from the materials used to construct the devices, which has led to a search for ways to produce major improvements in performance and the move to nanoscale materials. In all, there are over 1500 companies involved in nanotechnology R&D worldwide. It is not easy to extract from the data which companies are nanomaterials focused but, where the data is available, a rapid growth has observed.

Most of this growth has come through the establishment of small start-up compagnie, universitary spin off, or government related laboratories.

Although accurate data are difficult to obtain, there are probably in excess of 320 companies producing nanomaterials in various forms around the world today, of which about 200 are nanoparticle producers and in addition there are others making nanomaterials for using in their own products.

All the interest behind the nano material production is related to the possibility of re-engineering already existing materials down to the nanoscale allowing new performances and hence improved products.

Examples include cermet cutting tools, where smaller particle sizes translate into improved performance and lifetime; lapping and polishing compounds, where track dimensions on chips are approaching 90 nm so the polishing media need to be significantly less than this to keep defects small compared to the track dimensions; and magnetic recording media, where higher-density storage is driven by finer particle and grain sizes with the trend towards terabyte storage capacities. This type of evolutionary progression into nanoscale materials will continue as the benefits are realized.

However, the growth in interest cannot be totally explained by this evolutionary development and, as more research is directed towards investigating nanoscale materials, the ability to make a step-change in performance is being found all the time. This is opening up totally new applications and the possibility of making products that have been hypothesized about for many years, such as targeted drug delivery, new optoelectronic devices, and smaller, more efficient energy devices (table 2).

Table 2: A selection of current and future applications for nanoparticles

Field	Under development	Being introduced	Well estabished
Power and Energy	Dry solar-cells based on TiO2 H2 storage using metal hydrides Improved anode and cathode materials for fuel cells Thermal control fluids using Cu	Nanoscystalline Ni and metal hydride for batteries Environmental catalyst	Automotive catalyst
Healthcare and Medical	Nanocrystalline drugs for easier adsorption Inhalable insulin Bone growth promoters Virus detection using quantum dots Anticancer treatments Antioxidant drugs using fullerenes	Molecular tagging usinf CdSe quantum dots Drug carriers for drugs with low water solubility Marker particles for uses in assays Coating for implants (hydroxyhapatite)	Ag-based antibacterial wound dressings, ZnO fungicide Au dor biolabeling detection Magnetic resonance for image contrast (Fe2O3) Sunscreen using ZnO, TiO2
Engineering	Improved thermal barrier coatings Spark plugs using nanoscale metal Nanoporous silica based on aerogels for high efficiency insulators Controlled delivery of herbicides/pesticides Chemical sensors Molecular sieves	Absorption-resistant coatings (alumina, Y-Zr_2O_2) Lubrificant/Hydraulic additives (Cu, MoS_2) Pigments Self-cleaning glass with TiO_2 Propellents using Al	Structural enhancement of polymers and composites Thermal spray coatings based on TiO2, TiC-Co etc. Nanostructured alloys Processing catalyst Cutting tool bits: WC, TiC, Co Automotive tires
Consumer goods		Anticouterfait devices Nano-starch-based adhesives for cardboard packaging	Packaging using silicates Glass coatings for antiglare Ski wax Sport goods: tennis balls and nanoclays based rackets Water repellent textiles
Environmental	More sensitive sensors Environmentally friendly antitouling points and	Alumina fibers for water treatments Photocatalyst water	Self-cleaning glass using TiO_2 Antireflection

	coatings Self remediation using Fe	treatments using TiO_2	coatings
Electronics	EMI shielding with conducting materials Electrically conductive plastics Light-emitting Si LED nanoparticles for displays Electronic circuits, nonvolatile random access memory (NRAM) using Cu, Al Display technologies including field-emission devices with conducting oxides	Ferrofluids using magnetic materials Optoelectronics devices using rare-earth doped ceramics Smaller multilayer capacitors using Ni/Cu nanopowders Nano magnetic particles for high density storage	Chemical-mechanical planarization (Al, Ce) Coatings and joining materials for optical fibers

Carbon nanotubes are proving to have some unusual properties, such as being able to convert light into electric current, which could enable an enormous range of new applications. This is prompting some companies to gear up to produce significant quantities of these materials, of the order of hundreds of tonnes per year.

Looking at the major markets for functional nanomaterials today, the largest by volume are automotive catalysts, chemical-mechanical planarization (CMP), magnetic recording media, and sunscreens with 11 500 tonnes, 9 400 tonnes, 3 100 tonnes, and 1 500 tonnes, respectively. The scope and number of applications for nanoparticles continues to grow and companies are finding more and more uses for these materials.

The following works have been performed in order to produce based manganese and cobalt nanoparticles even investigating the operating conditions which determine the formation of products having the smallest possible sizes. Keep working in the "Material Processing Field", cobalt and manganese have been chosen among all metals because of the future ambition to produce nanostructured materials as downstream of hydrometallurgical processes to valorize spent batteries. The study related to the manganese nanoparticles resulted in a paper: "*Nanoparticles of manganese carbonate by microemulsion mediated route: production and characterization*".

Reference

M.J. Pitkethly. Nanomaterial the driving force, Nanotoday, ISSN:1369 7021 © Elsevier Ltd, 2004.

4.1 Nanoparticles of manganese carbonate by microemulsion mediated route: production and characterization

4.1.1 Introduction

Manganese oxides have been extensively studied in the last years because of the large number of manganese oxidation states which allows to have many different manganese products with a large range of applications, from the battery technologies to the catalysis. Among all manganese oxides Mn_3O_4 is known to be an active catalyst in several reactions such as the oxidation of methane and carbon monoxide, [1] for the selective reduction of nitrobenzene [2] and recently for the

combustion of organic compounds at low temperatures [3-4]. Moreover the using of Mn_3O_4 nanoparticles as capacitor material has been studied [6-7].
There is also a big interest in Mn_2O_3 because it can be used as catalysts for removing carbon monoxide and nitrogen oxide from waste gas [8, 9] but recently researchers have also shown considerable interest in lithium intercalated Mn_2O_3 as an electrode material for rechargeable lithium batteries [10, 11].
Nowadays many synthesis routes can be used to produce these kinds of nanomaterials but those solvo-hydrothermals seems to be the most popular because of their easiness and reproducibility in a larger scale. Surfactant mediated ways by DMF or DMSO has been used by A. Vàzquez-Olmos et al. [12] to produce nanorods of Mn_3O_4, at room temperature but in a long time. Among all solvo-hydrothermal routes the reverses micelles can be used to create structures like micro-reactors in which the precipitation of many kind of products takes place [13]. A microemulsion is a thermodynamically stable dispersion of two immiscible fluids stabilised by adding a surfactant. Among all kinds of microemlusions the "water-in-oil" having spherical shape is the most common one. It self-aggregates in this form in order to minimize the surface Energy when water is added in a hydrocarbon based continuous phase in presence of a surfactant. In literature there are many works about microemulsion mediated synthsis of nanocrystals. Marie-Paule Pileni produced in 2003 an exhaustive work [14] which well explained the based theory of reverse micelles. In 2007 Julian Estoe et al. showed the relationship between size of several reverse micelles and main operating conditions such as temperature, water-surfactant molar ratio and reagent concentrations [15]. In the same year M.A. Michaels at al. formulated a quantitative model to relate the size of nonionic reverse micelles to most important operating variables [16]. Another interesting reviews which well explained the use of microemulsion mediated route in the production of nanocrystals have been published furthmore by Ashok K. Ganguli et al. (2009) [17].

In particular, regarding manganese-based material produced by microemulsion-mediated synthesis several works have been published in the last decade. Y. Liu et al. (2003) prepared Manganese oxide (hausmannite) nanowires by annealing precursor powders which were produced in a novel inverse microemulsion with non-ionic Nonylphenol Ethoxylate (NP9) [18]. Tokeer Ahmad et al. (2004) used the reverse-micellar method with CTAB to produce Nanorods of anhydrous manganese oxalate. They investigated the manganese calcinations, under specific reaction conditions, in order to produce some manganese oxides such as MnO, Mn_2O_3 and Mn_3O_4 having average sizes included between 30 and 100 nm [19].
Xinglong Wu et al. (2006) used a CTAB microemulsion method followed by a thermal treatment to synthesize $MnCO_3$ nanocrystals performing also a shape control by a modification of operating variables such as concentration of reactants and water-surfactant molar ratio [20].
By this paper we wanted to produce nanocrystals of manganese carbonate, without any thermal treatment investigating also how the most important operating conditions such as water-surfactant molar ratio and reactants' concentrations are able to influence the final size and dispersion of the produced carbonate. A manganese carbonate produced by this route could also be used, after characterization, as precursor for the synthesis of manganese oxides.

4.1.2 Experimental

All chemicals used for this work ($MnCl_2$, $(NH_4)_2CO_3$, cyclohexane, n-penthanol, ethanol) were analytical grade reagents purchased from Kanto Chemicals Co. and CTAB (99+%) was purchased from ACROS ORGANICS. A ternary phase microemulsion of Cyclohexane (20 g) + n-penthanol (1.5 g) - CTAB (2g) – Water ($MnCl_2$ and $(NH_4)_2CO_3$ solutions) was employed as media in which to perform the reactions. As shown in figure 1, the $MnCl_2$ and $(NH)_4CO_3$ solutions were slowly added by dropwising in their respective organic phases until they became optically transparent and then the reaction (1) was carried out, under nitrogen atmosphere, mixing the two different microemulsions at controlled temperature (30 °C), under stirring, for 2 hours.

$$MnCl_2 + (NH_4)_2CO_3 \rightarrow MnCO_3 + 2NH_4Cl \qquad (1)$$

As showed in table 1 water-surfactant molar ratio (w) was investigated in the range 5-7.5 whilst reactants' concentration ($MnCl_2$ and $(NH_4)_2CO_3$) have been investigated in the range 0.25-1.0 M. Water-surfactant molar ratio was investigated by keeping constant the amount of surfactant (2 g) and by modifying the amounts of aqueous solutions in the in the microemulsions: 0.49, 0.62 and 0.74 g of aqueous solutions were added in their respective systems in order to reach respectively w=5, w=6.25 and w=7.5. Reactants' concentration was investigated by modifying the concentration of their aqueous sources. The precipitate was collected by centrifuging and it was washed several times, at first twice with absolute ethanol and then twice with distilled water. When the thermal treatment was tested it was carried out in a teflon-lined autoclave reactor at 120°C for 4 hours after dropwising. Size and morphology of the synthesized particles were estimated by Scanning Electron Microscope (JEOL JSM-5510LV) and Transmission Electron Microscope (JEOL JEM-2100 in ISSP, Univ. Tokyo) and a software for image analysis, "JImage", was used in order to determine the size distributions of particles. For each sample the particle size distribution was evaluated by analyzing four TEM images resulting in a number of analyzed particles included between 550 and 1150. Samples for microscopic observations were prepared by adding acetone and by dispersing the particles in an ultrasonic bath. After ultrasonication, a drop of the suspension was put on a copper grid and dried at air before microscopic observation. Samples were also analyzed by MacScience X-ray diffractometer M03X (XRD), with Cu Kα radiation (λ = 1.5406 Å) operated at 40 kV and 20 mA emission condition to determine the composition of products.

Table 1: investigated factors of full factorial experimentation

n test	Ctot [M]	w
1	0.25	5
2	0.25	6.25
3	0.25	7.5
4	1.0	5
5	1.0	6.25
6	1.0	7.5

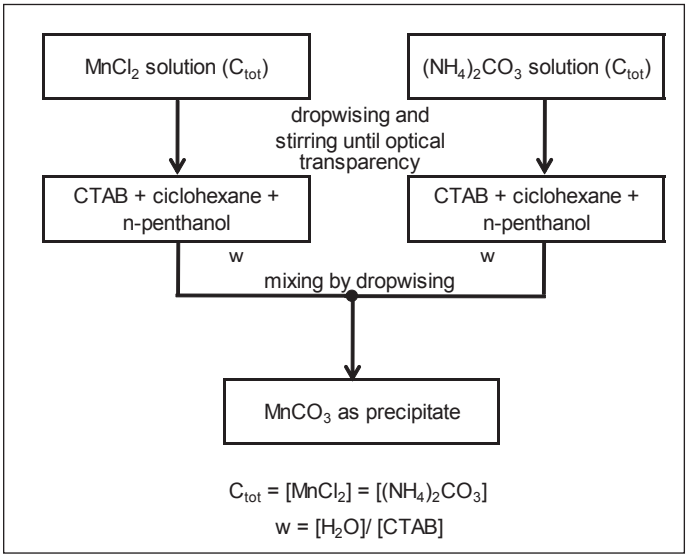

Fig.1: flowchart for the synthesis of nano-crystalline manganese carbonate

4.1.3 Results and Discussion

Results of characterization

According to the SEM images 2a and 2b, by performing a thermal treatment after mixing the two microemulsions (as done by several authors), the particle size increased a little (2b). For this reason we have confirmed our intent to carry out all synthetic procedures without any thermal treatment.

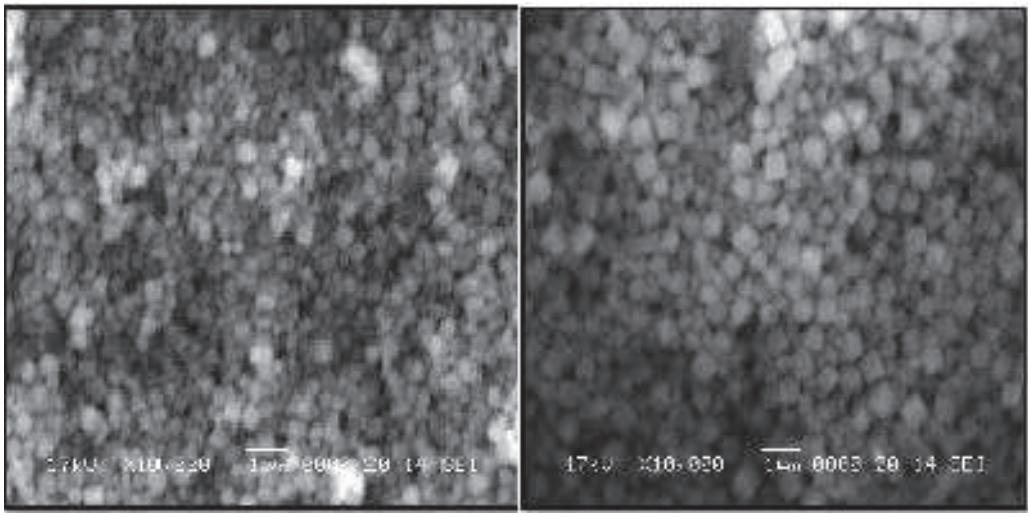

Fig 1a:particles obtained for w=20, 0.5 M at 30 °C
Fig 1b:particles obtained for w=20, 0.5 M at 90 °C for 4 hours

Observing the XRD patterns of the products obtained for w = 7.5 (3a), w = 6.25 (3b) and w = 5 (3c) all reflection peaks can be indexed as a rhomb-centered hexagonal (rch) phase of $MnCO_3$ with lattice constants α=4.790 Å. Anyway the XRD pattern of the sample obtained at the lowest water-surfactant molar ratio showed a small presence of oxidized manganese (peaks marked with *). Since all reactions were carried out at the same way, even working under a nitrogen atmosphere,

we could suppose that the very small size of products (see TEM characterizations) and hence its very high surface area, resulted in easy oxidation of surface portions.

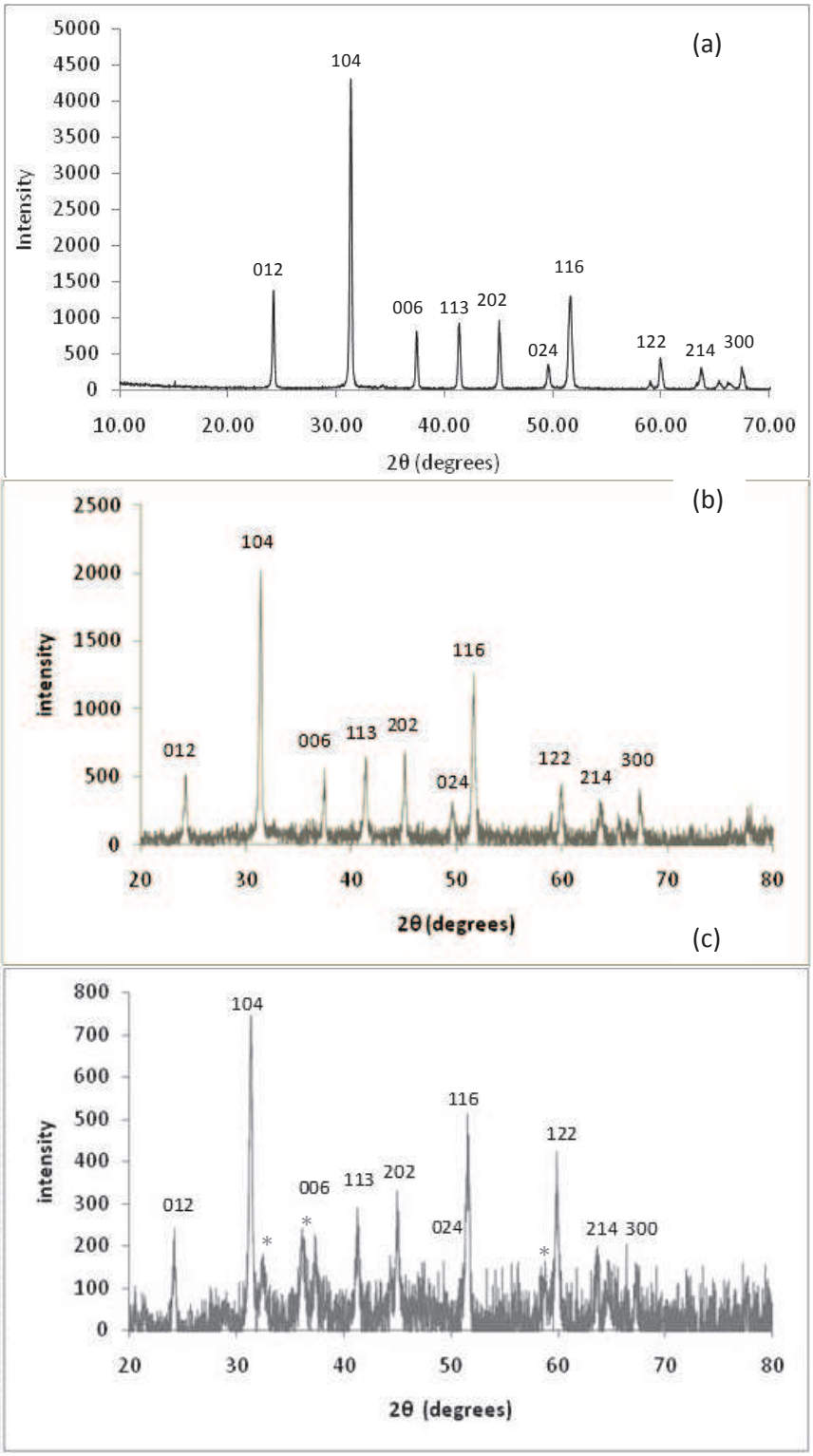

Fig2: X-ray diffraction patterns of nanocrystalline $MnCO_3$ obtained for w=7.5 (a),w= 6.25 (b) and w=5 (c)

Water-surfactant molar ratio (w) exhibited a relevant influence on particles size and distribution (evaluated by the dispersion around the average size) and also on particles shape. For w = 5 the particles had a spherical shape and they were smaller than 10 nm with a narrow dispersion (fig. 4). Increasing this ratio to 6.25, the particles become mainly rhombohedral (and also cubic) and their size and dispersion increased (fig. 5). Working at w = 7.5 (fig. 6) the particles were larger (around 100 nm) with a higher dispersion around the average size (fig. 6). Though cationic surfactant can lead to an anisotropic growth because of assembling phenomena on negatively charged surface of forming particles, the obtained shapes (spherical and cubic) are the result of an isotropic growth of particles.

For all investigated water-surfactant molar ratios by an increasing of the reactants' concentration from 0.25 M to 1.0 M, only a little increase of particle size was observed, as showed in figure 7 (w=5), figure 8 (w=6.25) and figure 9 (w=7.5).

These results have been different from those shown by Xinglong Wu et al. (2006) because they had reported that reactants concentration was able to influence the particle size more than water-surfactant molar ratio. Moreover, even if they had performed a thermal treatment, the particle size of their manganese carbonate increased by decreasing w.

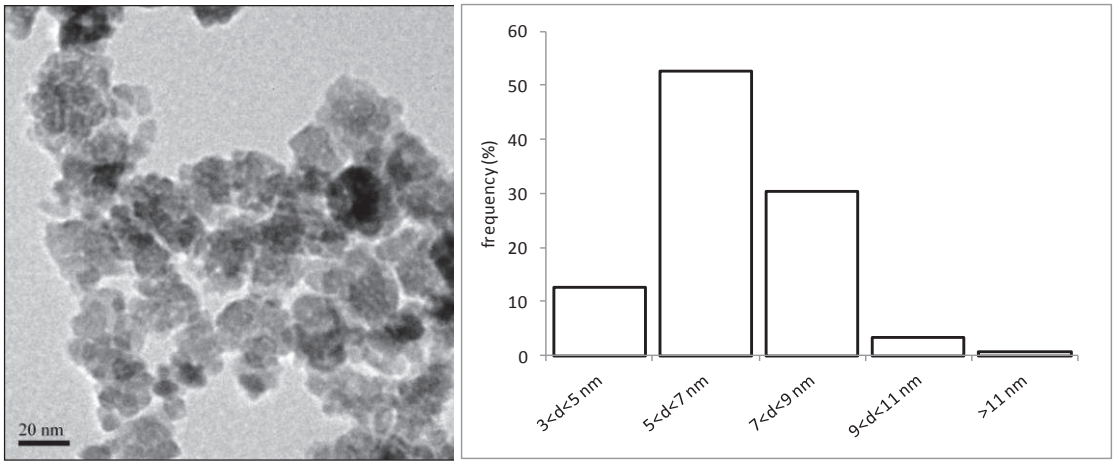

Fig 3: particles obtained for w=5, 0.25 M at 30 °C and their size distribution (b)

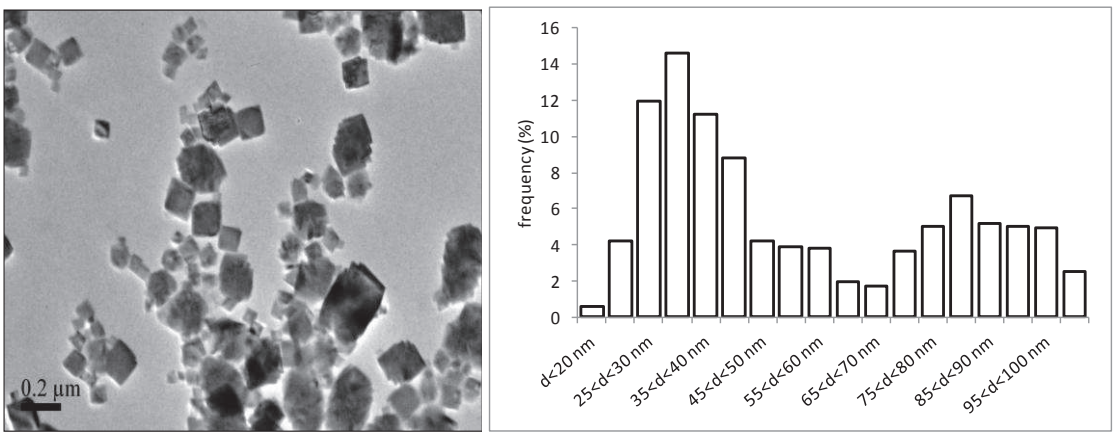

Fig 4: particles obtained for w=6.25, 0.25 M at 30 °C (a) and their size distribution

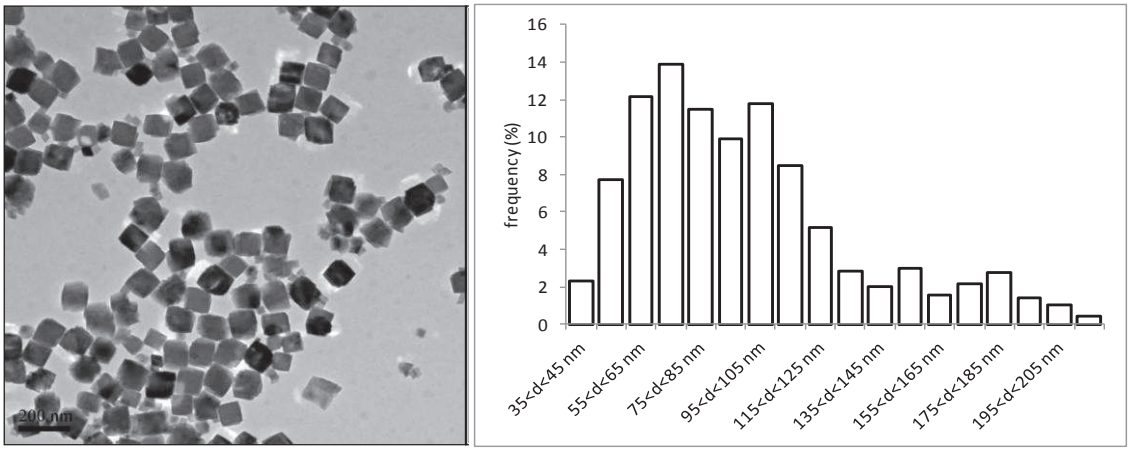

Fig 5: particles obtained for w=7. 5, 0.25 M at 30 °C and their size distribution

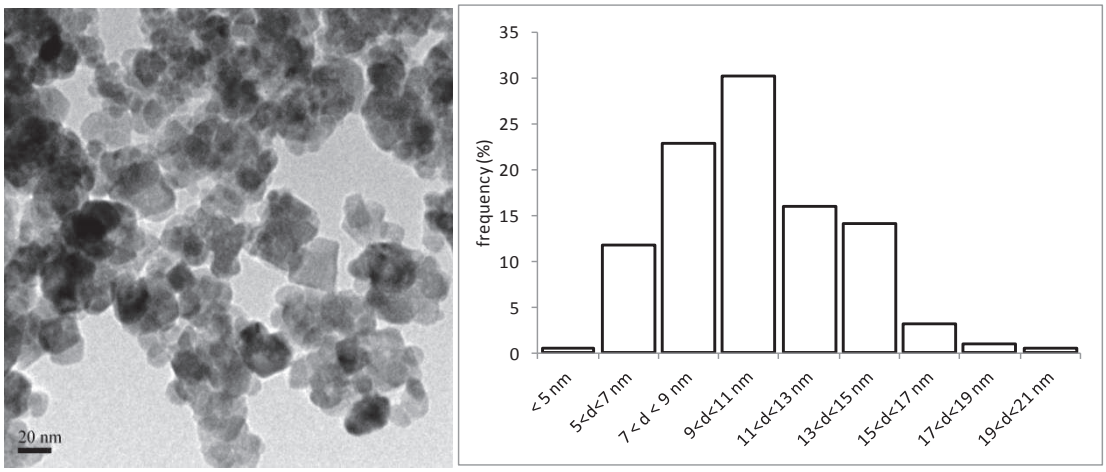

Fig 6: particles obtained for w=5, 1 M at 30 °C (a) and their size distribution (b)

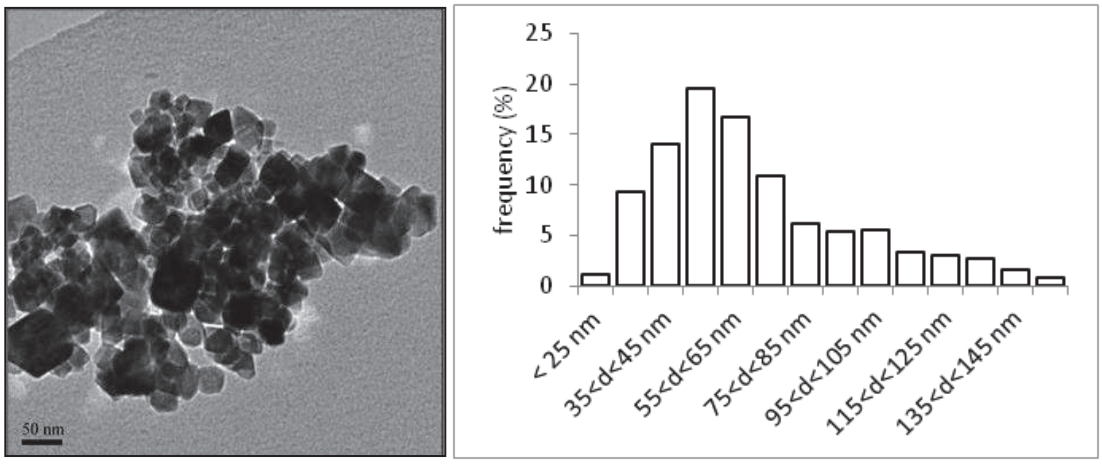

Fig 7: particles obtained for w=6.25, 1 M at 30 °C (a) and their size distribution (b)

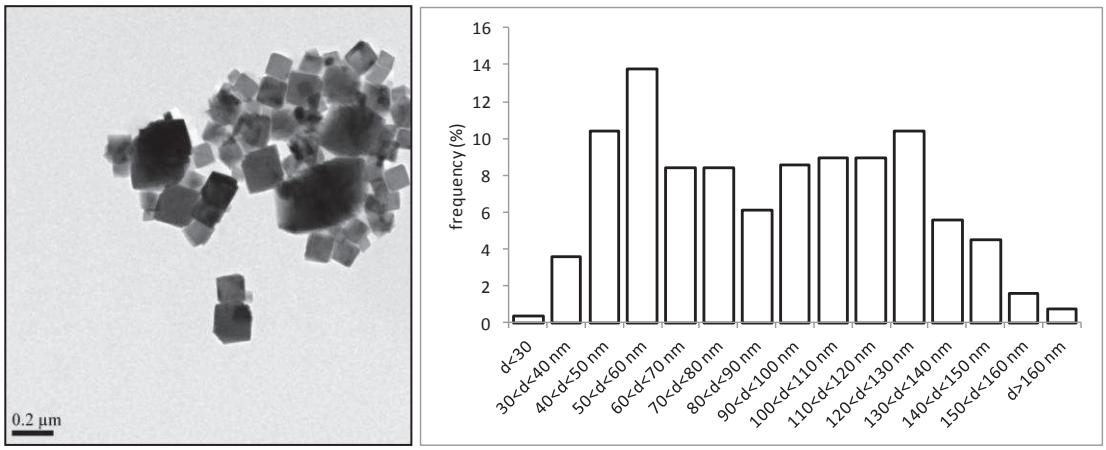

Fig 8: particles obtained for w=7. 5, 1 M at 30 °C (a) and their size distribution (b)

Statistical analysis

Experimental tests were performed according to a full factorial design with two factors (A=w and B=C_{tot}), where w is the water- surfactant molar ratio and C_{tot} is the molar concentration of reactants, the first at three levels (5, 6.25 and 7.5) and the second at two levels (0.25 and 1.0 M).

Different statistics such as mean and standard deviation were evaluated for particle populations obtained in the different treatments (i.e. different operating conditions used in factorial design). In particular the mean (µ) was calculated as the average value of N particle sizes (x_i) (2) whilst the standard deviation was calculated as the square root of the sum of square deviations between each particle size (x_i) and their mean (µ), divided by the number of particles (N) less one (3).

$$\mu = \frac{1}{N}\sum_{i=1}^{N} xi \qquad (2)$$

$$s = \sqrt{\frac{1}{N-1}\sum_{i=1}^{N}(xi-\mu)^2} \qquad (3)$$

In Figure 10 the values of these statistics for each treatment were reported. It is possible to see that w is the most influencing factor for all statistics, meaning that by increasing w in the investigated range an increase of mean (Fig. 10a) and standard deviation (Fig. 10b) of particle populations was determined. Thus increasing water-surfactant molar ratio both size and heterogeneity of particle populations tend to increase. On the other side increasing the reactants' concentration no relevant effects on estimated statistics were observed meaning that in the investigated range this factor do not affect neither size nor heterogeneity of particle populations.

The process of ANOVA analysis including numerical results should be given as Supporting Information .

These qualitative observations were confirmed by ANOVA [21] considering as output variables the statistics estimated for particle populations (mean and standard deviation). Further information about ANOVA (definitions and numerical results) are provided by supporting material.
Estimate of variance component due to error (MSE) was obtained by independent replicated tests and takes into account the variability associated to random experimental errors, the variability due to image choice for statistic determination, and variability due to image analysis uncertainties. In this context eight TEM images from two replicates (four images for each replicate) of the same treatments were used to estimate variability due to random errors.

ANOVA put in evidence that only A factor has a significant effect on all investigated outputs, while B factor and AB interactions are not significant (99% confidence level).
Estimates of the effects were evaluated considering the higher and lower levels for each factor (w = 5 and 7.5 and C_{tot}= 0.25 and 1 M) and all effects were reported in figure 11 along with the confidence bands (dashed lines) for each statistic ($\pm t_{\alpha/2,n-1}\sqrt{(MS_E/n)}$, where α=0.01 and n=8). Estimates of the effects which are larger than the confidence bands are those statistically significant (99% confidence level).
As for the interpretation of these graphs consider for example the effect of A factor (w) on population mean (figure 11a): this effect was estimated to be 84.4 nm meaning that by changing A factor from the lowest to the highest level it was determined an increase of population mean of 84.4 nm. Similarly the effect of A factor on population standard deviation (11b) was estimated to be 31.8 nm meaning that by changing A factor from the lowest to the highest level the standard deviation of population increased of 31.8 nm.
A series of hypotheses can be made to provide a phenomenological interpretation of obtained results. Considering the inverse micelles as microreactors where reactions take place, the mechanism of particle formation is characterized by subsequent steps such as intermicellar reactant transfer, intramicellar reactant diffusion, nucleation and growth. Upon mixing, nucleation occurs on the micelle edges as the water inside them becomes supersaturated with reactants. Growth then occurs around this nucleation point, with the arrival of more reactant fed via intermicellar exchange. According to several articles and reviews the intermicellar transfer can be often considered as the slowest step on particles formation [22,23] and this step plays a key-role in the obtaining of nanoparticles.
The values of factors like water-surfactant molar ratio and reactants' concentration can influence also the intermicellar transfer of reactants and hence the average size of particles and their heterogeneity can change too.
For example by raising water-surfactant molar ratio the average size of micelles increases [17] and this results in two main effects:

- a decrease of the specific surface area of micelles negatively affecting intermicellar exchange

- an increase of the time necessary to diffuse inside the micelles

Thus transferring and mixing of reactants is faster in small micelles and it can result in something like instantaneous nucleation due to fast transfer and perfect mixing. On the other side in larger

micelles, some reactants are still diffusing while nuclei have been already formed and hence new nuclei continue forming gradually while others are still growing like in a progressive nucleation. Therefore if reactants' transfer was the limiting step of particles formation, larger particles with a higher heterogeneity could be obtained by working with larger micelles.

As for the insignificant effect of reactants concentration, it must be observed that other factors like the rigidity of micelles (strongly dependent from their composition) are greatly able control the intermicellar transfer of reactants. This mean that for a given system under intermicellar transfer control, even increasing four times the reactants concentration (like done by us) no effect on particles' size and heterogeneity could be noticed.

Another explanation about the insignificant effect of reactants concentration could be that the it is lower than the experimental error (see supporting material) and hence it can't be distinguished.

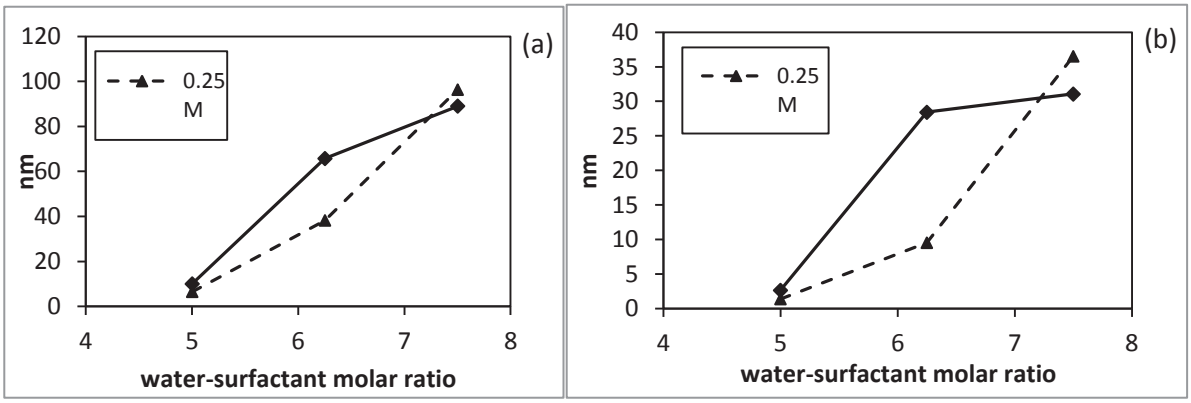

Fig 9: effect of treatments on mean size (a) and standard deviation (b)

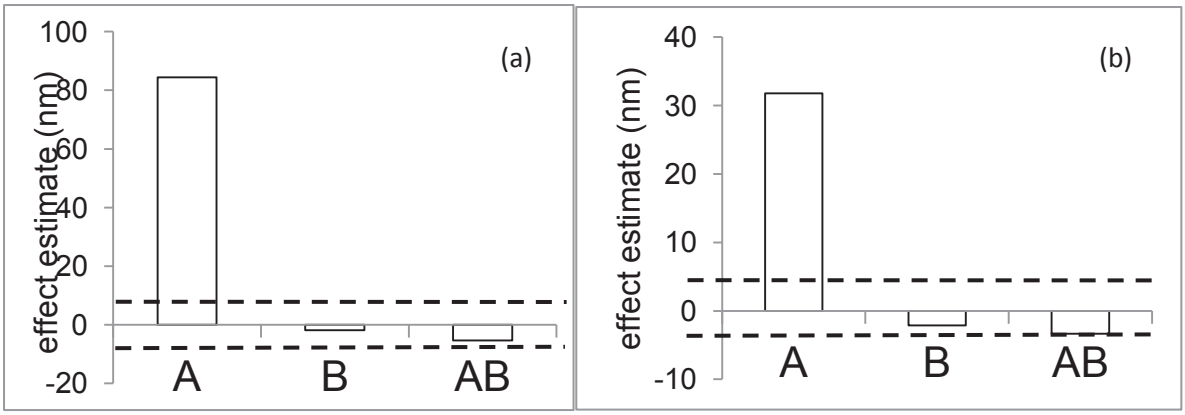

Fig 10: Estimates of effect with confidence bands

4.1.4 Conclusions

Nanoparticles of rhomb-centered hexagonal (rch) phase of manganese carbonate were obtained by a reverse micellar route at room temperature without any post-thermal treatment. Operating conditions allowing to obtain the smaller particles were w = 5 and C_{tot} = 0.25 M. The experimental

work and the statistical analysis revealed that in the investigated range, only the water-surfactant molar ratio has a significant effect on particle size and dispersion whilst reactants' concentration did not show any significant effects on the estimated statistics. Obtained results suggest that particles formations could be controlled by the reactants' transfer. Obtained products could be used as precursor for the production of manganese oxides.

4.2 Electrochemical study for production of nanostructured metallic cobalt

In this work an electrochemical study has been performed in order to investigate the electrochemical behavior of cobalt in an aqueous system even identifying how this metal nucleates on the electrodic surface. This is a preparatory study for the next production of nanostructured cobalt by electrodeposition, which is an efficient tool for preparing films for new technological applications. This method is cheaper in
terms of equipment and less time consuming than other available deposition techniques. The electrodeposition of cobalt metallic layers and alloys is of considerable interest due to its potential applications in several fields [1, 2], especially in microelectronics for magnetic recording systems [3, 4]. Cobalt is one of the most important ferromagnetic components of magnetic thin film materials. Electrodeposition is also of interest for the preparation of cobalt and cobalt alloys because it makes possible to modulate the structure of deposits and, hence, their magnetic properties. Depending on the preparation conditions, i.e. electrolyte composition, temperature, applied potential and presence of additives, materials with different structures, morphologies and magnetic properties can be obtained.
For this purpose several electroanalytical techniques, which mainly differ for the different electric signals used to describe the electrochemical process, have been employed.

4.2.1 Introduction: electrocrystallization and useful electrochemical techniques

A typical electrochemical process refers to the oxidation or reduction of electroactive species on the electrodic surface but the overall phenomena must take into account all single step determining the reaction. Actually whereas electroactive ions are contained in a solution they can move by:

- **diffusion**: spontaneous transportation of a substance under from a region of higher concentration to region of lowers concetration
- **convection**: trasportation of a substance related to the total physical motion of the liquid (i.e. solution under stirring)
- **migration**: transportation of ions under an electric field due to the attraction between opposite charges

Whereas these three mechanisms of transportation coexist the mass transfer rate J of a chemical species towards an electrode can be expressed by the Nernst-Plank equation. For a mono dimensional system it can be written as:

$$J(x,t) = -D_0 \frac{\partial C(x,t)}{\partial x} - \frac{zFD_0 c_0}{RT} \frac{\partial \Phi(x,t)}{\partial x} + c(x,t)V(x,t)$$

Where D_0 is the diffusion coefficient ($cm^{-2}*sec^{-1}$), $\delta c(x,t)/\delta x$ is the concentration time and position dependent, $\delta \Phi(x,t)/\delta x$ is the potential gradient, z and c_0 are respectively the charge and the concentration of the electroactive species, $V(x,t)$ is the hydrodynamic rate towards the x direction. Since the total current $I(x,t)$ is related to the flux by the expression:

$$I = -nFAJ\,(x,t)$$

Where *A* is the electrodic surface (cm^2).

Hence whereas the previous mechanisms of transportation coexist it become difficult to relate the total current conditions of the system. The migration contribution can be eliminated by the adding of supporting electrolytes whilst the convection transportation is unimportant by performing the measurements in a not stirred system. Whereas the diffusion become the only mechanism responsible for supplying the electrode surface with electroactive species the flux rate *J* can be expressed just by the first Fick's Law:

$$J(x,t) = -D_0\left[\frac{\partial c(x,t)}{\partial x}\right]$$

Hence, the total current becomes:

$$I(x,t) = nFAD_0\left[\frac{\partial c(x,t)}{\partial x}\right]$$

Considering also that the gradient depends on the time, for a mono dimensional system the total current should be described the second Fick's Law:

$$\frac{\partial c(x,t)}{\partial t} = D_0\left[\frac{\partial^2 c(x,t)}{\partial x^2}\right]$$

The resulting equation well describes the gradient of concentration through parallel plans placed at distance *x + dx* from the electrode surface.

4.2.1.1 Cyclic Voltammetry (CV)

Cyclic voltammetry is one of the most used analytical technique for investigations about electrochemical reactions. In spite of simple experiments, it allows to achieve many information about redox reactions in solutions, their reversibility and how they are influenced by operating conditions. It consists in a linear scansion of potentials imposed to a working electrode in a non stirred system, measuring at the same time the current passing through the electrochemical cell. The scansion-measuring operation result in a typical pattern *I vs E* called voltammogram and whereas a redox reaction takes place it results in a peak of current.

For instance, in a given system containing an electroactive species in its oxidized form Oxd^{n+} and under investigation by a *CV* (scansion of potential showed in fig. ..a) when approaching the thermodynamic reducing potential (E°) of the species Oxd^{n+} into new reduced species *Red*, there will be a reducing reaction according to the equation:

$$Oxd^{n+} + ne^- = Red \qquad\qquad E=E°$$

This reaction results in a peak of current like the in typical voltammogram showed in fig …b.

- For E>>E° the solution contains only the oxidized species Oxd^{n+} and no reactions are observed. Further decreasing of the working potential approaching the potential E°, results in the reaction * and hence in a current raise.
- For E=E°, according to the Nernst's Law, the concentrations of reducing and oxidized species are the same.
- For E<E° the reaction goes on until depletion of the electroactive species on the electrode surface determining the conditions where $C_{oxd}\,(0, t) = 0$ and C_{red} (0, t) = C_{max}

Performing also a scansion of potentials through the anodic branch, the reduced species get oxidized by the opposite reaction even determining the opposite limit conditions: $C_{oxd}(0, t) = C_{max}$ and C_{red} (0, t) = 0. The typical voltammographic peaks are the direct consequence of this time-dependent variation of concentrations on the electrodic surface.

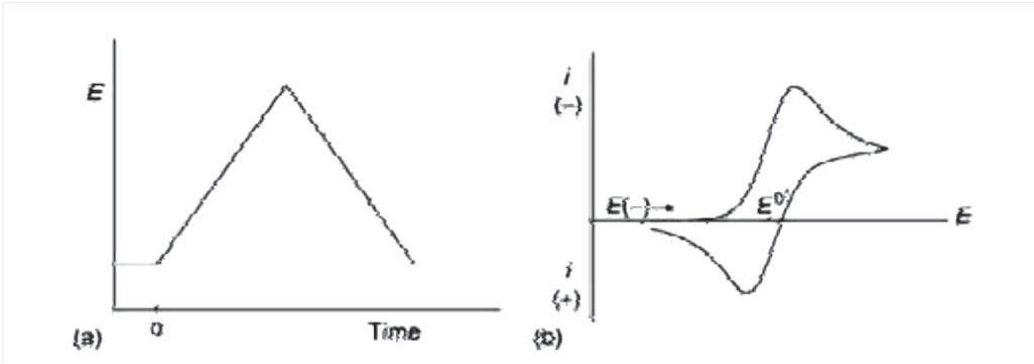

Fig. 11: Signals in a typical voltammetry

Solving the second Fick's Law (for a planar electrode in boundary conditions) and substituting in the expression of current, gives the Cottrell equation which well describes the I-V trend of a typical voltammogram:

Moreover in a typical voltammogram the current peak can be described by the Randles-Sevcik equation:

$$I_p = (2.69\times10^5)n^{3/2}Ac_0D_0^{1/2}v^{1/2}$$

Where v is the scansion rate, A is the electrode surface, D_0 is the diffusion coefficient, n is the amount of transferred electrons and c_0 is the bulk concentration of the electroactive species. According to this equation the current peak intensity increases proportionally to an increased bulk concentration and with a square root of potential scansion rate.
A CV experiment is also useful to estimate the reversibility of the electrochemical system. A reversible system is direct consequence of a fast electron transferring and it determines that:

- The ratio between the intensities of anodic and cathodic peaks must be 1, meaning that the same amount of substance gets reduced and oxidized.
- The half-wave potential is placed just halfway between the anodic and cathodic peak potential and hence for a reversible couple the peak potential gap is given by:

$$\Delta E_p = E_{pa} - E_{pc} = \frac{0.059}{n}$$

This implies the possibility to evaluate the number of transferred electrons by the experimental knowledge of ΔE_p.

4.2.1.2 Chronoamperometry

In a typical chronoamperometric experiment the potential of a working electrode is stepped up from the open-circuit potential to the potential at which a reducing the reduction of an ions take place according to the following reaction:

$$Oxd^{n+} + ne^- = Red \qquad E=E°$$

measuring the resulting current intensity during the time. potential Providing enough energy (E>>E°) the system made a transition from no reaction to the steady-state reaction, controlled by the rate of mass transfer of metal ions toward the electrode surface to determine the reaction.

Working in a non-stirred system containing only the electroactive species of interest, such transition is always followed by the current transient until the steady-state is achieved. Is such conditions the boundary conditions *c (x, t)* are:

- $c(x, 0) = c_0$
- $c(0, t) = 0$ (for $t > 0$) meaning the suddenly reaction on the electrode surface
- $c(x,0) \rightarrow c_0$ for $x \rightarrow \infty$ meaning the formation of diffusive layers

For these conditions the Fick's Law solution becomes:

$$c(x,t) = c_0\left\{1 - erf\left[\frac{x}{(4D_0t)^{1/2}}\right]\right\}$$

Deriving the Fick's Law solution towards *x* and replacing it in the general expression of current, it gives the Cottrell equation:

$$i = \frac{nFD^{1/2}C_0}{\pi^{1/2}t^{1/2}}$$

The Cottrell equation well describes the current trend during a chronoamperometric experiment once the diffusion zones have been formed.

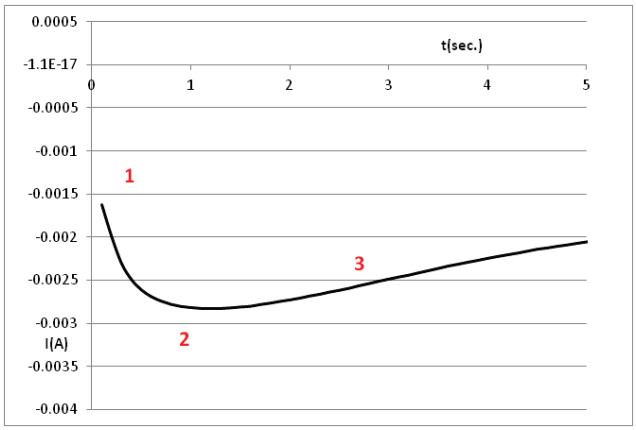

Fig.12: a typical chronoamperometric transient

Under these conditions, the nuclei formed on the surface contribute to the active surface area available for reaction. Initial current increase (1) for heterogeneous systems is due to the increase of surface area whenever the nucleation is involved.
As the nucleation progresses, the nuclei will begin overlapping and each nucleus will define its own diffusion zone through which metal ion has to diffuse, supplying mechanism for continuation of growth. Since the diffusion zones are much larger than the underlying nuclei, the overlapping zones would eventually include the entire electrode area. This results in a current peak (2). In a system under steady state conditions, further reaction is strictly controlled by the rate of mass transfer through the control area of the diffusion zone (3). Within the diffusion zone, growth of already-established metal nuclei can continue, or additional nucleation can be initiated on various sites, both governed by the steady state conditions, as described by the Cottrell equation. Because

of this equation chronoamperometry can be used either to estimate the diffusion coefficient when the electrode area is known or to do the opposite.
Moreover, the chronoamperometry is a very useful technique to identify the nucleation mechanism as it will be explained below.

4.2.1.3 Scharfcker-Hill's Model

A typical electrodeposition process from solution takes place by a first step of nucleation followed by the growing and coalescence of already formed nuclei. Once the nuclei have been formed they are stable and they can eventually grow only it their size is higher than a "critic size", evaluable from thermodynamic considerations. Moreover It must take into account that the whole phenomena includes also steps such as the transportation of electroactive ions to the electrode surface and the charge transfer. In many cases of the charge transfer is found to be fast and the rate of growth of mature nuclei can be described by the transportation of electroactive ions to the growing sites. According to Sharifker and Hill, the rate law for growth of 3D islands during electrochemical deposition is dependent on the mechanism of nucleation and growth and two limit cases can be distinguished:

a) Instantaneous nucleation. It corresponds to a slow growth of nuclei on a small number of active sites, all activated at the same time. In this case all active sites available on the electrode surface are occupied in a very short time period after applying overpotentials and then, the nuclei only grow. Instantaneous nucleation occurs with high nucleation rates and so:
   A >> 1, exp(-At)→0 and hence N(t) = N_0 meaning that the maximum density of nuclei can be reached just after the potential has been stepped up.
b) Progressive nucleation. It corresponds to a fast growth of nuclei on many active sites, all activated during the course of electroreduction. In this case nuclei are continuously formed during the whole time period at which overpotential is applied. So progressive nucleation occurs for low nucleation rateA<<1 and exp exp(-At)→1

Under the previous hypothesis Scharfcker and Hill proposed the following equations:

Table 1: equations proposed by Scharficker and Hill

S. no.	Instantaneous nucleation	Progressive nucleation
1.	$t_m = \left(\frac{1.2564}{N\pi kD}\right)$	$t_m = \left(\frac{4.6733}{AN_\infty \pi k' D}\right)^{1/2}$
2.	$I_m = 0.6382\, zFDc(kN)^{1/2}$	$I_m = 0.4615\, zFD^{3/4}c(k'AN_\infty)^{1/4}$
3.	$I_m^2 t_m = 0.1629\,(zFc)^2 D$	$I_m^2 t_m = 0.2598\,(zFc)^2 D$
4.	$\frac{I^2}{I_m^2} = \frac{1.9542}{t/t_m}\left\{1 - \exp\left[-1.2564\left(\frac{t}{t_m}\right)\right]\right\}^2$	$\frac{I^2}{I_m^2} = \frac{1.2254}{t/t_m}\left\{1 - \exp\left[-2.3367\left(\frac{t}{t_m}\right)^2\right]\right\}^2$

where D is diffusion coefficient, c the bulk concentration, zF the molar charge of the electrodepositing species, N the total number of nuclei, N∞ number density of active sites, Im and tm current and time coordinate of the peak and k and k‟ are numerical constant defined as:

$k = 8\pi cM\rho$

$k' = 43\ 8\pi cM\rho$

where M and ρ are molecular weight and density of the deposited material respectively.
Presenting the results of the chronoamperometry in a dimensionless form $(I/Im)^2$ vs. t/tm and comparing with the theoretical transients for instantaneous and progressive nucleations, it become possible to identify the nucleation mechanism of the process under exam.

4.2.2 Experimental

Reagent grade CoSO4*7H2O was used to prepare 0.005, 0.01 and 0.05 M Co(II) solutions. All solutions were prepared in bidistilled water contained 1 M reagent grade (NH4)2SO4 that served as a buffering agent and a supporting electrolyte, unless stated otherwise in the text. Solution pH was adjusted by adding dilute NH4OH (pH 6). The electrochemical setup was a standard three-electrode cell with copper as a working electrode, platinum foil as a counter electrode, and silver–silver chloride as a reference electrode (E^0_h = +0.222 V). Electrochemical experiments were controlled with a potentiostat/galvanostat (Amel potentiostat mod. 7060) under computerized control (Junior Assist software). The produced particles were observed by scansion electronic microscopy () with an EDS probe. Obtained images were analyzed by a software for image analysis (Jimage Software) in order to evaluate the particle size distribution. Thermodynamic calculations were performed by thermochemical software (Stabcal) [15].

4.2.3 Results

4.2.3.1 Voltammetry

Cobalt reduction thermodynamically occurs according to the following reaction:

$$Co(H_2O)_6^{2+} + 2e^- \rightarrow Co^0 + 6H_2O \qquad E0=-0.277\ V\ (E^0_{Ag/AgCl} = -0.499\ V)$$

Results of voltammetry showed that on a copper electrode the reduction toke place at cathodic potentials included between -0.7 and 1.0 V (vs reference) whilst its re-oxidation toke place between -0.4 and -0.2 V, suggesting that the difference between the equilibrium cobalt redox potential and the onset of cobalt deposition was due to the nucleation overpotential on copper electrode. The process wasn't completely reversible and this can be clearly seen looking at the two different intensity of oxidation and reduction peaks: their ratio is much lower than 1 meaning a non completely reversible process. As also reported by Grujic et al. in the oxidizing branch the metallic cobalt didn't get totally dissolved and by a second cycle in the cathodic branch a higher current was registered because the crystallization occurred on a surface already containing a small amount of cobalt and hence the resistance was lower. The current intensity peak increased linearly with the square root of the potential scanning rate according with the Randles-Sevcik equation:

$$Ip = cost\ nFAC(nFD/RT)^{1/2}$$

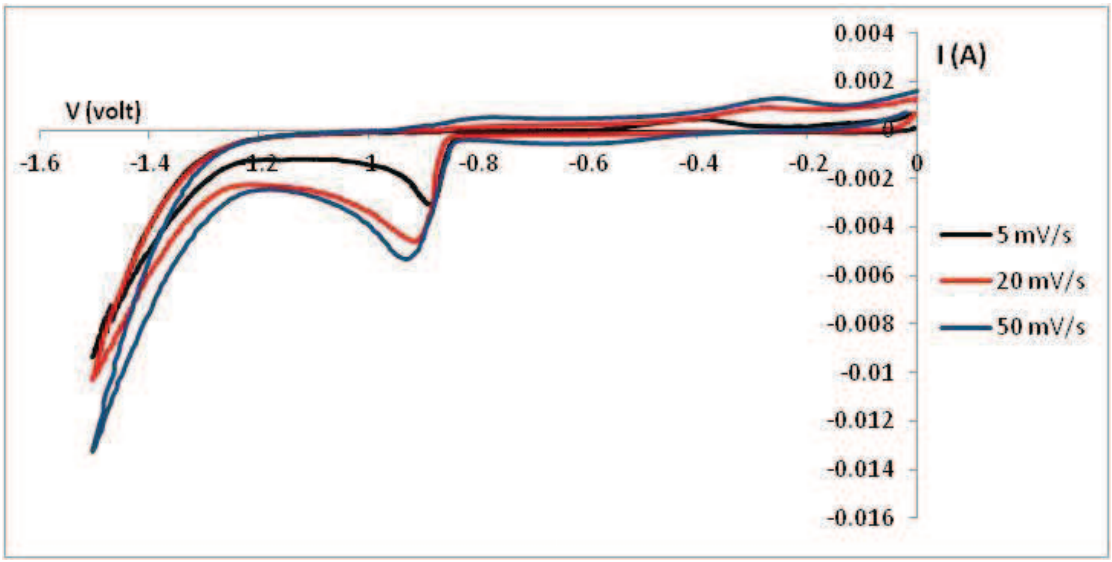

Fig.13: voltammetry performed at different potential scanning rate

The pH effect has been evaluated by performing several cycles at different pH's value and as can be seen in fig by increasing the pH value from 3 to 6 the reduction peak has been registered at higher cathodic potentials with more narrow shapes. In fact at pH 3 there was a high contribute to the current trace due to the hydrogen evolution such an extant than the cobalt reduction was visible just by a change in slope. When pH value increased the the hydrogen contribute to the total current also decreased determining more separation between reducing peaks of Cobalt and hydrogen ions .

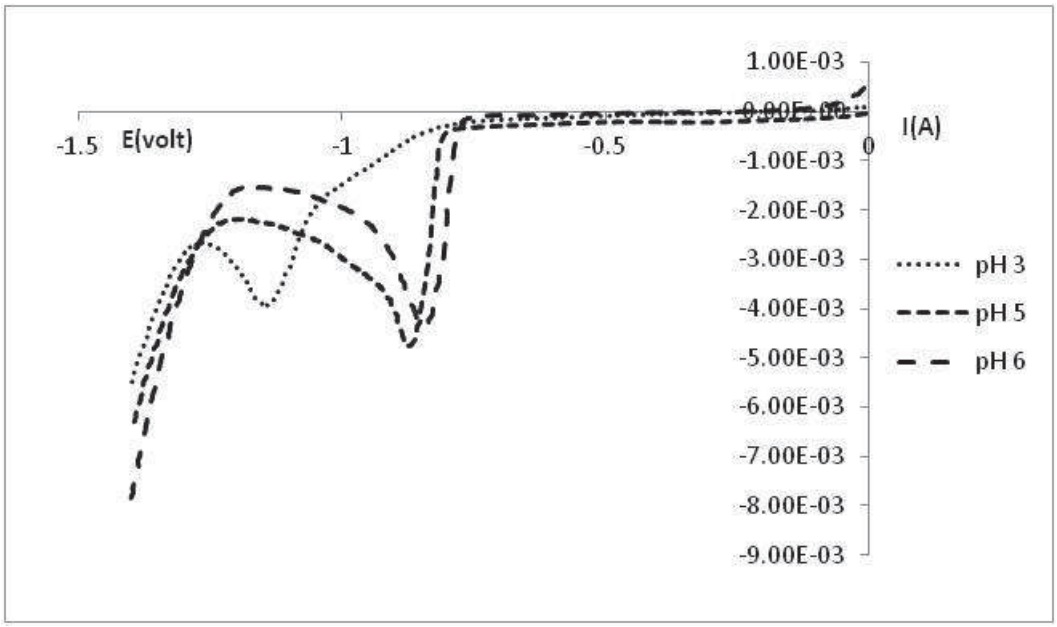

Fig. 14: voltammetry performed at different pH values

Cobalt (II) concentration is very effective on both its own reducing potential and current intensity at the reduction peak. The magnitude of the current peaks increased proportionally to the increase of Co(II) concentration, as expected, since the process in under diffusive control and well desribed by Cottrell equation. The peak due to the reduction of cobalt shifts also to higher

potentials when cobalt contration increases and this effect is probably related to concentration overpotential, as the higher concentration of reacting species reduced the concentration overpotential for cobalt reduction [19].

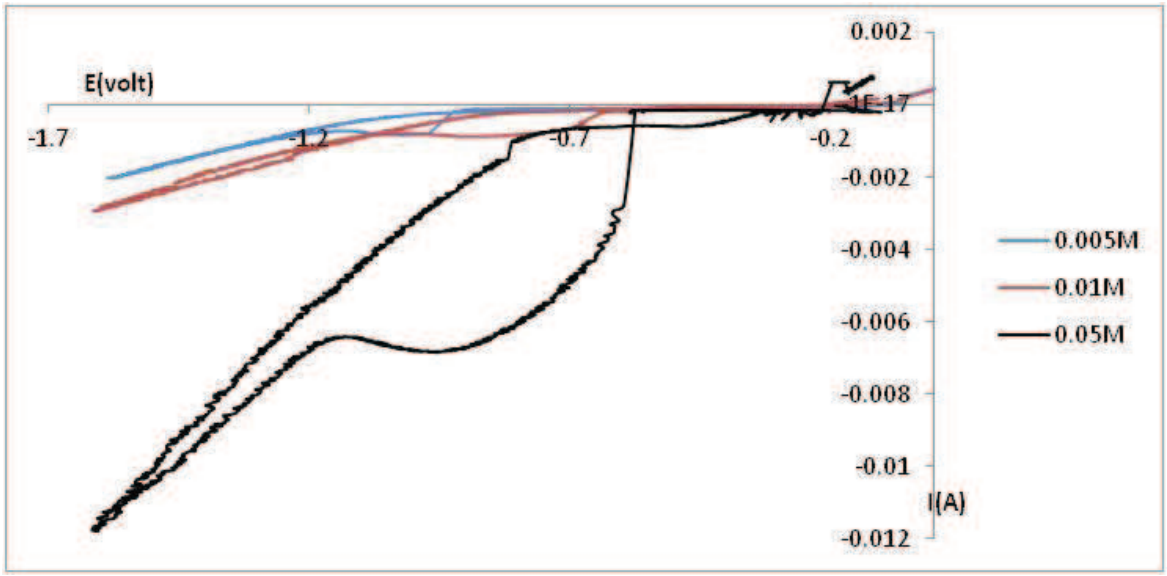

Fig. 15: effect of cobalt concentration on voltammetry

4.2.3.2 Chronoampermetry

Chronoamperometry experiments have been performed with the aim to get more information about cobalt nucleation on copper electrode. The investigation has been made on a 0.005 M cobalt sulphate solution in a range of deposition potentials included between -1.0 and -1.2 V, as previously suggested by results of voltammetry. The obtained trends well represent what expected by these kind of transient: At first, stepping up the potential to a value at which the reduction takes place, a current rising due to a charge transfer was observed. When the reaction occurred and cobalt nuclei formed creating a a diffusion zone which controls further supply of cobaltous ions to the electrode surface. The overlap of these zones results in a peak that is characteristic for nucleation and as it can be seen in fig. higher overpotential promoted faster nucleations. After this peak, the current is well described by the Cottrell equation meaning that the whole process become controlled by the trasnfer of cobaltous ion to the electrode surface.

The experimental data from Fig. were used to obtain reduced currents versus reduced time plots, according to Scharicker-Hill's equations. As can be seen in fig… the initial stages of cobalt nucleation occurred according to an instantaneous mechanism meaning that a process completely controlled by the diffusive transport of cobaltous ions was taking place. Hence a slow growth of nuclei on a small number of active sites, all activated in the same time should take place.

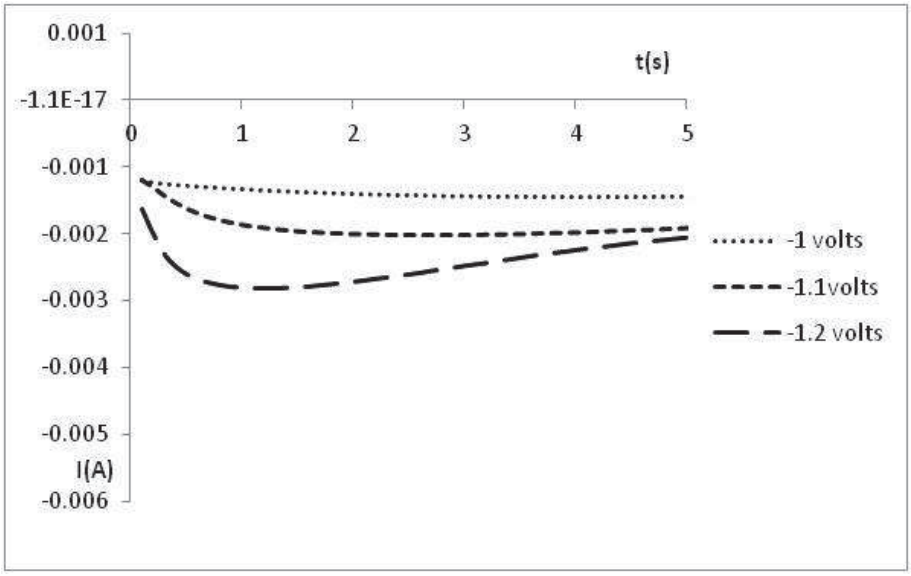

Fig.16: chronoamperometry performed on a 0.005 M cobalt solution

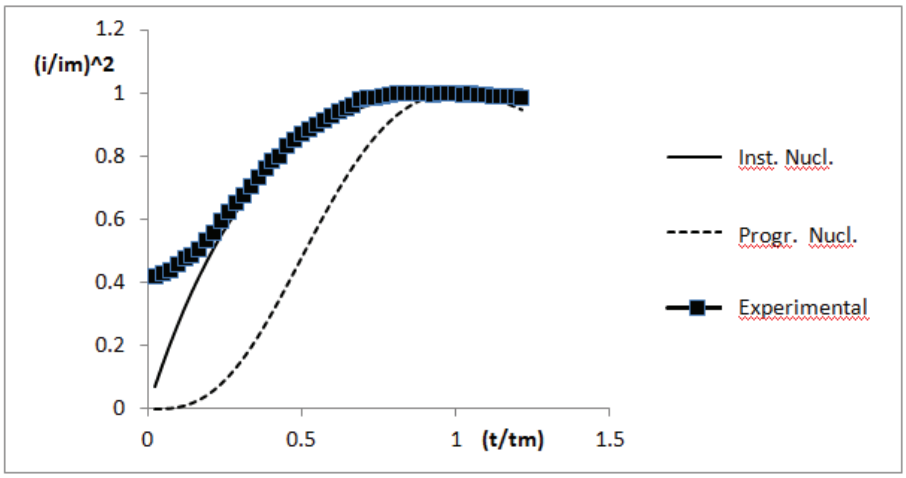

Fig. 17: Reduced current versus reduced time plots, obtained at -1.0 V from data in fig. 16

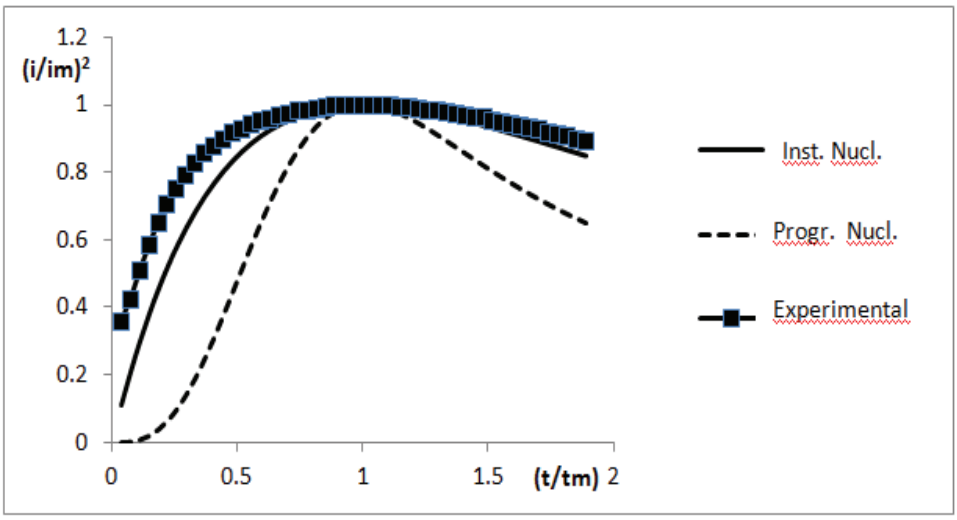

Fig. 18: Reduced current versus reduced time plots, obtained at -1.1 V from data in fig. 16

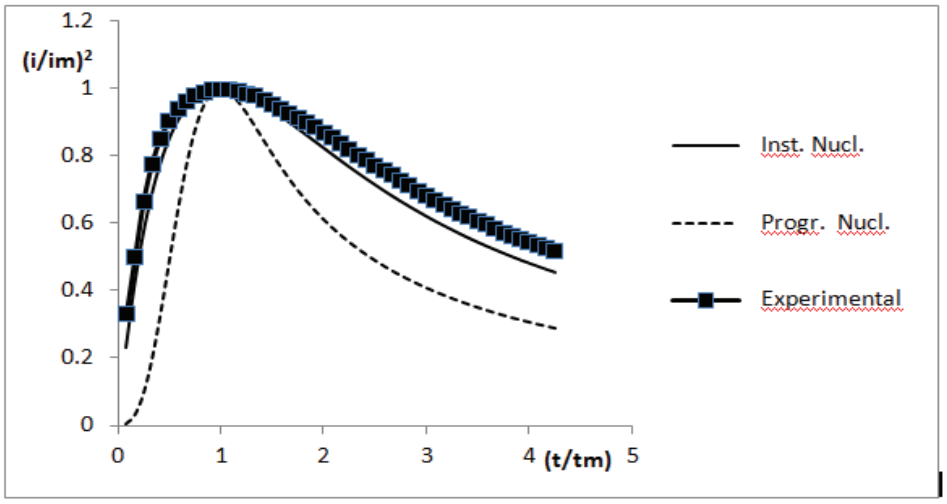

Fig. 19: Reduced current versus reduced time plots, obtained at -1.2 V from data in fig. 16

The electrodes used in the chronoamperometry experiments were also observed by a scansion electron microscope in order to verify the results obtained by the reductive transient. In fact an instantaneous mechanism should result in an electrode covered with cobalt nuclei of similar sizes, meaning that nuclei formed at the same time. The obtained images were first elaborated by Adobe Illustrator software and then, the resulting images were analyzed by a software for image counting (Jimage) to obtain a a particle size distribution. Results are listed figures 20, 21 and 22. showing that the obtained particles were included in a relatively small range but since no progressive mechanism was observed in the present experiments, the obtained results couldn't be compared with something which should theoretically promote a wider dispersion.

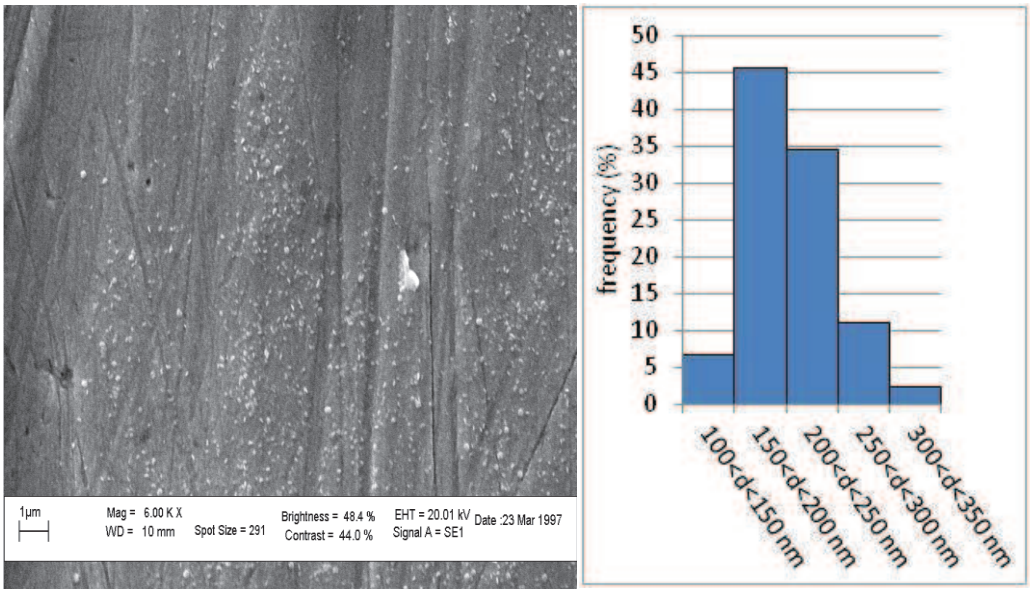

Fig. 20: cobalt particles on copper electrode and their distribution at -1.0 V

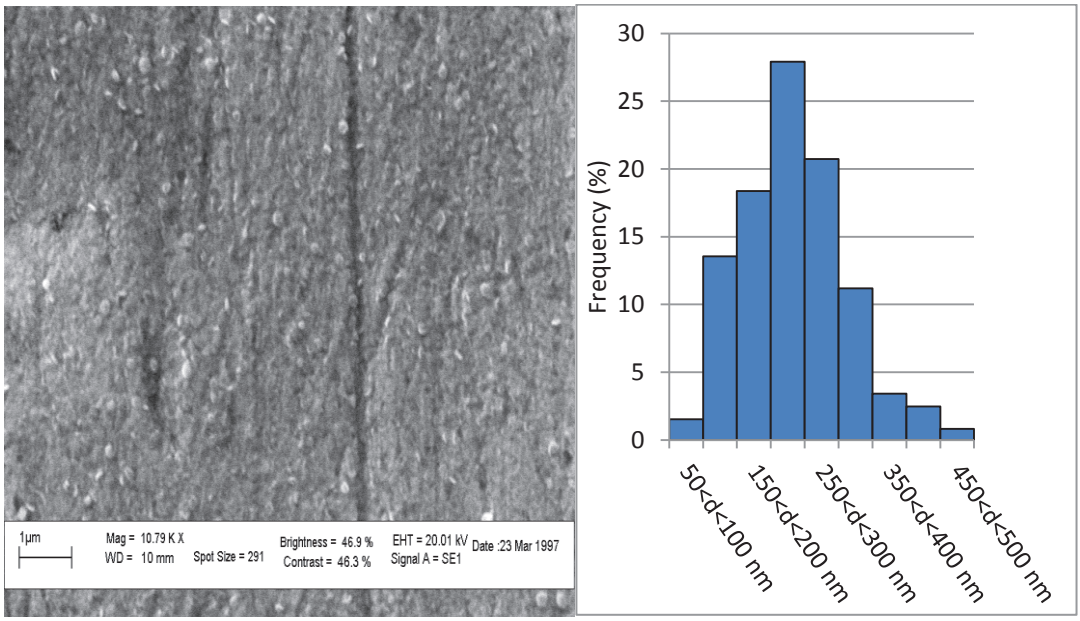

Fig. 21: cobalt particles on copper electrode and their distribution at -1.1 V

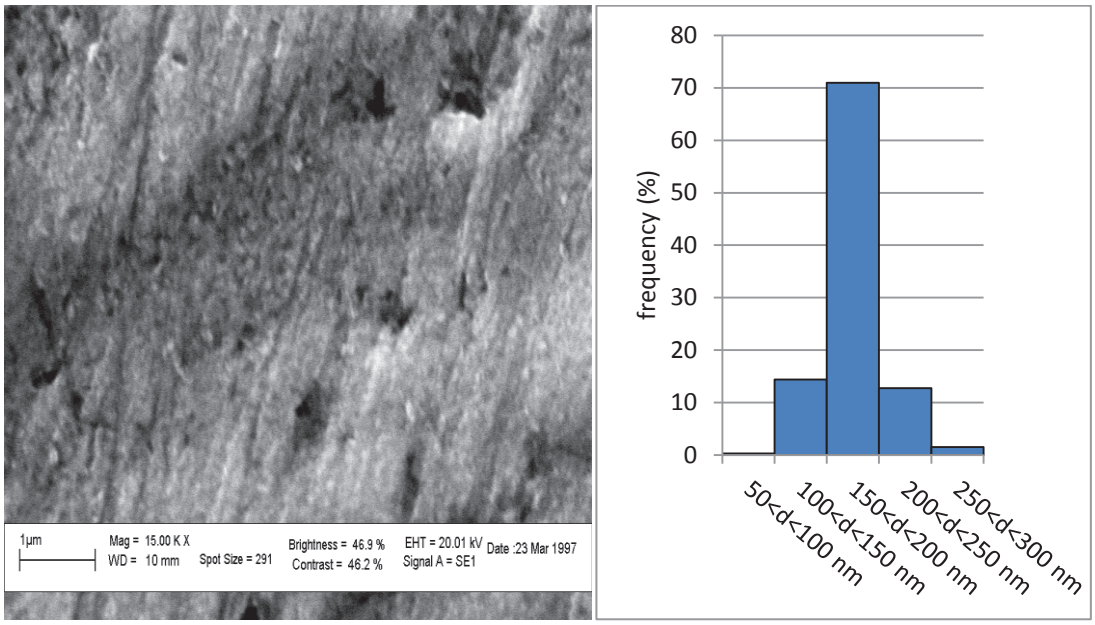

Fig. 22: cobalt particles on copper electrode and their distribution at -1.2 V

Since presumably the smallest nuclei will produce smaller crystallites, in this preparatory study the effect of deposition potential on cobalt nuclei was investigated. This effect was evaluated by performing several depositing transient at different cathodic potentials but since according to the Faraday's law the total reacting species (and hence the final size of nuclei) are proportional to the total electrodic charge, the total amount of charge itself was kept constant by modifying also the transient time. Results are showed in fig. where it can be seen that the increasing of the depositing potential resulted in larger nuclei and -1.0 V was found to be the optimal depositing potential for obtaining the smallest nuclei.

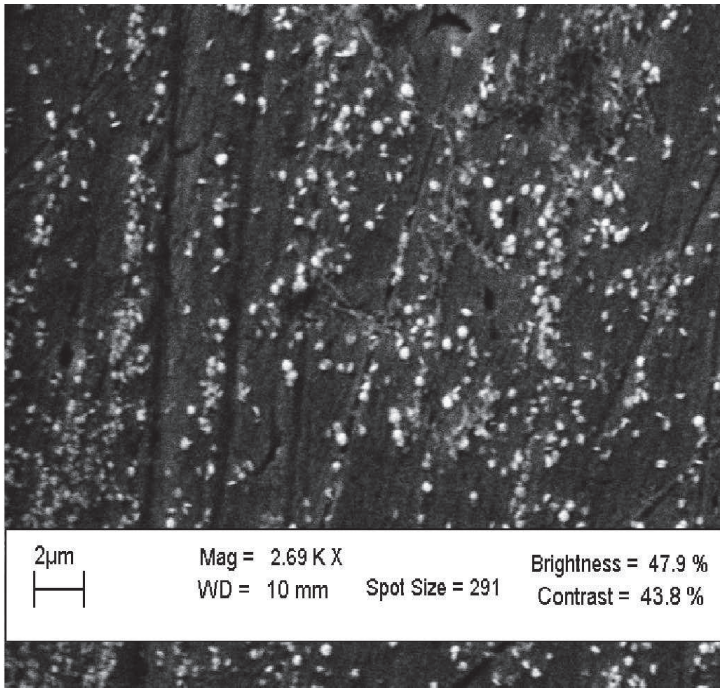

Fig 23: copper electrode surface depositing cobalt at -1.0 V

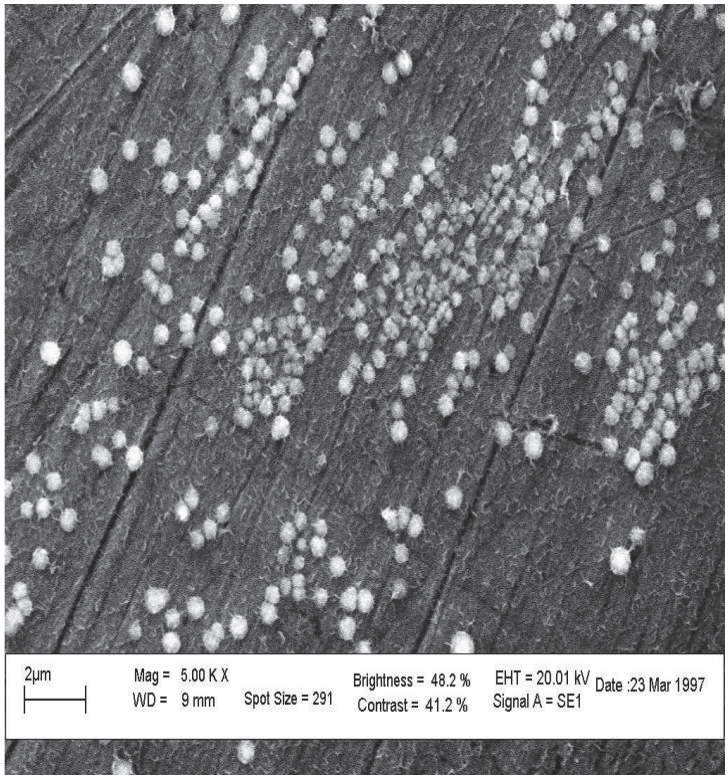

Fig 24: copper electrode surface depositing cobalt at -1.0 V

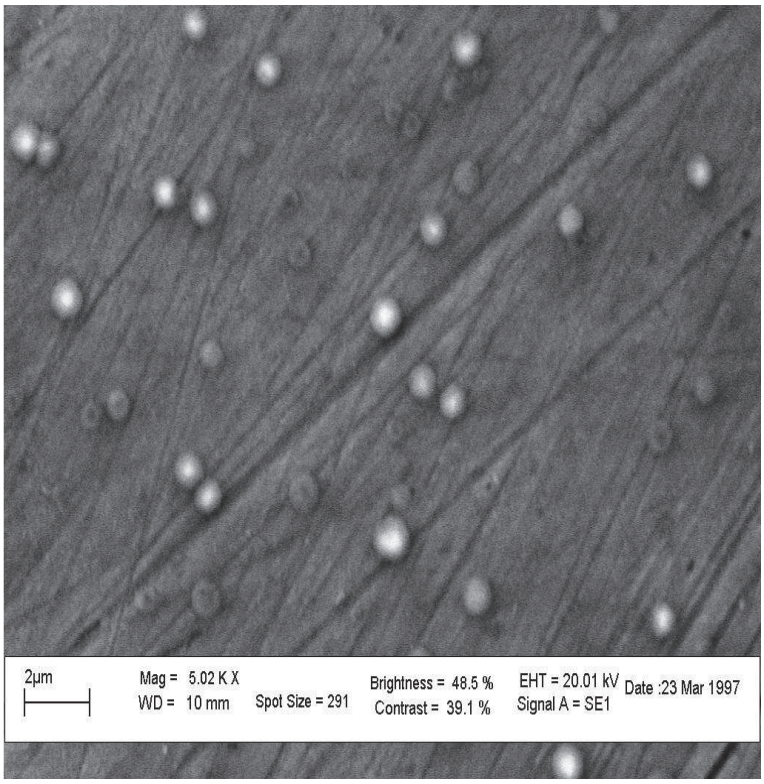

Fig 25: copper electrode surface depositing cobalt at -1.0 V

References

[1] Stobhe, E. R.; Boer, B. A. D.; Geus, J. W. *Catal. Today* 1999, 47, 161

[2] Grootendorst, E.; Verbeek Y.; Ponce, V. *J. Catal*. 1995, 157,706

[3] Pang, S.C.; Anderson, M.A.; Chapman, T.W. *J. of Electrochem. Soc.* 2000, 147, 444–450

[4] Baldi M.; Finocchio E.; Milella F.; Busca, G. *Appl. Catal.* 1998, B, 16, 43.

[5] Zwinkels, M. F. M.; Jaras, S. G.; Menon P. G.; Griffik, T. A. *Catal. Rev.* 1993, 35, 319.

[6] Nam, K.W.; Kim, K.B. *J. Electrochem. Soc.* 2006, 153, 81–88.

[7] Chang, J.K.; Tsai, W.T. *J. Electrochem. Soc.* 2003, 150, 1333–1338.

[8] Baldi, M. *Appl. Catal*. 1998, B, 17, L175.

[9] Zhang, H. M.; Teraoka, Y. *Catal. Today*, 1989, 6, 155.

[10] Tabuchi M.; Ado, K. *J. Electrochem. Soc.* 1998, 145, L49.

[11] Nakamura T.; Kajiyama, A. *Solid State Ionics*, 1999, 45, 124.

[12] Vàzquez-Olmos, Redòn, R.; Fernàndez-Osorio A.L.; Saniger, J.M. *Appl. Phys*. 2005, A 81, 1131–1134.

[13] Pileni, M. P. *Nat. Mater.* 2003, Vol. 2, 145-150.

[14] Pileni, M.P. *J. Phys. Chem*. 2007, 111, 9019-9038.

[15] Eastoe, J.; Hollamby, M. J.; Hudson, L. *Adv. Colloid Interfac.* 2006, 128-130, 5-15.

[16] Michaels, M.A.; Sherwood, S.; Kidwell, M.; Allsbrook, M.J.; Morrison, S.A.; Rutan, S.C.; Capenter, E.E. *J. Colloid Interf. Sci*, 2007, 311, 70-76.

[17] Ganguli, A. K.; Ganguly, A.; Vaidya, S. *Chem. Soc. Rev*., 2010, 39, 474-485.

[18] Liu, Y.; Liu, Z.; Wang, G. *Appl. Phys*. 2003, A 76, 1117–1120.

[19] Ahmad, T.; Ramanujachary, K. V.; Lofland, S. E.; Ganguli A. K. *J. Mater. Chem*. 2004, 14, 3406–3410.

[20] Wu, X.; Cao, M.; Lu, H.; He, X.; Hu, C. *J. Nanosci. Nanotechno*., 2006, Vol.6, 2123-2128,.

[21] Montgomery, D.C.; Runger, G.C. Applied Statistics and Probability for Engineers

[22] Lopez-Quintela, MA.; Tojo, C.; Blanco, MC.; Garcıa Rio, L.; Leis, JR. *Curr. Opin. Colloid Interface Sci* 2004;9:264.

[23] Uskokovic, V.; Drofenik, M. *Surf Rev Lett* 2005;12:239.

[24] Allen J. Bard, Larry R. Faulkner. Electrochemical Methods, Fundamentals and Applications;

[25] D. Grujicic, B. Pesic. Electrochimica Acta 47 (2002) 2901_/2912

[26] D. Grujicic, B. Pesic. Electrochimica Acta 49 (2004) 4719–4732.

5. Conclusions

By the following work two processes to recover metals from spent batteries such as lithium ion and nickel metal hydride have been developed.

The process for the valorization of lithium ion batteries has been developed studying at first in medium scale the mechanical operations required to dismantle the spent devices recoverying interesting fraction such as ferrous metals, non ferrous metals and the electrodic powders enriched in cobalt and lithium ($LiCoO_2$). This study resulted in a route composed by primary crushing, sieving at 1mm and secondary crushing of the fraction > 1 mm followed by another sieving at 1 mm in order to separate a fine electrodic powder and a bigger fraction of ferrous and non ferrous metals then separated by an eddy current splitter. A leaching operation has been optimized in order to maximize the extraction of cobalt and lithium from the mechanically recoverd electrodic powders. The optimized operation required 2g of suphuric acid for g of electrodic powder at 70-90°C for 2 hours and in presence of a reducing agent (glucose) able to reduce cobalt from Co^{3+} to Co^{2+} determining its solubilization. Since also other metals acting like impurities (Fe, Al, Ni) were solubilyzed a primary purification has been carried out by a precipitation of iron and aluminum at pH 4.5-5. Separation cobalt- nickel was then optimized by a selective extraction of Co using Cyanex 272 in a stoichiometric ratio 3.5:1 with cobalt at pH 5.5. After purifications the lithium and cobalt was recovered as carbonates from their respective streams by carbonatation and precipitation. Performing these operation after solvent extraction the obtained carbonate had a cobalt content around 46-47% but without solvent extraction the obtained product contained also nickel and the cobalt content was about 36-37%. Process analysis reveled that performing the solvent extraction operation to sell a higher purity cobalt carbonate (selling price 45 $/kg) the process would be always economically feasible. The process without solvent extraction would be conomically feasible only by selling the lower purity carbonate for at least 10 $/kg and by selling it for 18 $/kg both processes with and without solvent extracton would give the same economical outputs.

The process to valorize spent nickel metal hydride devices has been developed at fist studying a mechanical route to dismantle the devices recovering 3 fractions: ferrous metals, non ferrous metals and a fine electrodic powder containing nickel, cobalt, manganese and rare earth. Therefore the hydrometallurgical operations have been studied in order to extract metals from the powder, to purify the resulting solutions and to recover products. Optimized conditions for leaching were: 2 M sulphuric acid, for 2 hours ar 25°C. Rare earths were recovered as sulphates after leaching by a precipitation at pH 1.5. Leach liquor purification was optimized extracting the manganese by an extractive multistep with D2EHPA in a molar ratio 2:1 with manganese at pH 4. The number of step were proportional to the manganese concentration. After manganese removal the cobalt was transferred into an organic phase made up of Cyanex 272 (stoichiometric ratio Cyanex/Co 3,5-4:1, pH 6) leaving the nickel in the aqueous phase. Once separated Ni, Mn and Co were recovered by precipitations from their respective streams. In particular Mn and Co were precipitated as carbonates whilst nickel was recovered as hydroxide. Simulations showed this process was always economically feasible in the investigated ranges and in spite of higher costs

and higher revenues it gave economical outputs similar as for the process of lithium ion valorization.

With the future ambition to produce based Co, Ni and Mn nanomaterials as downstream of hydrometallurgical processes for waste valorization, a further experimentation has been carried out studying the production of nanoparticles.

Nanoparticles of manganese carbonate were produced by a microemulsion mediated route investigating the effect of operating conditions such as water-surfactant molar ratio and reactants concentration. The smallest particles were obtained working at 5 as water-surfactant molar ratio and 0.25 M as reactant concentrations. All produced samples, after characterization by SEM, TEM, XRD and TGA, were calcinated at 500°C for 4 hours under Ar atmosphere in order to obtain a more useful product like Mn_3O_4.

A preparatory study for the production of nanostructured metallic cobalt by electrodeposition has been performed. The aim of the study was to identify the cobalt electrochemistry and its nucleation mechanism on a copper cathode. Cobalt nucleated at around -1.0 V as cathodic potentials (vs Ag/AgCl reference electrode) following an instantaneous mechanism according which nuclei form very fast in the same range of time and they grow slowly only on a small number of active sites. This results in the formation of nuclei having similar sizes which presumably will carrie out to the formation of particles with a narrow dispersion.

This study is still under exam and starting from obtained results it will be completed by electrodepositing cobalt in a nanostructured form by pulsed current.